The design and synthesis of boronic acid dye molecules

Ward, Christopher James

Award date:
2001

Awarding institution:
University of Bath

THE DESIGN AND SYNTHESIS OF BORONIC ACID DYE MOLECULES

submitted by Christopher James Ward

for the degree of PhD

of the University of Bath

2001

Signed: C. J. Ward

ProQuest LLC
789 East Eisenhower Parkway
P.O. Box 1346
Ann Arbor, MI 48106-1346

"I remember when I found out about chemistry,

It was a long, long way from here,

I was old enough to want it but younger than I wanted to be,

Suddenly my mission was clear.

So for a while I conducted experiments,

And I was amazed by the things I learned..."

Semisonic, 'Chemistry' from the album 'All About Chemistry', 2001

Abstract

The detection of saccharides is of crucial importance in many medicinal and industrial applications. In the last decade there has been an explosion in the use of boronic acid technology for the recognition of saccharides. Whilst a number of successful fluorescent sensors have been reported, there has been relatively little activity in the development of colorimetric systems using the boronic acid moiety.

A novel and facile synthetic route to boronic acid azo dyes has been developed. UV-VIS absorption studies have shown that boronic acid dyes containing a secondary anilinic nitrogen centre give significant visible spectral changes at high pH upon complexation with saccharide. A dye that is nitro-substituted in the phenylazo *para*-position, has shown the largest response. The proposal of a saccharide bound species containing a boron-nitrogen bond explains the enhanced response of the dyes containing a secondary anilinic amine compared to those with tertiary centres. A boronic acid dye with a tricyanovinyl chromophore has also shown large spectral changes upon addition of saccharides, but at the biologically acceptable pH of 8.21.

The boronic acid dyes' interaction with fluoride has also been evaluated. All the dyes studied have shown spectral changes upon addition of potassium fluoride in methanol, with selectivity for fluoride over other halide ions. The breaking of the boron-nitrogen bond in these molecules by fluoride is proposed to explain the spectral behaviour.

In a reversal of the above research, a colorimetric sensor for boronic acids has been identified. The commercially available Alizarin Red S has been shown to be a particularly effective receptor for a range of boronic acids. Large spectral shifts occur on addition of boronic acid to free Alizarin Red S at pH 8.21. It is thought that this system will be of value to the many users of boronic acids in a variety of disciplines.

Acknowledgements

I would like to take this opportunity to thank the many people who have provided me with help and encouragement over the past three years. Without them, I almost certainly would not be here now having written this thesis. First and foremost, I would like to thank Dr Tony James for giving me the fantastic opportunity of a PhD place within the legendary Boronic Acid Research Team (BART) and for his guidance, encouragement and friendship. I could not have asked for a better boss. I would also like to thank the past and present members of BART for their assistance, Dr Christopher Cooper, Dr James Hartley, Dr Susumu Arimori, Karine Frimat, Suvi Pettersson and Laurence Bosch. I am extremely grateful to Dr Prakash Patel, my industrial supervisor, for his colour knowledge and for his guidance during my placement in Manchester.

I also wish to thank the people and organisations that have funded my PhD life in all its guises – the EPSRC, Avecia Ltd, the Universities of Bath and Birmingham, and, of course, my parents. I must also acknowledge the various technical and analytical staff of both universities for their help and expertise in matters spectrometric and spectroscopic.

I have been lucky enough to meet some great characters during my PhD life, making work and play that bit more interesting. I've tried to mention you all, apologies if I've missed anyone out. The Birmingham Crew - Coops, Jim, Monkey, Ally, Duane, Mikee, Paul, Rich, Dan, Phil, Suzi, Kate, Taryn, Karine, Sam, Sarah, Julie, Pete, Dave, Darren, Mal, Elwyn, Matt, Andy, Steve V, Baldrick, Scroat, Mike O'D, Steve S, Jodi, Rick, Marcus and the rest of the Usual Suspects. The Bath Mob – JP, Stav, Christelle, Piers, Tim, Ross, Mike G-C, Koko, Kelly, Steve F, Phil P, Cath, Aaron, Phill B, Lara, Vincente, Steve D, Joe, Chris C, Fred, Selma, Claudia, Mike E and Mark. Thanks to all the members of the 6- and 11-a-side football teams in Birmingham, the Bath 7-a-side team, and the Mermaids and Venturers Staff Cricket Clubs, for some enjoyable, and sometimes successful, sporting moments.

Finally, and most importantly, thank you to all of my family for their love and constant support and encouragement throughout my time at university.

Table of Contents

Abbreviations

Ar	Aryl
br	Broad
δ	Chemical shift
d	Doublet
D	^2H
D-	Dextrorotatory
dec.	Decomposed
DMF	*N*,*N*-dimethylformamide
DMSO	Dimethylsulphoxide
EI	Electron impact
ESI	Electrospray ionisation
FAB	Fast atom bombardment
g	gram
hν	Light
HPLC	High performance liquid chromatography
HRMS	High-resolution mass spectrometry
IR	Infra-red
k	Rate constant
J	Coupling constant
K_a	Association constant
L-	Leuvorotatory
LFER	Linear free-energy relationship
lit.	Literature
LSI	Liquid secondary ion

m	Multiplet
m-	*Meta-*
Me	Methyl
MHz	Megahertz
mmol	Millimole
mp	Melting point
MS	Mass spectrometry
m/z	Mass to charge ratio
NBS	*N*-bromosuccinimide
NMR	Nuclear magnetic resonance
o-	*Ortho-*
p-	*Para-*
PBA	Phenylboronic acid
PET	Photoinduced electron transfer
Ph	Phenyl
ppm	Parts per million
rt	Room temperature
s	Singlet
st	Strong
t	Triplet
THF	Tetrahydrofuran
TLC	Thin layer chromatography
UV-VIS	Ultraviolet-visible
v/v	Volume for volume
w/w	Weight for weight

1 Introduction

"Twenty years from now you will be more disappointed by the things you didn't do than by the ones you did do. So throw off the bowlines. Sail away from the safe harbour. Catch the trade winds in your sails. Explore. Dream. Discover."

Mark Twain, 1835-1910

1.1 Overview of Introduction

This section is designed to provide a general summary of boronic acid dye molecules and the current state of play in the field as regards to their application as sensor systems for saccharides and the fluoride anion. Illustrations from the literature are given where appropriate. The introduction will be split into two main sub-sections. These will focus initially upon saccharide sensors, and finally on receptors for fluoride.

Firstly, boronic acids will be introduced in a historical perspective. The manner in which they bind to polyols or fluoride will be briefly discussed. This will be followed by a look at the development of boronic acids as sensor systems, concentrating in particular on coloured examples. Mention will also be made of some non-boronic acid based receptors. It should be noted that this section is not intended to be a comprehensive review of the area of boronic acid sensor systems.

If the reader is interested in more detailed discussion, they are directed to two recent review articles.[1, 2] The use of boronic acids in the palladium assisted Suzuki cross-coupling reaction has now become widespread in organic synthesis.[3] Although this is an excellent application of boronic acid chemistry, it is not considered relevant to be discussed here.

1.2 Sensor Systems for Saccharides

1.2.1 Context of Research

The chemistry of saccharides[†] plays an essential part in the metabolic pathways of living organisms, as the chemical breakdown of monosaccharides provides the energy source for physical activity. Determining the presence and concentrations of biologically important saccharides, such as glucose and galactose, in aqueous solutions is of crucial importance in many medicinal, industrial and research environments. The detection of D-glucose is of considerable benefit since a breakdown in the transport of glucose in humans has been linked to such conditions as diabetes,[4, 5] cystic fibrosis,[6] renal glycosuria[7, 8] and cancer.[9] Recent research provides clear evidence that tight control of blood-sugar levels in diabetics sharply reduces the risk of long term complications, which include blindness, kidney failure, heart attacks and gangrene.[10] Applications in industry include the assessment of fermentation processes and analysis of the purity of synthetic drugs.

The majority of current medicinal detection systems for glucose are based on the glucose oxidase (GOD) enzyme.[11] Most use potentiometric techniques for detection purposes. Glucose oxidase catalyses the oxidation of glucose to gluconic acid. The basic reaction is the oxidation of an aldehyde group to a carboxylic acid group with the production of two electrons. The electron acceptor is usually molecular oxygen. The overall reaction can be written as follows.

[†] It is traditional in the field of boronic acid recognition chemistry to refer to the broad class of polyhydroxylated carbohydrates or sugars as saccharides. This convention will be followed throughout this thesis.

$$\text{Glucose} + \text{GOD}_{\text{oxidised}} \rightarrow \text{Gluconic acid} + \text{GOD}_{\text{reduced}}$$

$$\text{GOD}_{\text{reduced}} + O_2 + 2H^+ \rightarrow \text{GOD}_{\text{oxidised}} + H_2O_2$$

Monitoring either the production of hydrogen peroxide or the decrease in the amount of oxygen enables the quantitative determination of the glucose concentration. In media such as blood, where the presence of metabolites can interfere with the detection of oxygen or hydrogen peroxide, ferrocene derivatives (Figure 1) are used to mediate the redox process.

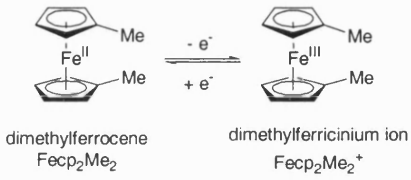

Figure 1: The oxidation of dimethylferrocene

In the glucose oxidase catalysed oxidation of glucose, the ferricinium ion acts as the electron acceptor and eliminates the need for oxygen. The overall reaction is represented in the following equations.

$$\text{Glucose} + \text{GOD}_{\text{oxidised}} \rightarrow \text{Gluconic acid} + \text{GOD}_{\text{reduced}}$$

$$\text{GOD}_{\text{reduced}} + 2\text{Fecp}_2\text{Me}_2^+ \rightarrow \text{GOD}_{\text{oxidised}} + 2\text{Fecp}_2\text{Me}_2 + 2H^+$$

In this method, the potential is held at that required to oxidise dimethylferrocene to the dimethylferricinium ion (+ 160 mV). When glucose is oxidised, the one equivalent of the reduced form of GOD produced reacts with the dimethylferricinium ion to produce an equivalent amount of dimethylferrocene. This is immediately oxidised back to the

dimethylferricinium ion at the set potential. The current is measured and is proportional to the concentration of glucose present.

There are a number of limitations in using glucose oxidase systems for the detection of glucose. The enzymatic nature of glucose oxidase means that it has an inherent instability and must be stored appropriately if it is to function properly and to prolong its lifetime. Specialist equipment, be it potentiometric or spectrophotometric, is required to monitor the output signal from the oxidation. This can make the cost of such systems prohibitive and limit the portability. Therefore, a diagnostic test paper for glucose incorporating a dye that gives a large visible colour change upon interaction with glucose, along the lines of universal pH indicator paper, would offer considerable advantages. There would be no need for specialist instrumentation, which would be of particular benefit to those in the developing world.

A great amount of attention continues to be devoted to the development of synthetic molecular receptors with the ability to recognise neutral organic species, including saccharides.[2] The vast majority of these systems have relied upon hydrogen bonding interactions for the purposes of recognition and binding of guest species. A recent review has described the progress of carbohydrate recognition through non-covalent interactions.[12] A few examples have been chosen below to give a brief illustration of how hydrogen bonding has been used in saccharide recognition.

A novel carbohydrate receptor from Davis and Wareham[13] was inspired by carbohydrate-binding proteins, which commonly place aromatic surfaces against patches of carbohydrate CH groups while accepting the hydroxyl groups into networks

of hydrogen bonds. The receptor (Figure 2) shows unusual levels of affinity and selectivity to octyl pyranosides in chloroform even in the presence of 8% CD_3OH.

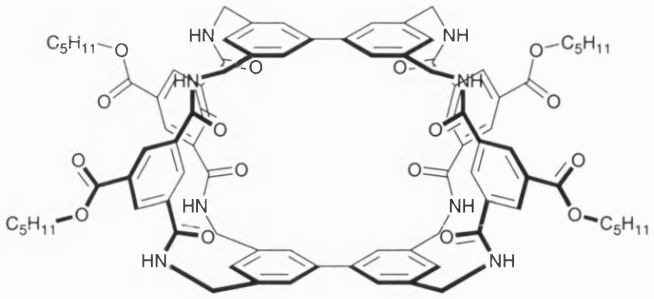

Figure 2: Carbohydrate receptor inspired by carbohydrate-binding proteins[13]

Davis has also developed a number of receptors for binding carbohydrates in non-polar media based on the inexpensive steroid cholic acid.[14-16] The designed cyclocholamide receptors use a rigid steroid backbone with a variable spacer for cavity size modulation.[14, 15] The hydroxyl groups present line the interior of the receptor and give a micelle-like character. 'Cholaphane' macrocyclic hosts again feature substantial cavities with inward-directed hydroxyl groups (Figure 3).[16] Both structural motifs proved suitable for carbohydrate recognition in non-polar solvents.

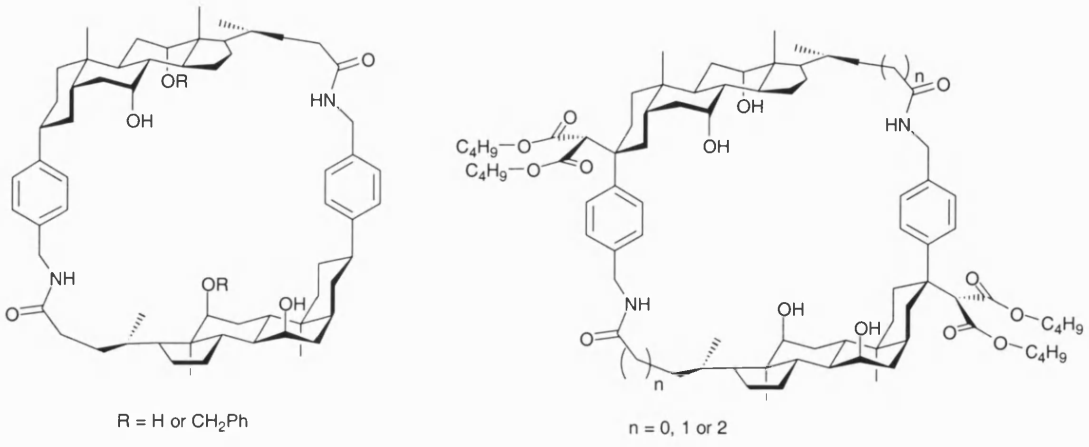

Figure 3: Davis' 'cholaphanes' for carbohydrate binding[16]

The hydrogen bonding interaction between phosphates or phosphonates and diols has been explored by a number of groups for carbohydrate recognition purposes. The basicity of the anionic centres enables the formation of extremely strong hydrogen bonds. Diederich has used 1,1'-binaphthalene-derived cyclophanes containing four phosphate residues (Figure 4a) to bind disaccharides in 1:1 complexes.[17] High affinities for disaccharide were observed, even in a competitive deuterated acetonitrile-methanol solvent mixture. An approach by Das and Hamilton involves the use of phosphonate-functionalised receptors (Figure 4b). A rigid spirobifluorene spacer was used to restrict the flexibility of the phosphonate groups and to impart chirality to the molecule.[18] Although the exact nature of the hydrogen bonding could not be determined, the anionic phosphonate was shown to be an excellent hydrogen bond acceptor for glycosidic hydroxyl groups. The monophosphonate binds various glycosides in a 1:1 stoichiometry. Selectivity and binding affinity is enhanced in the diphosphonate where two extra hydrogen bonding sites are available.

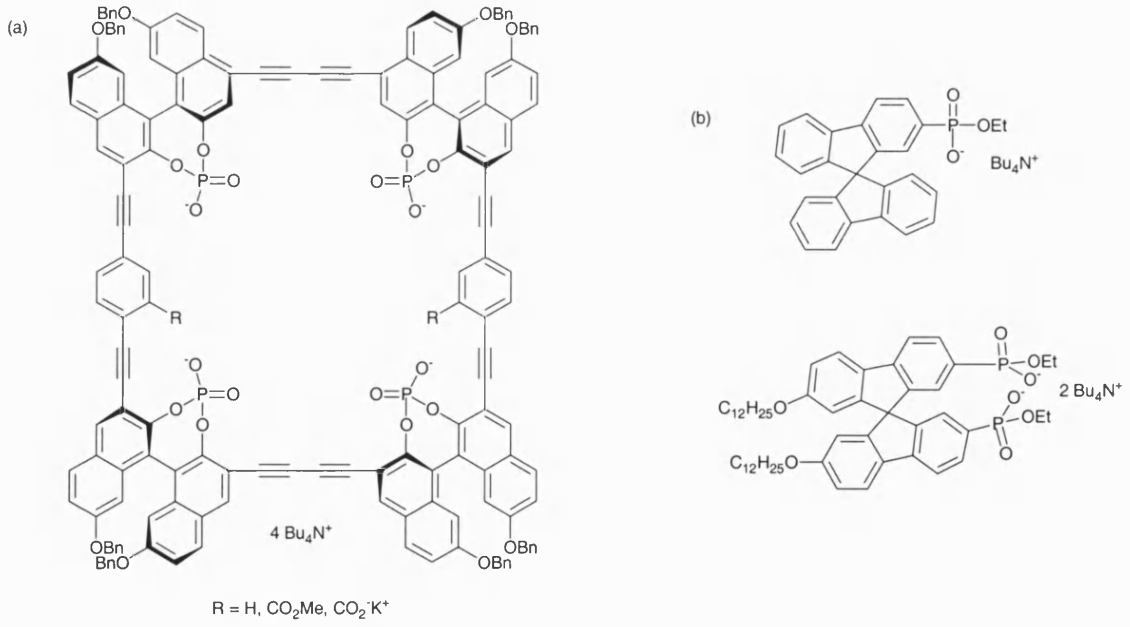

Figure 4: Phosphate-based receptors for carbohydrates: (a) Diederich's phosphate cyclophane receptor;[17] (b) Hamilton's spirobifluorene phosphonate receptors[18]

The major drawback of systems that rely on hydrogen bonding for recognition is that they are less successful in aqueous environments where guests may be heavily solvated. This is unfortunate, since most guest molecules, especially saccharides, require detection in aqueous media. Indeed, there is still no designed, monomeric hydrogen bonding receptor that can compete effectively with bulk water for low concentrations of monosaccharide substrates.[12] So what other chemistry can be used to overcome this problem, with specific attention to saccharides? The covalent interaction between boronic acids and saccharides can be utilised to conquer the obstacle of undesired solvent-guest competition.

1.2.2 Boronic Acids as Receptors for Saccharide

1.2.2.1 Background

The first recorded synthesis of a boronic acid was made by Michaelis and Becker in 1882.[19] They formed phenylboronic acid by reacting water with phenylboranodichloride, which they prepared from boron trichloride and diphenylmercury.[20] In 1931, Seaman and Johnson detailed the synthesis of phenylboronic acid derivatives from phenylmagnesium bromide and trimethylborate.[21] They also investigated the action of phenylboronic acid on bacteria. By the mid-1950's a number of review articles had appeared detailing the synthesis of numerous boronic acids.[22, 23] It was around this time that the binding properties of boronic acids were first investigated. Kuivila[24] and Solms[25] both observed that phenylboronic acid solubilised various polyols, including saccharides, and the formation of a cyclic boronate ester was postulated.[24] This agreed with the known ability of anionic borate to complex with compounds containing polyhydroxyl functionality.[26]

In a seminal paper in 1959, Lorand and Edwards were the first to investigate the binding affinity of phenylboronic acid for diols in a quantitative manner.[27] The work was performed in an attempt to clarify the structure of the phenylborate anion. A variety of polyols were added to a solution of phenylboronic acid at such a pH (8.8) that it existed in equal quantities of its neutral and anionic forms, i.e. its pK_a. It was found that the pH of the solution decreased as a range of polyols was added. Using the method of pH depression, they were able to calculate stability constants for the phenylboronic acid-polyol complexes. Table 1 shows a selection of their results.

Polyol	***K* / dm^3 mol^{-1}**
1,3-propanediol	0.88
Ethylene glycol	2.76
D-glucose	110
D-mannose	172
D-galactose	276
D-fructose	4370
Catechol	17500

Table 1: Some selected stability constants (*K*) for phenylboronic acid-polyol complexes[27]

The conclusion from their study was that phenylboronate anion has a tetrahedral, rather than a trigonal, geometry as shown in Figure 5.

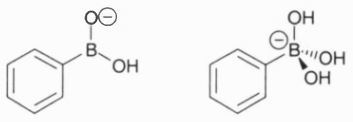

Figure 5: Proposed trigonal and tetrahedral forms of the anion of phenylboronic acid

Although the nature of the anionic structure has been known since 1959, there is still argument over the structure of the boronic acid-saccharide complexes formed in solution. The number of different conformational structures that saccharides can form in solution complicates the situation. Saccharides are polyhydroxyl aldehydes (aldoses) or polyhydroxyl ketones (ketoses) that constitute families of closely related stereoisomers. They exist as cyclic hemiacetals or hemiketals, either as six-membered pyranoses or five-membered furanoses. Furthermore, the newly built asymmetric centres at C-1 can take either α- or β-configuration, giving rise to two anomers for both pyranoses and furanoses (Figure 6). D-glucose is present as 38.8% α-D-glucopyranose, 60.9% β-D-glucopyranose, 0.14% α-D-glucofuranose and 0.15% β-D-glucofuranose, measured in D_2O at 27 °C.[28]

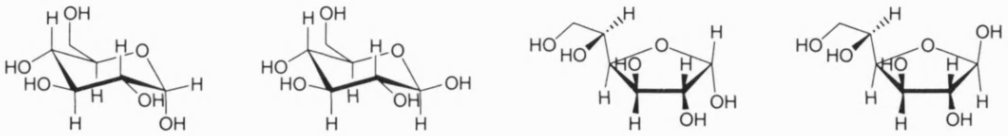

Figure 6: Cyclic hemiacetal structures of D-glucose: (a) α-D-glucopyranose; (b) β-D-glucopyranose; (c) α-D-glucofuranose; (d) β-D-glucofuranose

Shinkai *et al* have proposed that both 2,2'-dimethoxydiphenylmethane-5,5'-diboronic acid[29-31] (Figure 7a) and an anthracene-derived diboronic acid[32] (Figure 7b) bind D-glucose as 1:1 complexes, where binding occurs through the 1,2- and 4,6-hydroxyl groups of the α-D-glucopyranose conformer. Norrild and Eggert have since re-investigated the binding characteristics of the two molecules.[33-35] They studied the ^1H and ^{13}C NMR spectra and concluded that both diboronic acids bind D-glucose as the 1,2:5,6-α-D-glucofuranose conformer.

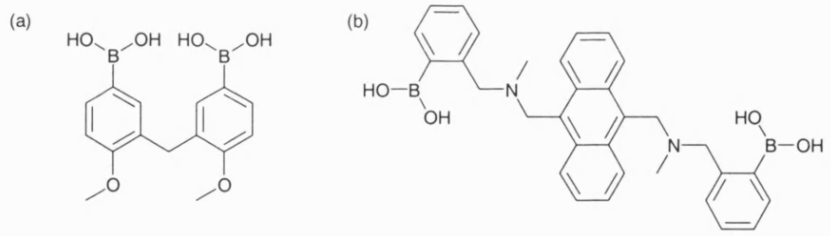

Figure 7: Diboronic acid receptors for D-glucose: (a) 2,2'-dimethoxydiphenylmethane-5,5'-diboronic acid;[29-31] (b) anthracene-derived diboronic acid[32]

What is probable is that the most stable solution boronic acid-saccharide complexes depend on a number of experimental factors, not least the concentration of species being studied and the solvent mixture. It is, therefore, possible that both parties are correct in their conclusions under their own experimental conditions. The issue of binding conformations, with respect to boronic acid sensor design, is actually, for the most part, irrelevant. All that is required for qualitative applications of a sensor is the accurate knowledge of the binding stoichiometry between the boronic acid and saccharide. As seen above, the binding stoichiometry of the complex is the same for both of the diboronic acids, whether the glucose is bound in its pyranose or furanose form. More recently, computer-aided design by Drueckhammer[36] has led to the development of a diboronic acid receptor attached to a polycyclic framework. Fluorescence and NMR studies have shown that the receptor is selective for D-glucose and binds it in its pyranose form.

Whatever the exact bound conformer of monosaccharides with boronic acid, it is now well established that boronic acids readily and reversibly form cyclic esters with diols in aqueous basic media. The most common interaction is with 1,2- and 1,3-diols to form five or six-membered rings respectively via two covalent bonds (Scheme 1). Saccharides contain a linked array of hydroxyl groups that are ideal for binding to boronic acids. As described earlier, Lorand and Edwards determined the selectivity and

first stability trends of various polyols and saccharides towards phenylboronic acid.[27] From Table 1, it can be seen that there is an increase in complex stability from 1,3-propanediol to D-fructose, i.e. from the simple acyclic diols to the rigid, vicinal *cis*-diols of saccharides. The planar aromatic catechol has the largest stability constant. This observed selectivity order has subsequently been shown to be common to all monoboronic acids, not just to phenylboronic acid.[1]

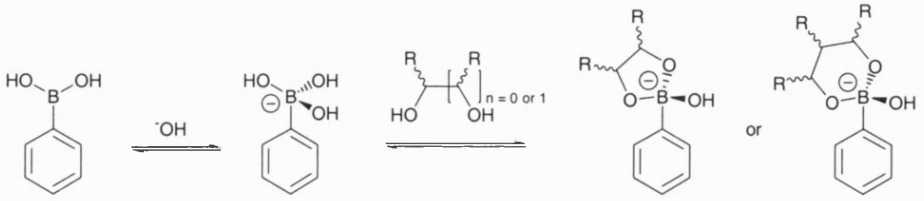

Scheme 1: Formation of 5- and 6-membered ring cyclic boronate esters

The suitability of the boronic acid functionality as a receptor for saccharides has been established by using a number of different techniques in a variety of environments. The following section will describe a selection of these applications, including fluorescence sensors, porphyrin-based receptors, saccharide transporters, protecting groups for diols, and usage in metal co-ordination complexes.

1.2.2.2 Applications of Boronic Acids

Photoinduced electron transfer (PET) has been widely used as the preferred tool in fluorescent sensor design for atomic and molecular species.[37] It is, therefore, no surprise to learn that numerous PET systems for saccharides have been developed. The first fluorescence PET sensors for saccharides were based on relatively simple fluorophore boronic acids, such as 2-anthrylboronic acid and 2-naphthylboronic acid.[38-40] However, fluorescence changes with these molecules are small and facile boronic acid-saccharide complexation only occurs at high pH.

To overcome these disadvantages 'off-on' fluorescent sensors were developed, containing a boronic acid group and a neighbouring amine group. The amine plays two roles. The first is to lower the pH at which boronic acids can bind to saccharide from high pH to near neutrality. The second is to control the fluorescence intensity. When there is no saccharide present, the lone pair of electrons on the amine nitrogen is free to quench the fluorescence of the system through photoinduced electron transfer. The fluorescent sensor is 'off'. When saccharide is added, the boron-nitrogen interaction between the nitrogen lone pair of electrons and the boronic acid boron centre is strengthened and the lone electron pair is now unavailable to quench the fluorescence. Hence strong fluorescence is observed and the sensor is 'on'.

James *et al* prepared the first fluorescent PET sensor for saccharides (Figure 8a).[41] The simple monoboronic acid shows the D-fructose selectivity that is inherent to all monoboronic acids.[27] This system was improved by the addition of a second boronic acid group (Figure 7b), leading to D-glucose selectivity.[32] Since this discovery, several diboronic systems have been synthesised showing selectivity for a variety of saccharides,[2] including a two-dimensional PET sensor (Figure 8b).[42] Boronic acid PET sensors have also been used in combination with other binding sites. Cooper and James have developed a D-glucosamine selective sensor (Figure 8c) based on a boronic acid and aza crown ether.[43, 44] The glucosamine hydroxyl groups bind to the boronic acid, while the sensor's crown ether interacts with the glucosamine ammonium group. A few non-PET saccharide receptors have also been reported. Sandanayake *et al*[45] and James and co-workers[46] have both prepared Internal Charge Transfer (ICT) chromophores. In these cases, the nitrogen is directly connected to the chromophore and can affect both the fluorescence intensity and the wavelength. Sandanayake's amino coumarin based

system shows only small shifts in intensity and wavelength upon adding saccharide, compared to the large shifts observed in the James sensor (Figure 8d).

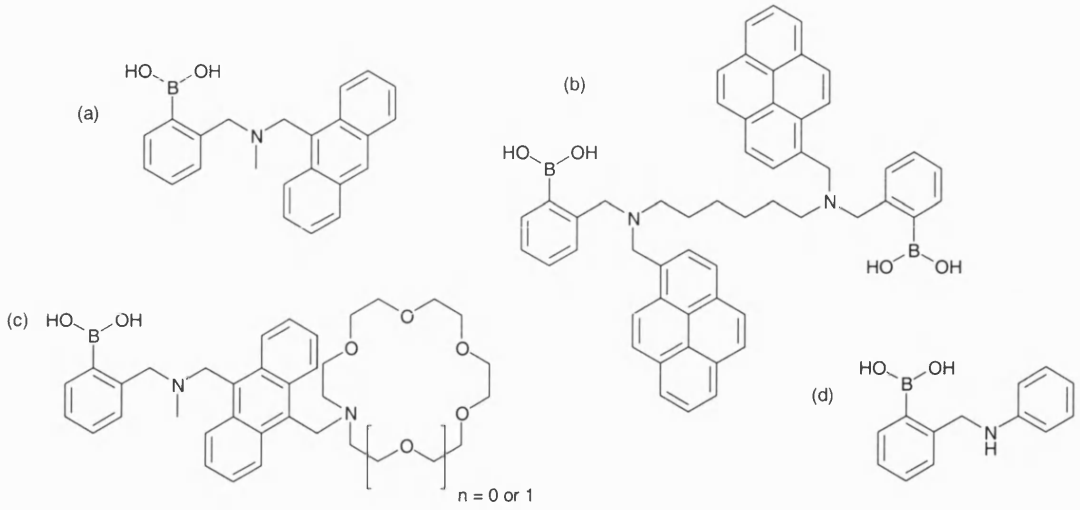

Figure 8: Fluorescence saccharide sensors: (a) the first fluorescent PET sensor for saccharides;[41] (b) two-dimensional PET sensor;[42] (c) D-glucosamine PET sensor;[43, 44] (d) fluorescent ICT saccharide sensor[46]

Porphyrin assemblies have been revealed to be attractive building blocks for saccharide receptors. Most have been based on the structure shown in Figure 9, although the metal centre and the number and ring position of the boronic acid groups have varied. Imada's monoboronic acid derivative has shown glucose-6-phosphate selectivity.[47, 48] It is thought that binding by the glucose to the boronic acid is complemented by the interaction of the phosphate with the zinc metal centre. Takeuchi *et al* have used the iron μ-oxodimer of the porphyrin structure in Figure 9 to form a tweezers-like molecule that shows strong binding with D-glucose and D-galactose.[49, 50] Arimori *et al* have also used the cationic form of this molecule to form 1:1 dimers with cationic porpyrins.[51] The dimers bind saccharides with glucose and xylose selectivity.

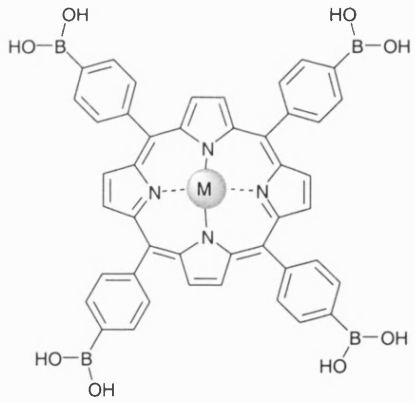

Figure 9: A boronic acid appended porphyrin

The use of metal centres in boronic acid-saccharide recognition has not been limited to porphyrin assemblies. A number of metal co-ordinated saccharide receptors have been reported.[2] Mizuno *et al* have used chiral salen cobalt(II) complexes for the purpose of saccharide detection.[52, 53] Saccharide complexation was monitored by spectroscopic changes in the metal complexes. The complex in Figure 10a showed an interesting two-fold selectivity increase for L-allose over D-allose. Smith and Deetz have investigated a ruthenium(II) complex (Figure 10b) as a heteroditopic receptor.[54] Binding of saccharide and phosphate was shown to have positive cooperativity, with phosphorylated saccharides displaying enhanced binding.

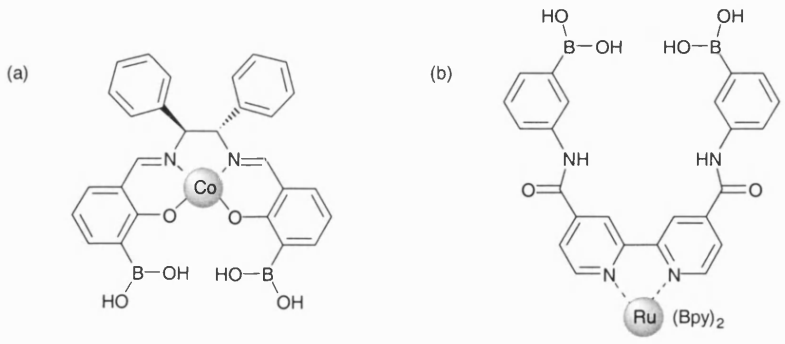

Figure 10: Metal co-ordinated saccharide receptors: (a) chiral salen cobalt(II) complex;[52, 53] (b) heteroditopic receptor for phosphate and saccharides based on a ruthenium(II) complex[54]

Boronic acids have been used in a number of molecular imprinting techniques, including polyion complexes that can create a memory for adenosine monophosphate (AMP).[55, 56] The boronic acid binds to the ribose *cis*-diols in AMP. After removal of AMP, a 'cleft' is created which has memory for the AMP template. Shinkai has used saccharides as template molecules to regio- and chiroselectively introduce boronic acid groups into [60]fullerene.[57, 58]

Boronic acids can promote the transport of a sugar out of an alkaline aqueous departure phase, through a lipophilic membrane, and into a slightly acidic aqueous receiving phase. Smith and co-workers have led the way in this field. They have investigated the selective transport of D-fructose through supported liquid membranes using both mono- and diboronic acids (Figure 11a).[59, 60] They have also facilitated catecholamine transport using boronic acids in combination with crown ethers (Figure 11b).[61] Duggan *et al* have also reported high fructose selective transport promoted by boronic acids based on a pentaerythritol core.[62] They have also reviewed the pioneering work of Ferrier[63] during the 1960's and 1970's in the use of boronic acids as protecting groups for diols. Phenylboronic acid has been shown to act as a labile protective agent for open-chain 1,2,3-triols, allowing the selective terminal derivatisation of D-mannitol.[64]

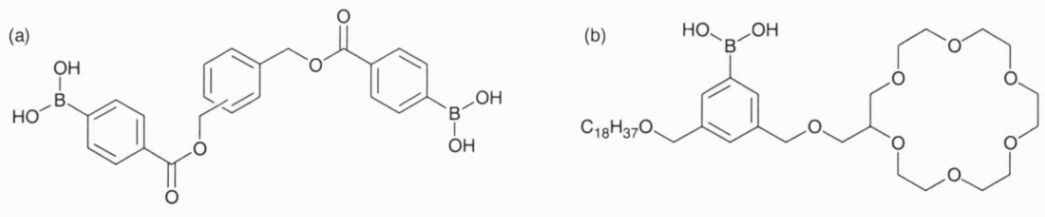

Figure 11: Boronic acid-based saccharide transporters: (a) D-fructose selective transporters;[59] (b) catecholamine transporter[61]

1.2.2.3 Boronic Acid Based Colorimetric Sensors

A fairly recent development has been the study of the effect of saccharides on the colour of dyes containing boronic acid functionality. Snyder *et al* synthesised the first boronic acid azo dyes over fifty years ago.[65, 66] It was shown that boronic acid functionality was compatible with diazo coupling reaction conditions.[65] Soon after, boronic acid azo dyes were used for investigations into the treatment of cancer and brain tumours by a technique called boron neutron capture therapy (BNCT).[66, 67] However, it has only been in the last decade that related dyes and their interaction with saccharides have been studied.

Russell has synthesised a boronic acid azo dye from *m*-aminophenylboronic acid that has been found to be sensitive to a selection of saccharides.[68] The usefulness of the dye as a glucose-monitoring agent in fermentation processes was proven by tests in beef-broth solution (used in the growth of bacteria) containing various proteins, lipids and salts. Nagasaki *et al* observed that chromophores containing boronic acid moieties (Figure 12a and b), which aggregate in water, changed colour and de-aggregated upon complexation with saccharide.[69] This was rationalised by the boronic acid-saccharide complexation increasing the hydrophilicity of the bound species. Shinmori *et al* have shown that a boronic acid appended spirobenzopyran (Figure 12c) undergoes changes in its absorption spectra upon addition of diols and sugars.[70] Added saccharide changes the merocyanine to spiropyran equilibrium position and hence the colour of the system. Takeuchi *et al* have prepared a boronic acid dye (Figure 12d) that undergoes an absorption spectral change on addition of nucleosides.[71] The boronic acid can bind with the ribose hydroxyl groups and the dimethylaminophenylazo moiety can stack with the adenine of the nucleoside.

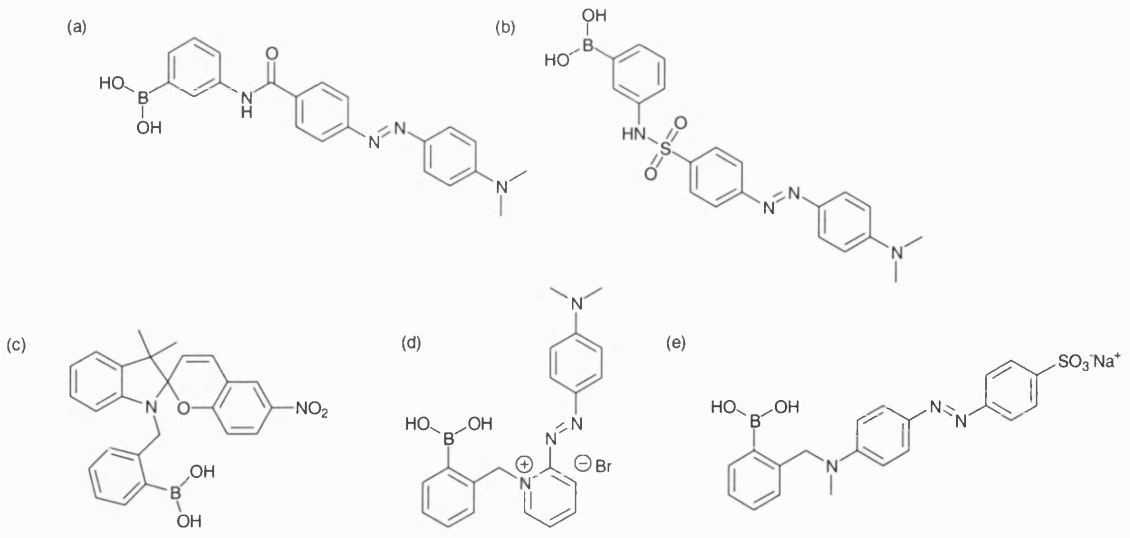

Figure 12: Colorimetric saccharide receptors from the Shinkai group

In 1994 Sandanayake and Shinkai reported 'the first known synthetic molecular colour sensor for saccharide utilising the boronic acid-amine interaction'.[72] This designed molecular internal charge transfer (ICT) sensor (Figure 12e) is based on the intramolecular interaction between the tertiary amine and the boronic acid group. The electron-rich amine creates a basic environment around the electron-deficient boron centre. This has the effect of inducing the boronic acid-saccharide interaction and reducing the working pH of the sensor. The electronic change associated with the decrease in the pK_a of the boronic acid moiety on saccharide complexation is transmitted to the neighbouring amine. This creates a spectral change in the connected ICT chromophore, which can be detected spectrophotometrically. The pK_a value associated with the boron-nitrogen interaction shifted on saccharide addition. The largest shift was seen for D-fructose (ΔpK_a = 3.31) and the smallest for ethylene glycol (ΔpK_a = 0.22), with D-glucose somewhere in between (ΔpK_a = 1.47), which is in agreement with Lorand and Edwards' findings. As seen earlier, this boron-nitrogen interaction has also been elegantly used as the foundation for certain photoinduced electron transfer (PET) sensors.

More recently, Shinkai's group have synthesised a diboronic acid saccharide receptor bearing a photoresponsive azobenzene group (Figure 13a) suitable for use as a light-gated saccharide sensor.[73] When the azobenzene unit is switched from the more stable *trans*-conformation to the thermodynamically unfavourable *cis*-isomer, it shows high D-glucose and D-allose selectivity. The formation of cyclic 1:1 complexes between saccharide and the dye in its *cis*-geometry explains the selectivity order. Koumoto and Shinkai have also demonstrated that azobenzene derivatives bearing one or two aminomethylphenylboronic acid groups (Figure 13c and d) can be used for practical colorimetric saccharide sensing in 'neutral' aqueous media.[74] The preparation of an electron-rich dye-conjugated nitrogen that strengthens the boron-nitrogen interaction is said to be behind the enhancement of the dye system's response to saccharide, compared to previous systems.

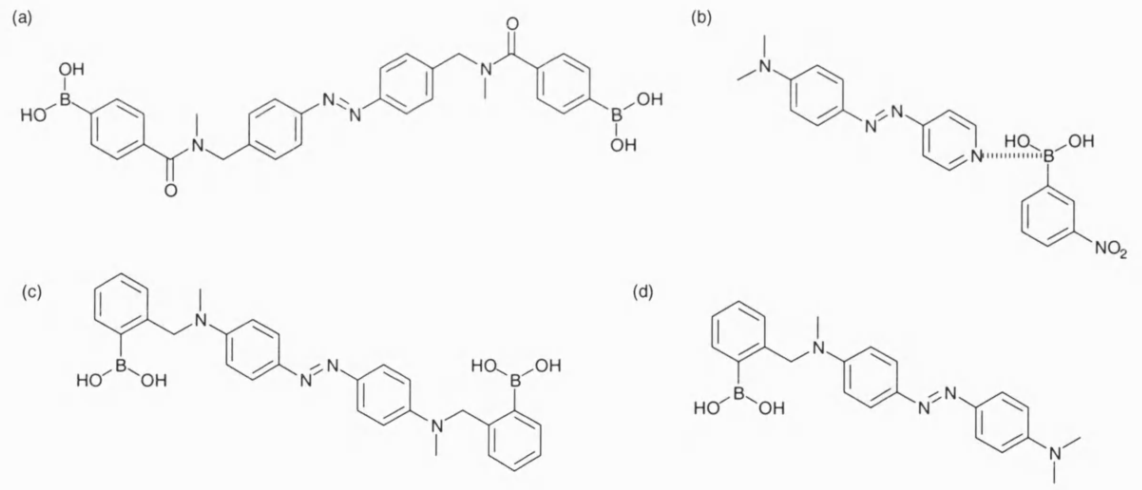

Figure 13: Further colorimetric saccharide receptors from the Shinkai group

Shinkai has applied the boronic acid-amine interaction to the molecular design of a visualized intermolecular sensing system for saccharides.[75] 3-nitrophenylboronic acid interacts with the pyridine nitrogen of 4-(4-dimethylaminophenylazo)-pyridine (Figure 13b) in methanol and changes its colour from yellow to orange. Added saccharides form

complexes with the boronic acid and enhance the acidity of the boronic acid group. As a result, the boron-nitrogen interaction becomes stronger and the intensified intramolecular charge-transfer band changes the solution colour to red. The largest effect is experienced with D-fructose.

Strongin has prepared a tetraboronic acid resorcinarene system for the visual sensing of saccharides (Figure 14a).[76] Characteristic colour changes were observed for specific carbohydrates, glucose phosphates and amino sugars. However, for a colour change to be observed the saccharide and receptor must be heated to 90 °C in DMSO. This reaction is irreversible so cannot be applied as a sensor system. Further work with another resorcinol derivative[77] (Figure 14b) has shown that oxygen consistently promotes the colour changes and that the resorcinol hydroxyl groups play a key role in the colour formation of the receptor solutions.

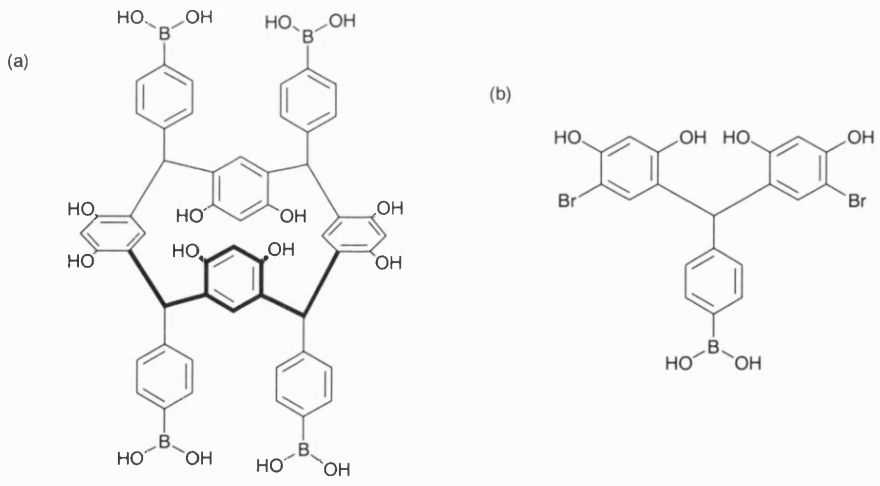

Figure 14: Strongin's resorcinol-derived visual saccharide sensors: (a) tetra-arylboronic acid resorcinarene;[76] (b) a tri-aryl receptor[77]

Further applications of boronic acid dye molecules can be found in the preparation of biochemical assays and in inkjet printing. Frantzen *et al* have developed some water-soluble 'dye-phenylboronic acid conjugates', possessing strong absorption of visible

light.[78] These have been used as reagents in the determination of glycohaemoglobin, which is important in the monitoring of diabetes. A Hewlett-Packard patent describes the synthesis of a number of phenolic-based boronic acid azo dyes.[79] These water-soluble species show good water-fast printed images on paper with improved colour strengths compared to standard sulphonated dyes. Binding of the dyes to the paper occurs via boronic acid-saccharide interactions with the starch and cellulose found in all paper.

Anslyn has recently reported two very interesting systems based on boronic acid receptors. The Anslyn approach involves competitive spectrophotometric assays. The first system is a receptor for glucose-6-phosphate (Figure 15a).[80] The binding of glucose-6-phosphate is measured through the competitive displacement of 5-carboxyfluorescein from the receptor, which provides a spectrophotometric change in the indicator.

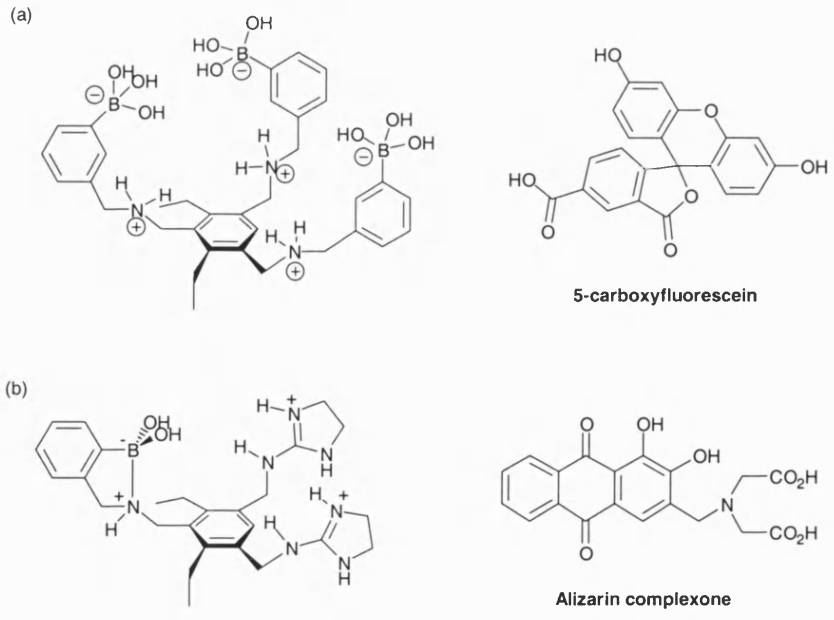

Figure 15: Anslyn's competitive spectrophotometric assays: (a) receptor for glucose-6-phosphate;[80] (b) receptor for tartrate and malate[81]

The second system is a receptor for tartrate and malate (Figure 15b) and works in a similar way to the previous receptor.[81] The binding of the tartrate or malate anions can be detected in this instance through the competitive displacement of alizarin complexone.

Hartley and James have developed an attractive catalytic system based on boronic acid imines (Figure 16).[82] With this system, enhanced rates of hydrolysis of the imine bond are observed when saccharide binds to the boronic acid centre. The system is not strictly a colour receptor, however the system could be used to measure saccharide concentrations by monitoring the rate of disappearance of the imine absorbance signal at 320 nm.

Figure 16: Boronic acid imines[82]

The main drawback in the development of coloured boronic acid-saccharide sensors, so far, has been the relatively small shifts achieved in the absorption bands of the chromophores upon saccharide binding. The work outlined above has provided excellent foundations for the study of boronic acid appended chromophores. With further research, it is hoped that a boronic acid system can be developed that shows large spectral shifts upon saccharide interaction.

1.3 Sensor Systems for Fluoride

1.3.1 Context of Research

Among the range of biologically important anions, fluoride is of particular interest due to its established role in the prevention of dental caries. The fluoride anion has also been explored as a treatment for osteoporosis. Recently there has been concern about overexposure to fluoride, which can cause fluorosis, a type of fluoride toxicity that can manifest itself by increasing bone density. The fluoridation of water supplies and the monitoring of groundwater contamination from certain industrial plants are also important areas for the accurate determination of fluoride concentrations. This diversity of function makes the problem of fluoride anion detection one of considerable interest.

In 1966, it was discovered that a slice of a single crystal of lanthanum fluoride (LaF_3) attached to the end of an electrode barrel could be used to sense the fluoride anion in aqueous solution.[83] This technology continues to be used today for the majority of fluoride determinations. Although LaF_3 electrodes are sensitive and selective, there has recently been increased activity to find alternative methods of fluoride anion analysis, including the use of specific chemosensors.[84] Systems that can recognise fluoride in solution and signal its presence via an easy to detect optical signature would be of considerable value.

The following two sections will describe firstly the use of synthetic receptors for the recognition of anions, focusing in particular on the fluoride anion and colorimetric systems, and secondly will illustrate the use of boronic acid-based fluoride sensors.

1.3.2 Synthetic Receptors for Anion Recognition

Supramolecular cation coordination chemistry has progressed rapidly since the advent of macrocyclic ligands such as the crown ethers, cryptands and the large range of other multidentate hosts.[2] Although the first synthetic organic ligands for anions were reported at the same time as Pedersen's discovery of crown ethers,[84] the growth in anion coordination systems is a more recent development. This is probably as a consequence of the large ionic radii of anions, high free energy of solvation and the wide range of topologies encountered, resulting in difficulties designing receptors with appropriately situated Lewis-acidic or acceptor sites. Anions are of key importance across many scientific fields making their selective binding and sensing a critical research target. Therefore, in recent years, increasing attention has focused upon supramolecular anion complexation.[84-86] Of particular interest are 'colorimetric anion sensors', species that allow the so-called 'naked-eye' detection of anions without the resort to any spectroscopic instrumentation. However, few such systems exist at present.

The use of alizarin complexone (Figure 15b) for the qualitative and quantitative analysis of fluoride was first proposed by Belcher, Leonard and West in the late 1950's.[87-91] They found that fluoride produces a coloured complex with the cerium(III) chelate of alizarin complexone. In an acetate buffer the red colour of the cerium(III)-alizarin complexone changes to the lilac-blue colour of the double complex upon addition of fluoride. Other common anions were shown not to interfere with the method. A few years later, Yamamura *et al* found that that use of a 20% acetonitrile or acetone medium, rather than water alone, increases both the sensitivity of the reaction and the stability of the complexes.[92] This method for the determination of fluoride continues to be used today.

Pyrrolic NH groups can be combined with electrostatic interactions to produce receptors that have an extremely high affinity for anions. Sessler *et al* demonstrated that sapphyrins (pentapyrrolic expanded porphyrins) are capable of coordinating anions. The core of a sapphyrin macrocycle (Figure 17a) can be doubly protonated to form a receptor with a positive charge and an array of five NH hydrogen-bonding groups. Solution-phase experiments indicated that fluoride ions bind over 10^3 times more strongly to diprotonated sapphyrin than either chloride or bromide ions.[93, 94] X-ray studies revealed that the fluoride ion is held in the plane of the sapphyrin by five NH hydrogen bonds.[95]

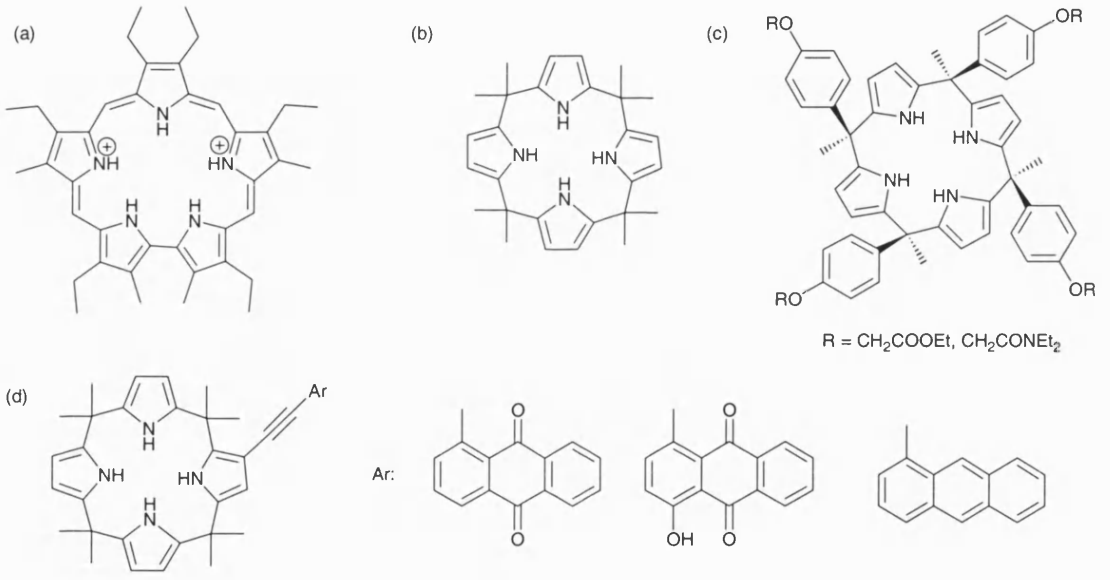

Figure 17: Pyrrole-based fluoride receptors: (a) sapphyrin macrocycle;[93, 94] (b) octamethylcalix[4]pyrrole;[96] (c) 'super-extended cavity' calix[4]pyrrole;[97] (d) colorimetric anion sensor based on calix[4]pyrrole[98]

Sessler has also reported that calix[4]pyrroles (*meso*-octaalkylporphyrinogens) coordinate to anions.[99] *meso*-octamethylcalix[4]pyrrole (Figure 17b) was shown to form the strongest complex with fluoride in CD_2Cl_2, with weaker binding to chloride and dihydrogen phosphate ions. This calixpyrrole has also been used in combination with the 4-nitrophenolate anion to make a colorimetric anion sensor.[96] The intense yellow

colour of the 4-nitrophenolate anion in dichloromethane or acetonitrile dissipates upon addition of calix[4]pyrrole as a consequence of the formation of a complex between the two species. The addition of anions, including fluoride, displaces the phenolate ion and regenerates the yellow colour. The intensity of the colour is dependent upon the binding affinity of the added anion to the calixpyrrole. Gale has extended the calix[4]pyrrole cavity to incorporate ester and amide functionality (Figure 17c).[97] Both derivatives show exclusive binding to fluoride in deuterated DMSO solution. Sessler has recently prepared anthraquinone-functionalised systems that bear an appended chromophore directly linked to the calix[4]pyrrole skeleton through a conjugated alkyne bond (Figure 17d).[98] Binding of fluoride to the calixpyrroles produced visible colour changes. To a lesser extent, the addition of chloride and dihydrogenphosphate ions also caused spectral changes. Adjustment of the anthraquinone unit to a hydroxy-substituted system allows a degree of 'colour tuning', as this modifies the absorption wavelength of the chromophore.

Reinhoudt and co-workers have developed a new class of anion selective receptors based upon the neutral uranylsalophene building block as a Lewis acidic binding site (Figure 18a).[100] Additional hydrogen bond accepting or donating moieties near the anion binding site offer the possibility of varying the binding selectivity. Salophenes with amido substituents result in high fluoride selectivity, even in the presence of 0.1 M chloride. Sessler *et al* have reported that 2,3-dipyrrol-2'-ylquinoxalines, such as that in Figure 18b, allow the detection of fluoride ions in DMSO and dichloromethane under both visual and fluorescence emission conditions.[101] A colour change from yellow to purple is only observed upon addition of fluoride. Other anions have no effect on the colour. The colour change is reversed upon addition of water to the DMSO solution. This is presumably due to the water competing with the pyrrolic NH hydrogen bond

donating sites for fluoride. Sessler has also screened a number of 'off-the-shelf' molecular entities, including 4-nitroaniline, alizarin and 9(10*H*)-acridone, for use as colorimetric anion sensors.[98] All of the molecules studied showed colour changes with a variety of anions. However, anion specificity was lacking in the majority of cases. Bowman-James and co-workers synthesised an aza cryptand (Figure 18c) and investigated its selective binding to fluoride by ^{19}F NMR and crystallographic techniques.[102] They found that the cryptand can encapsulate anions over a significant pH range.

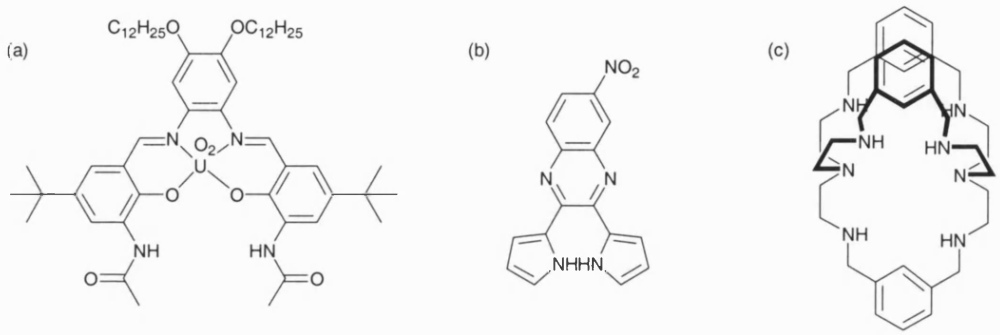

Figure 18: Fluoride receptors: (a) an uranylsalophene derivative;[100] (b) a dipyrrolylquinoxaline;[101] (c) an aza cryptand[102]

Anslyn's research group have developed a number of anion receptors using a displacement-assay approach. Nitrate ions have been detected using an ensemble of a trigonal amide box (Figure 19a) and colorimetric dyes, such as Methyl Red, as indicators.[103] Adding nitrate perturbs the equilibria between the dye and receptor, resulting in the formation of a receptor-nitrate complex. Displacement of the dye causes a large absorbance change in the chromophore. The citrate anion has been detected in a similar manner using a pre-organised guanidinium-based receptor and a carboxyfluorescein fluorescent probe.[104, 105] In an extension of this work, Anslyn has designed a metal containing fluorescent sensor for the quantification of citrate in beverages. The sensor consists of Cu(II) bound by a phenanthroline ligand which is

attached to a bis(aminoimidazolium) receptor (Figure 19b).[106] Binding of the metal creates an additional binding site for citrate and also quenches a photo-excited state of the phenanthroline fluorophore. Addition of citrate to the system results in an increase in the fluorescence.

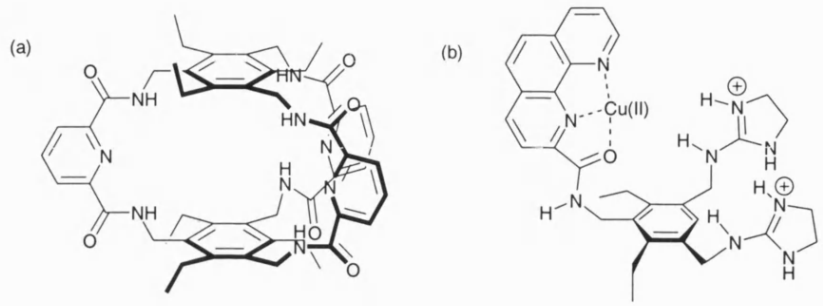

Figure 19: Selected anion chemosensors: (a) nitrate receptor;[103] (b) metal-triggered fluorescent sensor for citrate[106]

The main disadvantage of the systems described above is that the majority of them have only been studied in organic solvents. For such systems to be really useful, the detection of anions needs to be performed in aqueous conditions. Some of the systems are also based on a competition-assay approach, relying on detection methods containing two components. Boronic acids, which can recognise fluoride in aqueous environments in a unimolecular fashion, can offer a distinct advantage in this respect.

1.3.3 Boronic Acid Receptors for Fluoride

The recognition of fluoride by boron-containing systems is based on the Lewis acid-base interaction between the boron and anions. When boron binds to certain anions, including fluoride, the hybridisation changes from sp^2 to sp^3. Katz was the first to study boron-centred fluoride receptors. Using a 1,8-diborylnaphthalene design motif (Figure 20a), Katz showed that it was possible to trap fluoride, as well as chloride and hydride anions, between the two boron atoms.[107-109] Crystal structures of the hydride and chloride

complexes have shown that the ion is bound to both boron atoms with short strong bonds. It is thought that fluoride binds in the same manner. Reetz *et al* have synthesised a crown ether appended phenylboronate (Figure 20b) that is capable of coordinating to potassium and fluoride ions simultaneously.[110, 111] The potassium ion is bound by the crown ether moiety, whilst the fluoride ion is held by a combination of orbital overlap with the Lewis-acidic boron atom and electrostatic interactions with the potassium ion.

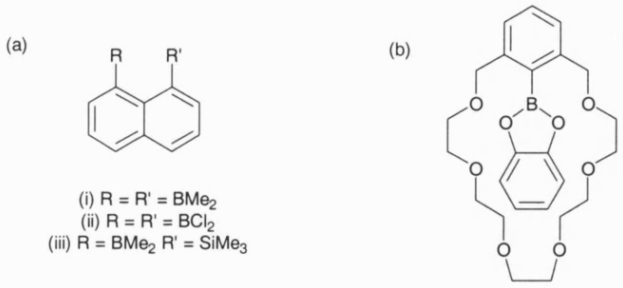

Figure 20: Boron-based Lewis acidic receptors for anions: (a) 1,8-diborylnaphthalene unit;[107-109] (b) crown ether appended phenylboronate[110, 111]

Shinkai and co-workers have used ferroceneboronic acid (Figure 21a) as a fluoride receptor. The original work measured the binding electrochemically, as the boronic acid binding site is intramolecularly connected to the redox-active ferrocene moiety.[112] The fluoride binding event occurring at the boronic acid centre can be read out through the shift in the redox potential of the ferrocene. Selectivity for fluoride has been established in the presence of other halides and common anions, such as sulphate and thiocyanate. Later work has shown that ferrocenylboronic acids (Figure 21a and b) can detect fluoride by a colour change when mixed with dyes that contain appropriate redox potentials.[113] As an aside, the chiral ferrocenylboronic acid (Figure 21b) has also been used electrochemically for the chiral discrimination of certain linear saccharides, including D-sorbitol.[114]

Cooper and James have developed fluorescent fluoride sensors from phenylboronic acid, 2-naphthylboronic acid and 2-[benzyl(methyl)aminomethyl]phenylboronic acid (Figure 21c). The latter sensor was shown to stabilise the mono-fluoride adduct by hydrogen bonding to the protonated amine,[115] whereas the simpler boronic acids formed tri-fluoride adducts. Yuchi *et al* have also investigated some arylboronic acids for fluoride recognition and confirmed the proposal of the tri-fluoride adduct for these molecules.[116] In further work, they have demonstrated that the introduction of an electron-withdrawing substituent or a protonated substituent that can potentially be involved in hydrogen bonding, enhances the binding of fluoride to the arylboronic acids.[117]

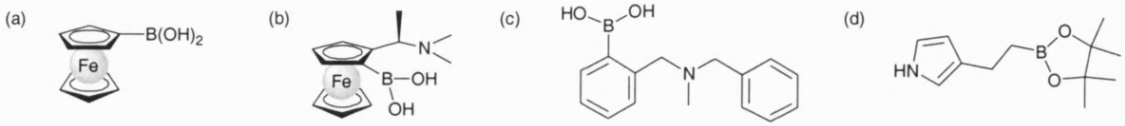

Figure 21: Fluoride receptors: (a) ferroceneboronic acid; (b) chiral ferrocenylboronic acid;[112] (c) fluorescent PET sensor;[115] (d) boronate substituted pyrrole[118]

Shiratori *et al* have used fluoride binding with boron to modulate the electron transfer pathways in zinc porphyrin systems. Fluoride coordination at a boronate bridge either suppresses intramolecular electron transfer[119] or switches the electron transfer path,[120] depending on the porphyrin assembly. Fabre and co-workers have produced some novel electropolymerisable boronate-functionalised polypyrrole (Figure 21d), polythiophene and polyaniline membranes that are selective for fluoride over other anionic guests.[118, 121] The electrochemical responses of the materials were changed upon binding of fluoride to the immobilised boron, with the strongest modifications observed for the polypyrrole derivative. They have also investigated the electrochemical behaviour of a boronic acid-substituted 2,2'-bipyridine iron(II) complex in the absence and presence of fluoride.[122]

The binding of the halide to the boron led to a shift in the Fe(II)/Fe(III) oxidation peak towards less positive potentials.

1.4 Summary of Introduction

- The detection of saccharides is of vital importance in many medicinal and industrial applications.
- A number of synthetic receptors for carbohydrates have been developed based on hydrogen bonding interactions. However, most struggle to compete with bulk water in competitive solvent systems.
- Boronic acids rapidly and reversibly form cyclic boronate esters with 1,2- and 1,3-diols in aqueous media.
- The cyclic boronate has been exploited in various applications, including the development of sensors for saccharides; protection of diols; and transport of nucleosides and nucleotides, as well as saccharides.
- Although a relatively large number of boronic acid fluorescent sensors for saccharides have been reported, there are few examples of colorimetric systems.
- The recognition of anions, including fluoride, has received much attention due to their essential roles in many biological and industrial processes.
- Colorimetric systems for the 'naked-eye' detection of the fluoride anion are known, but most only work in organic solvents.
- The Lewis acid-base interaction between the boron centre in boronic acids and fluoride has been used in a variety of sensor systems for the detection of fluoride under aqueous conditions.
- There are currently no reported molecular colour sensors for fluoride based on boronic acid technology.

2 Results & Discussion

"In the field of observation, chance favours only the prepared mind."

Louis Pasteur, 1822-1895

2.1 Aims and Objectives

The synthesis of a range of novel boronic acid appended chromophores was attempted in order to assess their potential as colour sensors for saccharides and the fluoride anion. Following successful preparation, the dyes' interaction with, firstly, saccharides, through binding to the boronic acid moiety, will be investigated using UV-VIS spectrophotometry. The same method will then be used to probe the binding properties of fluoride to the boron centre of the dyes.

Initial studies will focus on the widely used azo dye system.[123, 124] The electronic configuration of the azo chromophore will be subtly altered by varying the substituent group on the azo aromatic ring, and also by changing the size of the aromatic rings present in the molecule. Modification of the electronics of the boronic acid aromatic ring will also be examined. Different chromophores (e.g. the tricyanovinyl group) will then be looked at for their ease and compatibility of synthesis with the boronic acid group. An effort to introduce a second boronic acid binding site to a coloured system will be made, as diboronic acid fluorescent sensors have shown D-glucose selectivity.[41] A colour sensor for D-glucose could find significant applications in various fields, including the treatment of diabetes.

Finally, in a reversal of the above work, coloured systems for the detection of boronic acids will be explored. The diethanolamine group[125] and alizarin-based systems[126, 127] have both been proposed as suitable fluorescent receptors for boronic and boric acids. However, no colorimetric systems for boronic acids have been developed using these receptors. As such, both will be tested for their usefulness as colour sensors for boronic acids.

2.2 Synthesis of Boronic Acid Dye Molecules

2.2.1 Azo Dye Systems

Griess's discovery, in 1862, of the diazotisation reaction, was of fundamental importance to the dye industry.[124] He found that when a primary aromatic amine was treated with a nitrosating agent, such as nitrous acid, an unstable diazonium salt was formed. When he reacted this salt with a phenol or aromatic amine, a highly coloured azo compound was the resulting product. Azo dyes now form the largest group of all synthetically derived colorants.[124]

2.2.1.1 Boronic Acid Appended Azo Dyes

Scheme 2 shows the three-step synthetic route used to prepare a small 'library' of boronic acid azo dyes. The synthesis is novel and facile and requires little or, in most cases, no need for purification. Commercial 2-formylbenzeneboronic acid is reacted with *m*-toluidine to form the imine **1**.[82] This is then reduced to the amine **2** using a standard sodium borohydride reduction.[44] The final step is to couple with the diazonium salt of a series of anilinic molecules (e.g. 4-nitroaniline) under normal azo coupling conditions,[123] to yield the boronic acid azo dyes (**3-7**) as single isomers. The complete synthetic details and full characterisation of these compounds can be found in the Experimental section of this report.

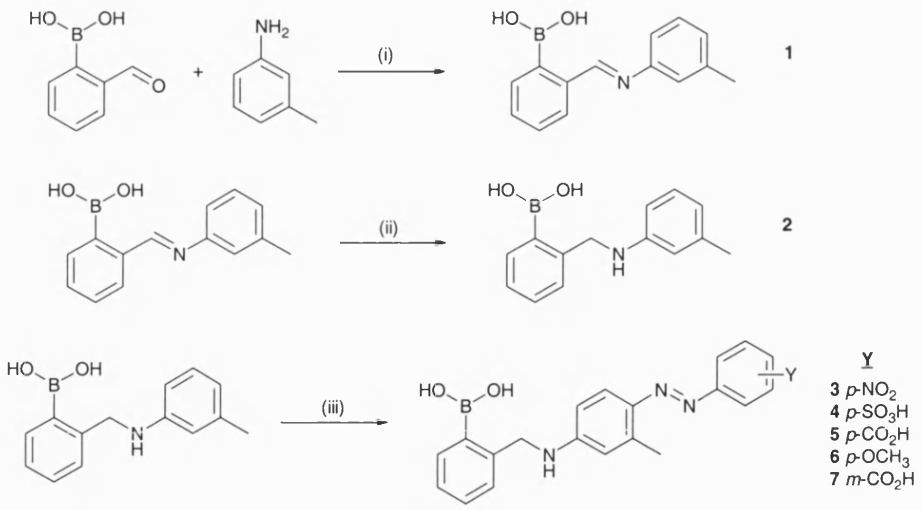

Scheme 2: Synthetic procedure for boronic acid appended azo dyes; (i) ethanol-benzene, reflux in Dean-Stark apparatus, 18 hr; (ii) $NaBH_4$, methanol, rt, 2 hr; (iii) $Y\text{-}C_6H_4N_2^+Cl^-$, pH 4, 0-5 °C, 2 hr.

The reaction of *m*-toluidine with 2-formylbenzeneboronic acid was performed in a refluxing ethanol-benzene solvent mixture, with azeotropic removal of the water produced by a Dean-Stark trap. This solvent mixture was used instead of toluene, the 'standard' Dean-Stark solvent, because the lower boiling point of the ethanol-benzene mix reduced the chance of product decomposition. In addition, the solubility of 2-formylbenzeneboronic acid in toluene is poor. The reaction works very well (isolated yield >90%) and shows 100% conversion to imine **1** by ^{1}H NMR. Consequently there is no need for any purification.

Imine **1** was reduced by sodium borohydride in methanol at room temperature. Amine **2** was obtained in good yield (81%) and excellent purity, after work-up by precipitation from water. ^{1}H NMR again showed total conversion to the amine. The characteristic imine singlet at around 9 ppm had completely disappeared, and a new singlet of double the intensity was apparent at 4.3 ppm, indicative of the reduced product's two benzyl protons.

The third and final step was to perform the azo coupling reaction. These aromatic electrophilic substitution reactions occur predominately *para* to the electron-donating anilinic nitrogen because of steric effects, but *ortho* substitution can also be observed.[123] However, it is known that by incorporating a methyl group *meta* to the anilinic nitrogen in the amine coupling agent, exclusive *para* coupling is observed.[124] Hence the inclusion of this design motif in the target dyes, in order to avoid potentially difficult separation of isomers. Azo coupling reactions were performed using the diazonium salts of 4-nitroaniline, sulphanilic acid (4-aminosulphonic acid), 4-aminobenzoic acid, *p*-anisidine (4-methoxyaniline) and 3-aminobenzoic acid, to yield the respective dyes **3**, **4**, **5**, **6** and **7**. For solubility reasons, the traditional water solvent employed in these coupling reactions was replaced by a mixed methanol-water solvent system.

The actual nitrosating species in the diazotisation reaction has been a subject of much debate, and varies according to the reaction conditions employed. Figure 22a shows some proposed nitrosating species.[123] The diazotisation process may be envisaged as occurring as in Figure 22b. At low acidities, it is thought that N_2O_3 is the effective agent.

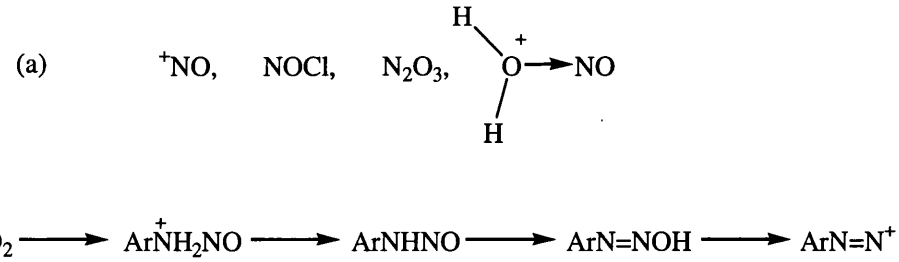

Figure 22: (a) Possible nitrosating species in diazotisation. (b) The diazotisation process.

The conditions employed in the preparation of dyes **3-7** involved forming nitrous acid *in situ* from sodium nitrite and concentrated hydrochloric acid, in the presence of the

amine. Excess nitrous acid was destroyed by adding sulphamic acid. This step is necessary to prevent diazotisation of the amine to which the diazonium salt is to be coupled.

Coupling can be viewed as an electrophilic substitution by a diazonium cation. As such, coupling occurs in positions at which there is increased electron density, including carbon atoms in aromatic systems. The diazonium cation is a relatively weak electrophile; therefore strong electron-donating groups are required to be present in the aromatic system of the coupling component for coupling to take place. These electron-donating groups are generally anilinic ($-NH_2$, -NHR, $-NR_2$) or phenolic (-OH) in nature. In the case of dyes **3-7**, a secondary anilinic amine (-NHR) is present. The couplings with the boronic acid amine **2** were carried out at approximately pH 4 in an acetate-buffered solution. This ensures that the reactive species is the necessary free, rather than protonated, amine molecule.

Dyes **3-7** precipitate from solution as the pH is raised to neutrality from low pH. Yields varied from below average to good, depending on the solubility of the dye in the water-methanol mixture. The only purification needed, in all instances, was the washing of the collected solids to remove residual acetic acid. Otherwise, the dyes precipitated with very high purity. This is fortunate, since boronic acids with neighbouring nitrogens are notoriously difficult to purify by conventional chromatographic techniques.[1] Other substituted anilines (including *m*-anisidine, aniline and 4-aminobenzonitrile) were diazotised and reacted with amine **2**. However, even though ^1H NMR identified the corresponding dye products, acceptable purification could not be achieved for further studies on them.

All of the dyes, and indeed all of the compounds described within the Results & Discussion section, have been fully analysed and characterised (see the Experimental section for full details). There are two points to note concerning the analysis. Firstly, elemental analysis of boronic acids has long been known to give poor correlations between calculated and found compositions.[21] This is usually attributed to the formation of highly stable boron nitride derivatives in the combustion process. Also, free boronic acids can readily and spontaneously form cyclic trimeric anhydrides, boroxines, at room temperature (Scheme 3).[1] Subsequently, this can lead to inaccuracies in the calculated composition values. Although some boron containing compounds did give a good match between calculated and found compositions, this was not always the case. This was not viewed as evidence of impurity, but due to the inherent problems of this technique in combination with boronic acids. For compounds where elemental analysis proved inconclusive, high-resolution mass spectrometry was performed instead.

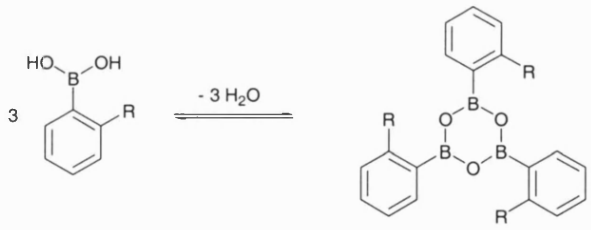

Scheme 3: Formation of boroxines from boronic acids

The second issue concerns the mass spectra of some boronic acids obtained using the technique of fast atom bombardment (FAB) mass spectrometry. FAB requires the use of a matrix, usually *m*-nitrobenzyl alcohol (NOBA), to mobilise the sample. Boronic acids readily bind to one or two hydroxyl groups of NOBA molecules to form adducts (Scheme 4) that are predominantly observed by FAB over the free boronic acid.

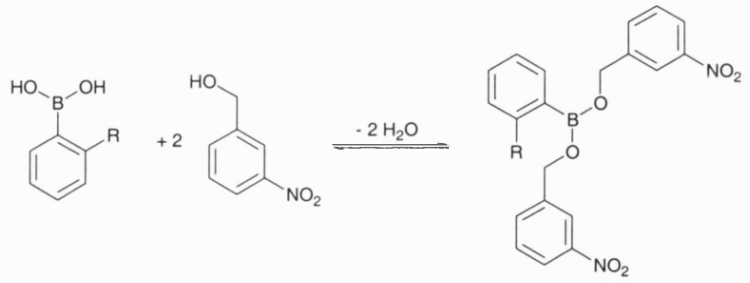

Scheme 4: *m*-nitrobenzyl alcohol adduct with boronic acid observed by FAB mass spectrometry

The novel route (Scheme 2) employed for the preparation of dyes **3-7** is synthetically simpler than previously reported procedures. For example, Shinkai's route[72] to an *N*-methylated azo dye derivative (Figure 12e) involved a moderately yielding lithiation reaction to make the boronic acid, followed by an azo coupling step that afforded two isomers requiring separation and purification. The method developed here involves a facile and mild reductive amination, followed by azo coupling that affords clean, single-isomeric products. There is no need for chromatography at any stage. The dyes' absorbance properties and interaction with saccharide and fluoride will be discussed later.

2.2.1.2 Model Azo Dye Systems

Two 'model' dyes were synthesised for comparison purposes with dyes **3-7**. Scheme 5 shows the synthesis of an *N*-methylated boronic acid azo dye, **10**. This dye is based upon Shinkai's similar *N*-methylated molecule (Figure 12e) and is prepared using a comparable synthetic route. Commercial *N*-methyl-*m*-toluidine was benzylated with 2-bromobenzyl bromide, by refluxing in acetonitrile using potassium carbonate as a base. The reaction proceeds quantitatively and efficiently to form the tertiary amine **8**. The aryl bromide in **8** was lithiated with *n*-butyllithium and reacted with trimethylborate at low temperature, to afford boronic acid **9**, after an acidic work-up. The yield for this step was below average (25%). However, the reaction was not optimised in any way,

the only criteria being the achievement of a satisfactory level of purity for the product. Standard coupling of **9** with the diazonium salt of 4-nitroaniline yielded the azo dye **10**.

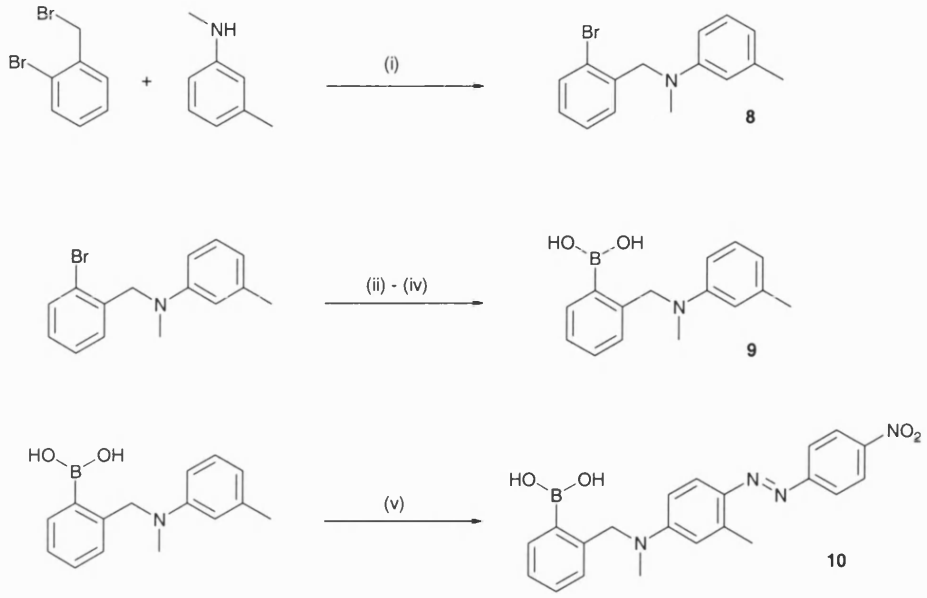

Scheme 5: Synthetic procedure for *N*-methylated boronic acid appended azo dye; (i) K_2CO_3, acetonitrile, reflux, 4 hr; (ii) *n*-BuLi, THF, -78 °C; (iii) $B(OCH_3)_3$, THF, -78 °C; (iv) H_3O^+; (v) $O_2N\text{-}C_6H_4N_2^+Cl^-$, pH 4, 0-5 °C, 2 hr.

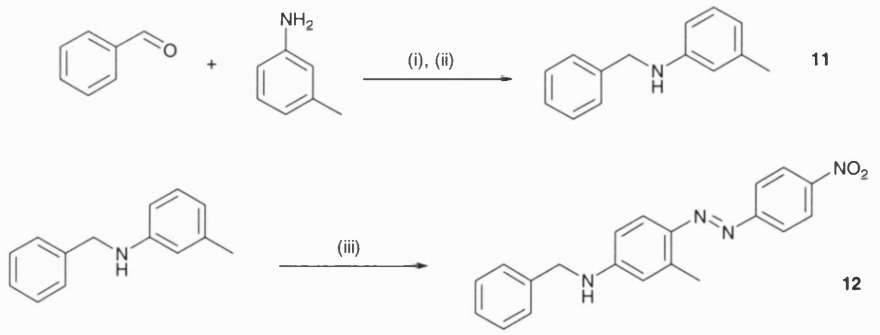

Scheme 6: Synthetic procedure for non-boronic acid azo dye; (i) ethanol-benzene, reflux in Dean-Stark apparatus, 18 hr; (ii) $NaBH_4$, methanol, rt, 2 hr; (iii) $O_2N\text{-}C_6H_4N_2^+Cl^-$, pH 4, 0-5 °C, 2 hr.

The second model, dye **12**, is a non-boronic acid analogue of dye **3**, as shown in Scheme 6. An identical synthesis to that used in Scheme 2 was repeated using benzaldehyde in place of 2-formylbenzeneboronic acid (Scheme 6). After reductive amination and azo coupling, analytically pure dye **12** was afforded after precipitation

from chloroform with hexane. The model dyes' absorbance properties and interaction with saccharide and fluoride will be discussed later.

2.2.1.3 Modification of the Azo Dye Aromatic Ring Size

The dyes synthesised to date exclusively contain benzene rings attached to the azo chromophore. Naphthalene derivatives have been used as coupling components in azo systems.[124] The larger aromatic ring size of naphthalene allows increased electronic conjugation. This results in a longer wavelength (lower energy) absorption by the azo chromophore. Molecules that absorb or are fluorescent at near infrared (NIR) wavelengths are desirable targets for the determination of analytes in biological systems, as this region of the spectrum is relatively free from interference.[128] The incorporation of a naphthylamine building block into a boronic acid appended azo dye would therefore make an interesting molecule to study.

It is known that 1-napthylamine derivatives couple to diazonium salts largely in the 4-ring position, although coupling can also be observed at the 2-ring position.[124] For this reason it was decided to try a test azo coupling reaction with 1-aminonaphthalene to see whether any of the 2-coupled product was formed. If so, it would not be worth trying to incorporate a boronic acid moiety into the molecule, as separation of the two dye isomers would be problematic. Hence the diazonium salt of 4-nitroaniline was coupled with 1-aminonaphthalene, using the procedure described earlier (section 2.2.1.1), to afford dye **15** (Figure 23). Fortunately, ^{1}H NMR showed evidence only for the 4-coupled product.

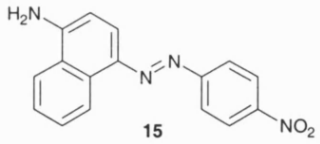

Figure 23: Model azo dye synthesised from 1-naphthylamine

Scheme 7 shows the synthetic route to a boronic acid appended naphthyl azo dye. The synthesis is very similar to that used earlier (section 2.2.1.1). The only alteration was in the step to form the imine. It was found that the naphthyl imine formed readily in methanol at room temperature, but was unstable when isolated from solution. Consequently, reduction of the imine with sodium borohydride was performed in the same one-pot reaction. The amine product **16** was cleanly isolated in good yield (68%) by precipitation after pouring on to ice. The previously discussed azo coupling reaction with the diazonium salt of 4-nitroaniline was performed on **16** to give the 4-coupled azo dye **17**.

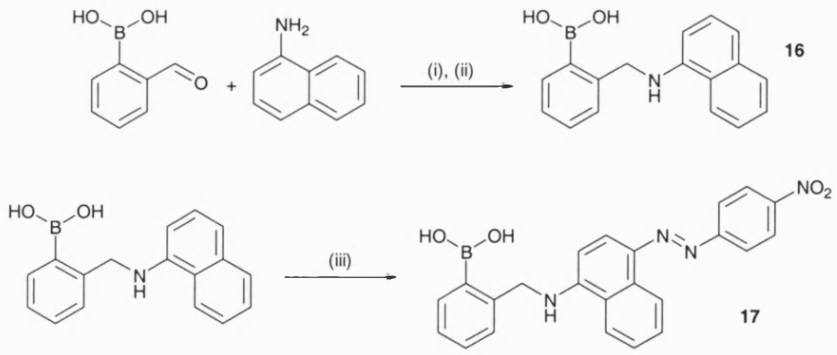

Scheme 7: Synthetic procedure for boronic acid appended naphthyl azo dyes; (i) methanol, rt, 1 hr; (ii) $NaBH_4$, methanol, rt, 1 hr; (iii) $O_2N\text{-}C_6H_4N_2^+Cl^-$, pH 4, 0-5 ^oC, 2 hr.

Extending the aromatic ring system further, to anthracene, was considered, as there are a number of aminoanthracene molecules commercially available. However, as the size of the ring is increased, the solubility of the dyes in the aqueous solvents used in absorbance studies decreases. Dye **17** was noticeably less soluble than the

corresponding benzene derived dye **3**. Also, aminoazo derivatives of anthracene have not been widely studied,[124] suggesting that their synthesis is not straightforward. As such, it was felt that it was not worth extending this investigation to the anthracene ring system.

2.2.1.4 Modification of the Electronics of the Boronic Acid Centre

The binding properties of boronic acids to saccharides or fluoride can be adapted through altering the electronic configuration of the boronic acid phenyl ring, by adding electron donating or withdrawing groups.[117] It was decided to try to incorporate a methoxy group and a chloro group into the boronic acid phenyl ring (Figure 24) to see how this would affect the chromophore upon saccharide or fluoride binding, compared to the non-substituted dyes synthesised earlier.

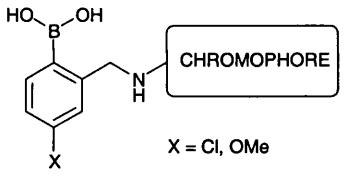

Figure 24: Modification of the boronic acid phenyl ring

Scheme 8 shows the synthetic route to the two target molecules. 4-methoxy-2-formyl-phenylboronic acid is commercially available and was reacted with *m*-toluidine, using the reductive amination conditions described earlier, to prepare the methoxy substituted boronic acid amine **19**. 4-chloro-2-formylphenylboronic acid could not be obtained commercially so was prepared from 2-bromo-4-chlorotoluene (Scheme 8). The bromide was reacted with magnesium powder in THF to form the corresponding aryl Grignard. The Grignard was used directly with trimethylborate at low temperature to yield boronic acid **20**, after acidic work-up and recrystallisation from methanol-water.

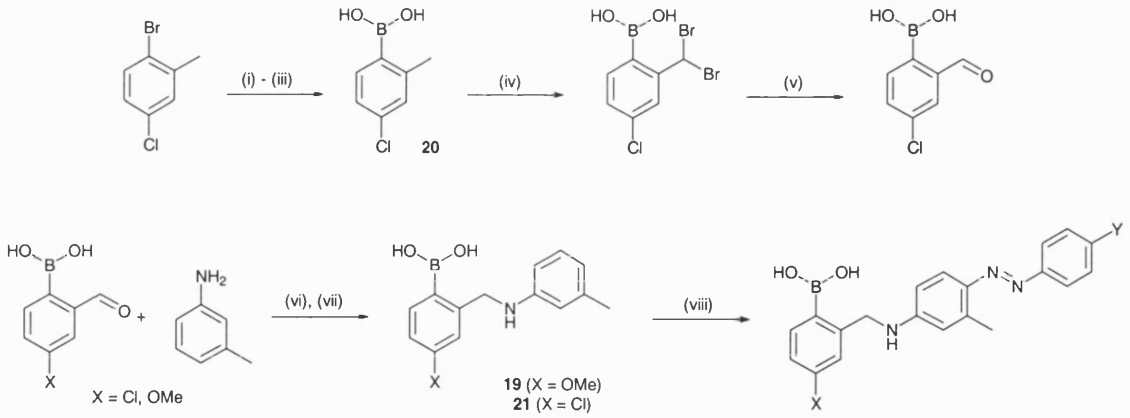

Scheme 8: Synthetic procedure for ring modified boronic acid appended azo dyes; (i) Mg, THF, reflux, 1 hr; (ii) $B(OCH_3)_3$, THF, -78 °C; (iii) H_3O^+; (iv) Br_2, CCl_4, hν, relux, 1 hr; (v) NaOH, $CHCl_3$, 0-5 °C; (vi) ethanol-toluene, reflux in Dean-Stark apparatus, 18 hr; (vii) $NaBH_4$, methanol, rt, 1 hr; (viii) Y-$C_6H_4N_2^+Cl^-$, pH 4, 0-5 °C, 2 hr.

The next step involved the dibromination of the methyl group of **20**. The reaction was performed with bromine rather than two equivalents of the standard brominating agent *N*-bromosuccinimide (NBS). Previous test reactions with NBS on similar systems showed that only a small amount of the dibrominated product was produced using this reagent. Using bromine increased the proportion of the dibrominated product formed relative to the monobrominated derivative. However, complete conversion to the dibrominated product could not be attained. The best conversion achieved (by ^{1}H NMR) was approximately 70%. Separation of the two brominated products proved problematic, so the subsequent step was carried out without further purification. The bromides were reacted with sodium hydroxide. The dibromide forms the dihydroxide substituted adduct, which undergoes immediate dehydration to form the aldehyde, whereas the monobromide forms the alcohol. In a fortuitious discovery, upon the first extraction of the basic layer, the alcohol was exclusively extracted. Later extractions removed only the aldehyde. The aldehyde was then reacted with *m*-toluidine in the usual manner to yield the chloro-substituted boronic acid amine **21**, after precipitation in water.

Having successfully synthesised the two boronic acid amine building blocks, an effort was made to introduce the azo chromophore to both molecules. A number of attempts on both amines were made using a variety of diazonium salts. Although there was evidence to suggest the dyes of both amine derivatives had formed, something else was happening in the reaction that gave rise to other products that could not be separated from the target dyes. It was decided not to continue any further with this line of investigation. However, this section of work has shown that it is possible to add substituents to the boronic acid phenyl ring, which may be of use in other non-colorimetric boronic acid applications.

2.2.2 Systems Containing Other Chromophores

The preceding work has shown that it is possible to introduce an azo chromophore into boronic acid appended molecules. The next section will describe the attempts made to replace the azo group as the chromophore. Although azo dyes can cover the whole visible spectrum in their hues,[124] the dyes synthesised to date have only shown yellow to red shades of colour. By selectively changing the chromophore, it should be possible to attain molecules that absorb in different regions of the spectrum.

2.2.2.1 A Boronic Acid Appended Tricyanovinyl Dye

McKusick *et al* first prepared tricyanovinylarylamine dyes in the late 1950's.[129, 130] In the last fifteen years, there has been a surge in the development of tricyanovinyl dye systems for use in non-linear optic (NLO) applications.[131-134] The use of tricyanovinyl substituents as acceptors in donor-acceptor substituted organic compounds leads to increased molecular second-order nonlinear optical susceptibilities, compared to

stilbenes and azo dyes.[135] In a similar manner to diazonium species, tetracyanoethylene readily performs electrophilic attack on aromatic rings at positions of high electron density, to form tricyanovinyl adducts.[136] The tricyanovinyl chromophore therefore seemed to be an ideal replacement for the azo group.

Scheme 9 shows the synthetic procedure towards a boronic acid appended tricyanovinyl dye. In an analogous procedure to the formation of amine **2**, 2-formylbenzeneboronic acid was reacted with aniline under reductive amination conditions to afford amine **13**. Reaction of **13** with tetracyanoethylene in DMF after gentle heating at 55 °C yields the *para*-substituted dye **14**. The product was precipitated from solution by addition to ice. ^{1}H NMR seemed to show the presence of a small amount of the potential *N*-substituted product. Recrystallisation from acetic acid afforded an analytically pure sample of **14**.

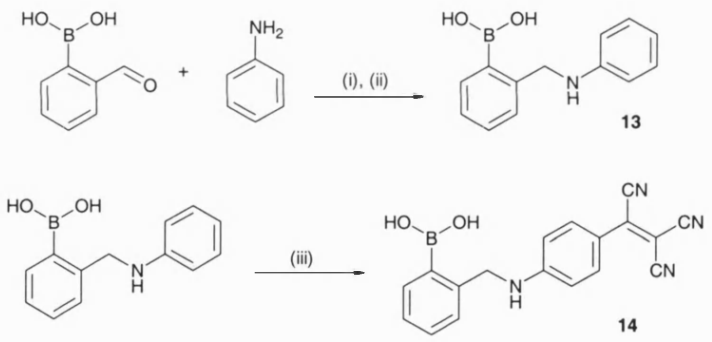

Scheme 9: Synthetic procedure for boronic acid appended tricyanovinyl dye; (i) ethanol-toluene, reflux in Dean-Stark apparatus, 18 hr; (ii) $NaBH_4$, methanol, rt, 2 hr; (iii) tetracyanoethylene, DMF, 55 °C, 1 hr.

The tricyanovinylation reaction was originally attempted on amine **2**. However, it was found that this led to a very messy crude reaction product, which proved impossible to purify. The reason for the failure of this reaction is probably steric in nature. Tetracyanoethylene contains four linear nitrile groups that protrude out from the centre of the molecule. Upon approach to amine **2**, there must be an unfavourable steric

interaction between one of the nitrile groups and the *meta*-methyl group in **2**. Hence, amine **13** derived from aniline and consequently missing the *meta*-methyl group, was synthesised.

Once more, the absorbance properties of dye **14** will be investigated later. An important point to note about tricyanovinyl dyes is that they are unstable if left for long periods in aqueous media. The dyes are especially prone to decomposition at high pH due to hydroxide attack at the vinyl carbon centre. However, for the purposes of this study, this issue should not cause any problems.

2.2.2.2 Other Boronic Acid Appended Chromophores

Figure 25 shows some dyes with different chromophores containing boronic acid functionality that were targeted for their interesting spectral properties.

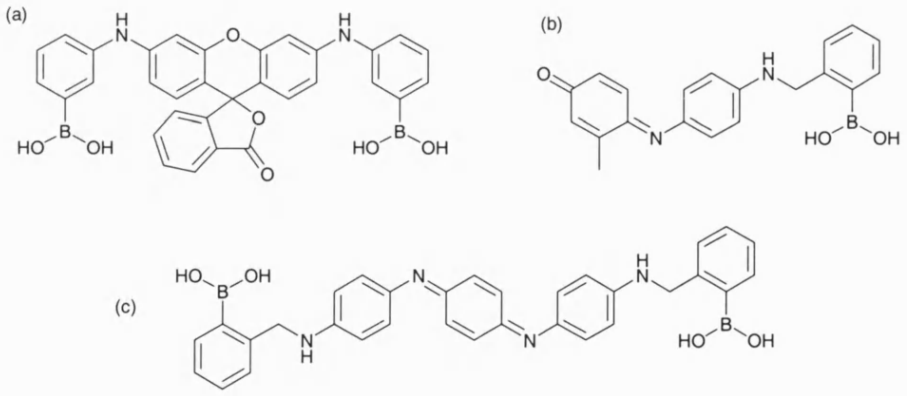

Figure 25: Some target boronic acid dyes; (a) a xanthene derivative; (b) an indoaniline derivative; (c) a quinonenediimine derivative.

Figure 25a shows a boronic acid appended xanthene, a representative of the oxygenated heterocyclic dyes. These dyes are derived from Fluorescein (Figure 26), which, as its name suggests, is highly fluorescent and as such is used in numerous applications as a marker.[124] When 3',6'-dichlorofluoran (Figure 26) is condensed with various anilines,

bright xanthene dyes can be formed. However, when 3-aminobenzeneboronic acid was reacted with 3',6'-dichlorofluoran, the dye product (Figure 25a) could not be isolated in acceptable purity.

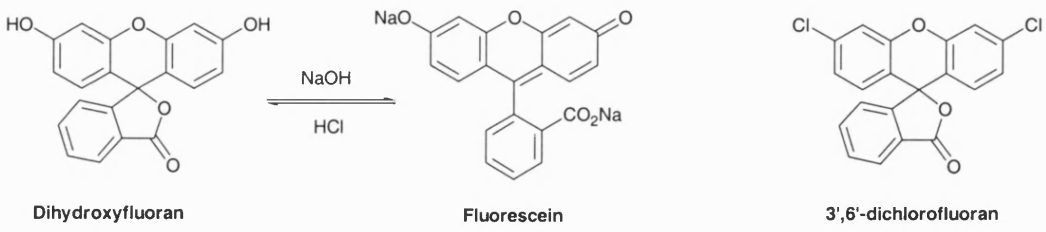

Figure 26: Fluorescein and some related structures

The indoaniline dye (Figure 25b) and the quinonenediimine structure (Figure 25c) are both examples of oxidation colours. Anilines are oxidised using suitable reagents, typically ammonium persulphate ($[NH_4]_2S_2O_8$), and then coupled to other anilines or phenols to form the respective dyes.[123] During the oxidation, radical species are formed. This can lead to side reactions occurring and consequent formation of unwanted impurities. Unfortunately this was the situation in the case of the dyes in Figure 25b and c, making purification extremely difficult. The two dyes decomposed very easily upon heating, making recrystallisation impossible, and were both unstable on silica. As a result, these chromophores were not pursued any further.

2.2.3 Towards D-Glucose Selective Sensors

The systems discussed to date have all contained a single boronic acid centre. Lorand and Edwards' work has shown that phenylboronic acid forms the most stable complex with D-fructose, when compared to other simple monosaccharides.[27] Subsequent work has confirmed that all mono-boronic acids have a preference for binding to D-fructose over the more biologically important D-glucose.[1] A number of sensor systems showing

D-glucose selectivity have been developed using di-boronic acid moieties.[31, 41] Figure 27 shows a schematic diagram of the macrocyclic structure formed upon 1:1 binding of saccharide to a di-boronic acid. Using D-glucose (in its preferred pyranose form) as an example, one boronic acid group can bind to the C-1 and C-2 hydroxyl groups of glucose, while the other can bind to the C-4 and C-6 alcohols, forming the 1:1 macrocycle.

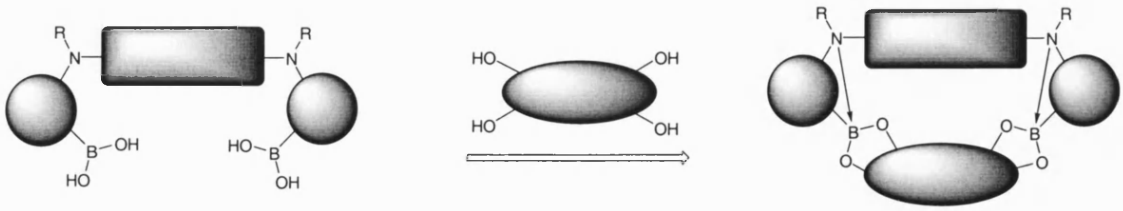

Figure 27: Schematic to show 1:1 binding between a di-boronic acid and saccharide

It was thought that by starting from a suitable anilinic diamine, a degree of D-glucose selectivity in a coloured boronic acid system could be achieved by utilising the successful synthetic procedure used previously to make dyes **3-7**. Commercially available 3,3'-methylenedianiline and *m*-phenylenediamine (Figure 28) were chosen as possible starting points for the syntheses of di-boronic acids. The difference in the spacing of the two amine groups in the two molecules might lead to a change in the selectivity order for monosaccharide.

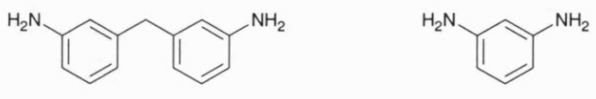

3,3'-methylenedianiline *m*-phenylenediamine

Figure 28: Some diamines suitable for use in the synthesis of di-boronic acid derivatives

Scheme 10 shows the synthesis of the di-boronic acids before azo coupling. Both 3,3'-methylenedianiline and *m*-phenylenediamine were reacted with two equivalents of 2-

formylbenzeneboronic acid, the former under reflux and the latter at room temperature. Attempts to isolate the di-imine from *m*-phenylenediamine at this stage led to decomposition of the product. Hence the resulting di-imines were both directly reduced with sodium borohydride to afford the respective di-boronic acids **22** and **23** in excellent purity, after acidic work-ups.

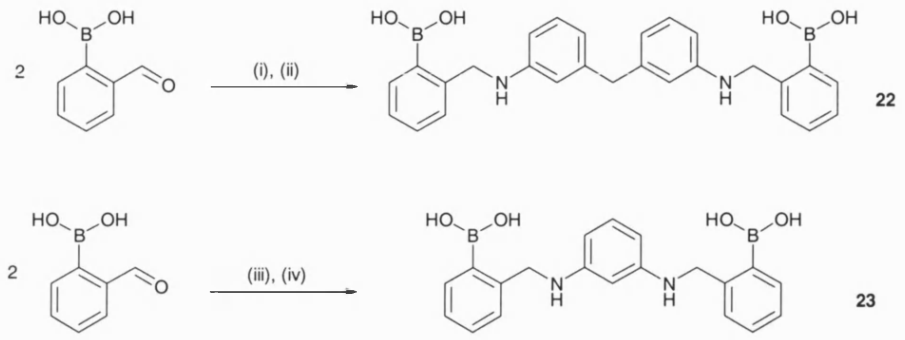

Scheme 10: Synthetic procedure for di-boronic acid amines; (i) ethanol-toluene, reflux in Dean-Stark apparatus, 18 hr; (ii) $NaBH_4$, methanol, rt, 2 hr; (iii) methanol, rt, 1 hr; (iv) $NaBH_4$, methanol, rt, 1 hr.

Attempts to couple **22** and **23** with the diazonium salt of 4-nitroaniline met with failure. ^1H NMR showed that the desired products had formed to some extent. However, satisfactory purification could not be achieved. The reason for the reaction not going to completion is probably steric in nature. If the diazonium ion is to couple *para* to the anilinic nitrogens, there must be an unfavourable steric interaction with the large and bulky groups that are in the *meta* position relative to the anilinic nitrogens in both **22** and **23**. Once more, after successful preparation of key intermediates, a promising idea failed at the last synthetic stage.

2.2.4 Summary

- A series of boronic acid azo dyes has been synthesised, and fully characterised, using a novel and straightforward three step synthetic route.

- Two model dyes have been prepared for comparison purposes – one a non-boronic acid derivative, the other an anilinic nitrogen *N*-methylated species.
- The aromatic ring size of the dye system has been successfully changed to incorporate an aminonaphthalene moiety.
- Three boronic acid amines with electronically modified ring substituents have been prepared. However, attachment of a chromophore has proved problematic.
- The chromophore has been effectively changed from the azo group to the highly electron-withdrawing tricyanovinyl moiety. Attempts to introduce other chromophores, including indoaniline and xanthene dyes, have failed because of difficulties in purification of the products.
- Two di-boronic acids, based upon anilinic diamines, have been synthesised for use as possible D-glucose selective receptors. Unfortunately, due to steric problems, the coupling with diazonium salts has shown to be ineffective.

2.3 Interaction of Boronic Acid Dyes with Saccharide

This section will examine the interaction of saccharide with the boronic acid dye molecules that were synthesised in the preceding chapter. Standard Ultraviolet-Visible (UV-VIS) spectrophotometry techniques were used to study the binding of the dyes to various saccharides and diols. The aim of the investigation was to see whether a spectral shift (colour change) would actually occur upon such a binding event. The development of boronic acid sensor molecules for saccharides has received much attention.[1, 2] A number of fluorescent sensors have been reported in the literature.[44, 137, 138] However, the progress of coloured sensors for saccharides has been a lot slower. If a system with a large colour change was to be developed, it could be incorporated into a diagnostic test paper for D-glucose, similar to universal indicator paper for pH. Such a system would allow the measurement of D-glucose concentrations without the need for specialist instrumentation. This would be of particular benefit to diabetics in developing countries.

The absorption of visible light by azo dye compounds can be described through a Linear Combination of Atomic Orbitals-Molecular Orbital (LCAO-MO) approach.[139] A non-bonding (n) electron from the azo nitrogen is excited, by the absorption of a photon of visible light, into the lowest antibonding (π^*) orbital in an $n \rightarrow \pi^*$ electronic transition (Figure 29). The energy, and hence wavelength, of this transition is dependent upon the substituents of the azo chromophore and the inductive and conjugation effects that these have on the energy of the n and π^* orbitals. In a similar manner, the tricyanovinyl chromophore's absorption can be described as a $\pi \rightarrow \pi^*$ transition, the electron being excited from the highest energy π-bonding orbital on the vinylic carbon.

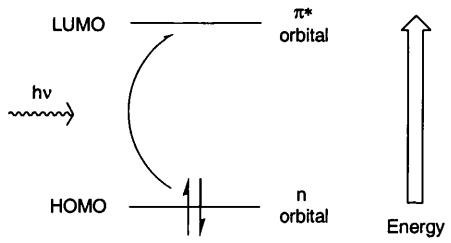

Figure 29: Schematic electronic energy level representation of the absorption of visible light by an azo chromophore

The anilinic nitrogens found in the boronic acid dye molecules are all in direct conjugation, through the linking aromatic ring system, with either the azo nitrogens or tricyanovinyl carbons. The anilinic nitrogen is also in close proximity to the boronic acid boron centre. The electronic changes associated with saccharide binding can be transmitted through a boron-nitrogen interaction to the azo chromophore. This will then hopefully create a spectral change in the molecule that can be detected in the UV-VIS absorption spectrum. It is well known that the electronic changes associated with saccharide binding to a boronic acid centre, are often manifested in a pK_a change.[1, 72, 137] This pK_a shift can be studied by UV-VIS absorption-pH titrations.

2.3.1 Absorption-pH Titrations with Boronic Acid Azo Dyes

Absorbance-pH titrations, from pH 2 to 12, with each of the boronic acid azo dyes (**3**, **4**, **5**, **6**, **7**, **10** and **17**) were performed in aqueous methanolic solutions containing 0.05 mol dm^{-3} sodium chloride. The sodium chloride present acts as a so-called 'osmotic buffer' because small amounts of sodium chloride are formed on adjustment of the pH with sodium hydroxide and hydrochloric acid. Because the titrations are carried out in a methanol-water mixture rather than simply water, the concept of pH is not strictly applicable to this situation. However, De Ligny and Rehbach have shown that for solutions in 50% methanol the pH is only changed by 0.1 of a pH unit compared to a 100% water solution.[140] At percentages lower than 84% methanol, the error does not

exceed 0.2 pH units, but for higher percentages it dramatically increases and for absolute methanol it is equal to 2 pH units.

The experiments were then repeated in the presence of 0.05 mol dm^{-3} D-fructose. D-fructose was chosen as the test saccharide as past studies have shown that it gives the largest pK_a shifts on binding to mono-boronic acids compared to other monosaccharides and simple diols.[27] Figure 30 shows the absorption-pH profile of unbound dye **7**. Three different species are observed as the pH is increased – one in the low pH region, one at around neutral pH and one in the high pH zone. Scheme 11 shows the proposed species present in each of these pH regions.

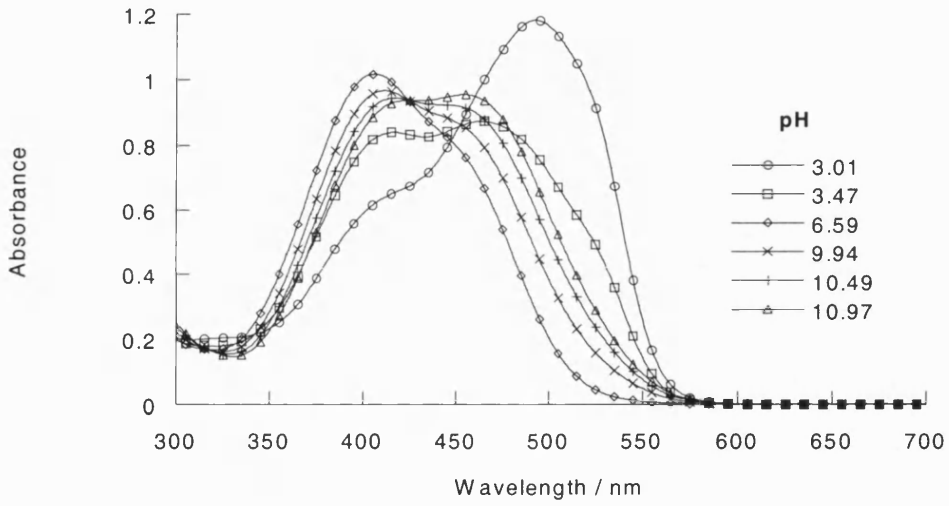

Figure 30: Absorption-pH spectral changes of dye **7** (5.34 x 10^{-5} mol dm^{-3})

At low pH's, protonation of 4-aminoazobenzene derivatives can occur either at the β–nitrogen atom of the azo group to give the azonium tautomer (**A** in Scheme 11), or at the terminal amino group to give the ammonium tautomer (**B** in Scheme 11). Ammonium tautomers no longer possess a free lone pair of electrons on the amino nitrogen. As such they resemble an azobenzene *para* substituted electron-withdrawing group and will absorb at shorter wavelengths than the neutral dye, with a lower

absorption coefficient (ε). On the other hand, azonium tautomers contain a positive charge that can be delocalised (**A** and **A'** in Scheme 11). These species are more bathochromic (absorb at longer wavelengths) and tinctorially stronger (larger ε) than the neutral dye. The azonium tautomer is generally stabilised by electron-donating groups (e.g. methyl groups) *meta* to the terminal amino group. Electron-withdrawing groups that are *meta* or *para* to the azo linkage also strengthen the azonium tautomer.

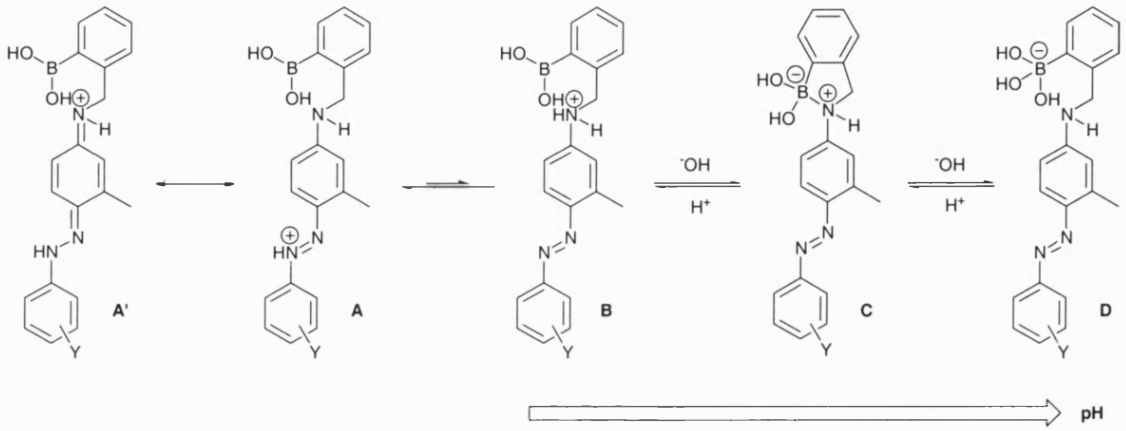

Scheme 11: Acid-base equilibria species of unbound boronic acid azo dyes

As the pH decreases, the spectra in Figure 30 clearly show a shift to longer wavelength as well as an increase in the absorption coefficients. This is good evidence that the azonium tautomer is the major species at low pH. This is to be expected considering there is an electron-donating methyl group *meta* to the terminal amino group, and an electron-withdrawing carboxyl group *meta* to the azo linkage. Although this is an interesting region of the acid-base equilibria, in the context of saccharide binding, it is irrelevant because the boronic acid-saccharide interaction only takes place at near neutral pH and above. As such, no further mention will be made of these low pH azonium species for the remaining azo dyes.

At intermediate pH, a boron-nitrogen interaction is prevalent (**C** in Scheme 11). The boron-nitrogen interaction has been widely used in the field of boronic acid-saccharide recognition, and is well established as a sensor design motif for lowering the pH at which boronic acids bind to diols.[1, 137] As the pH is increased further, the boron-nitrogen bond is broken by hydroxide ion to form the tetrahedral boronate anion species (**D** in Scheme 11). The pK_a of this equilibrium can be calculated from the absorption data obtained from the pH titrations. This will be discussed later in this section.

Figure 31 shows the absorption-pH profile of dye **7**, repeated in the presence of 0.05 mol dm^{-3} D-fructose. The low pH spectra have been omitted for clarity.

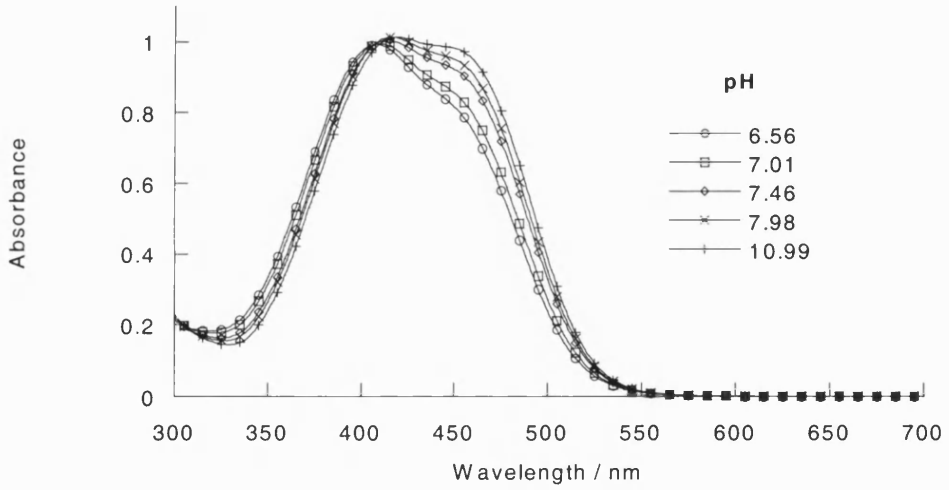

Figure 31: Absorption-pH spectral changes of dye **7** (5.34 x 10^{-5} mol dm^{-3}) with 0.05 mol dm^{-3} D-fructose

To examine the data obtained from Figure 30 and Figure 31 further, an absorption-pH profile can be constructed to see how the pK_a is affected upon saccharide complexation. Figure 32 shows a plot of relative absorbance of dye **7** versus pH at 450 nm, with and without the presence of D-fructose. The plot shows an unmistakable shift in the pK_a

upon the addition of D-fructose. This shift on saccharide binding (ΔpK_a) is in agreement with previous work.[72]

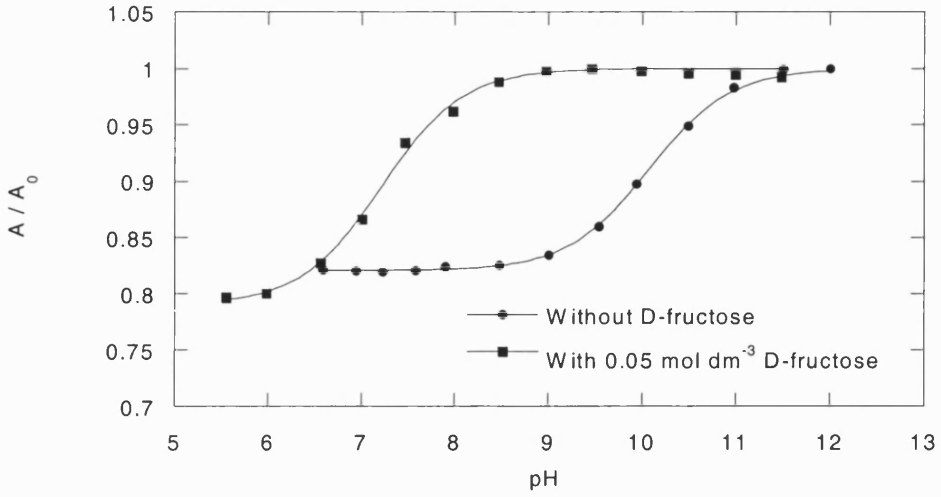

Figure 32: Absorption-pH profile of dye **7** with and without D-fructose at 450 nm

At this stage it is probably wise to discuss the concept of a boronic acid's pK_a and how it is affected upon interaction with saccharide. It has long been accepted that boronic acids bind rapidly and reversibly to 1,2- and 1,3-diols in basic aqueous media to form 5 or 6 membered cyclic boronate esters (Scheme 12). This interaction occurs most readily above the pK_a of the boronic acid, 8.8 for phenylboronic acid. However, as seen above, on binding the pK_a is reduced – this is referred to as the pK_a'. This interpretation is different to that adopted by Lorand and Edwards back in the 1950's.[27] They assumed that neutral binding K_a' was not appreciable, and therefore pK_a' could not exist. This means that anion formation must occur prior to complexation. However, since K_a' cannot be ignored, the possibility of anion formation after complexation must be considered. This will depend on the pH of the solution – highly basic solutions above the pK_a' of the boronic acid may well involve anion formation prior to complexation. It is therefore not possible to say for certain which pathway will occur. The possibility that either one pathway or the other may be in operation, or indeed that a combination of

both is observed, should always be considered.[141] For boronic acids with a boron-nitrogen interaction, including the dyes depicted in Scheme 11, the analogous pK_a of these molecules has traditionally been referred to as the breaking of the boron-nitrogen bond by hydroxide ion (species **C** going to species **D** in Scheme 11).[72]

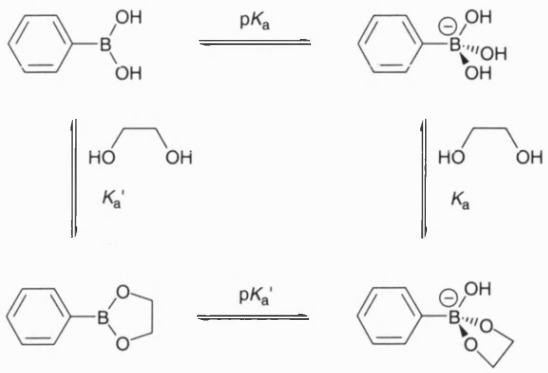

Scheme 12: Thermodynamic cycle for boronate ester formation

So why is the pK_a' of a bound boronic acid lower than the pK_a of an unbound boronic acid? There is no quantitative explanation in the literature, but Lorand and Edwards first proposed a rational qualitative description. They hypothesised that the reason for the increased acidity of the bound boronic acid centre was linked to the oxygen-boron-oxygen bond angle. In unbound boronic acid this angle is 120° as the boron atom is sp^2 hybridised (Figure 33a). This bind angle is reduced to 108° on binding to form the cyclic ester (Figure 33b). Since sp^3 hybridised orbitals have a tetrahedral geometry, with an ideal bond angle of 109.5°, formation of a *pseudo-*sp^3 boronate anion will dramatically reduce the ring strain (Figure 33c). The higher the binding constant and concentration of the saccharide or diol, the more sp^2 boron is bound in a strained manner and thus the greater the formation of the anionic boronate ester. The formation of the anion requires the release of H^+ from an associated or bound water molecule (Scheme 13). Hence, the larger the proportion of anionic boronate ester in solution, the lower the apparent pH. In other words, bound boronic acid is a stronger Brønsted acid.

The concept of boronic acid centres binding water molecules has been previously suggested,[82] but its relationship to pK_a has not been explored in any depth.

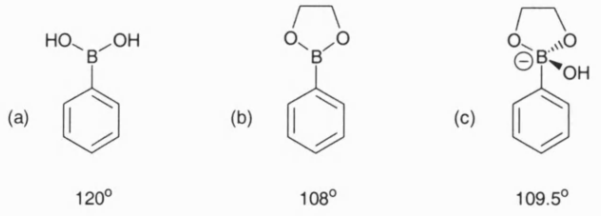

Figure 33: O-B-O bond angle variation during boronic acid binding and anion formation

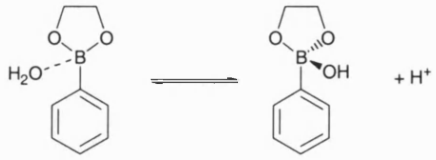

Scheme 13: An associated water molecule releases H^+ to form the tetrahedral boronate ester

Evidently, for molecules containing a boron-nitrogen interaction, the explanation above is a slight over-simplification as regards to the bond angles involved. However, the principle is still very much valid. It explains the well-known observation that the boron-nitrogen interaction is strengthened upon saccharide binding.[1, 142] The bound boronic acid, with its *pseudo-sp*^{3} conformation, is now more geometrically favoured to accept the lone pair of elecrons from the amine nitrogen. This phenomenon has been exploited in a number of Photo-induced Electron Transfer (PET) fluorescent saccharide sensor systems.[44, 137, 138] The strong association of the amine's lone pair of electrons to the bound boron centre prevents the fluorescent quenching that occurs with unbound boronic acid, where the boron-nitrogen interaction is significantly weaker.

The pK_a of this interaction can be calculated from the absorption data by using Equation 1.[44, 143] The pK_a curves were analysed in KaleidaGraph[‡] using non-linear (Levenberg-Marquardt algorithm) curve fitting of Equation 1. The errors reported are the standard errors ($\pm\sigma/\sqrt{N}$) obtained from the best fit. The curves in Figure 32 were fitted using this method. The calculation was performed for all of the dyes with and without D-fructose. The results of these calculations are summarised in Table 2. The spectra and absorbance-pH plots for all of the other dyes can be found in the Appendix.

$$A = (A_0 + A_{lim} K_a [H^+])/(1 + K_a [H^+])$$

Equation 1: A is the absorbance for a particular concentration of proton; A_0 is the initial absorbance; A_{lim} is the limiting (final) absorbance; K_a is the acid dissociation constant; $[H^+]$ is the concentration of protons.

Dye	Without D-fructose		With D-fructose		ΔpK_a
	pK_a	r^2	pK_a'	r^2	
3	10.19 ± 0.03	0.997	7.04 ± 0.04	0.998	3.15
4	10.01 ± 0.02	0.999	7.13 ± 0.03	0.998	2.88
5	9.93 ± 0.03	0.997	7.24 ± 0.04	0.995	2.69
6	10.22 ± 0.01	0.999	7.17 ± 0.02	0.999	3.05
7	10.07 ± 0.02	0.999	7.21 ± 0.04	0.996	2.86
10	9.68 ± 0.02	0.998	6.99 ± 0.04	0.996	2.69
17	9.72 ± 0.01	0.999	6.77 ± 0.04	0.997	2.95

Table 2: pK_a values and coefficients of determination (r^2) for boronic acid azo dyes

[‡] KaleidaGraph Version 3.09 for the PC, published by Synergy Software and developed by Abelbeck Software, 2457 Perikiomen Avenue, Reading, PA 19606. A user defined curve fit [1 + $m2$ $m1$ ($M0$)]/[1 + $m1$ ($M0$)] derived from Equation 1 was used in all calculations. The initial value of $m1$ (K) was set to 1 and the initial value of $m2$ (A_{lim}) was set to 1.1. The variable ($M0$) was $[H^+]$. The allowable error was set to 0.001%. For all curves the coefficient of determination (r^2) was > 0.99.

The results show that the applied equation is valid for calculating the pK_a's of the dyes as the coefficient of determination (r^2) values show an excellent fit ($r^2 > 0.99$). The pK_a values of the unbound dyes **10** and **17** are slightly lower than those of dyes **3-7**. This is because the electronic environment of the anilinic nitrogen is different for each of these two dyes. Dye **10** has a tertiary anilinic nitrogen compared to the secondary amine centre in dyes **3-7**, and dye **17**'s anilinic centre is attached to a naphthyl ring system rather than the phenyl ring of dyes **3-7**.

All of the dyes show similar magnitudes of ΔpK_a, although dye **3** (derived from 4-nitroaniline) shows the largest change. All of the dyes gave similar absorption spectra to dye **7**, with and without D-fructose (see Appendix). However, dye **3** showed an especially marked difference in its absorption spectra at high pH (Figure 34 and Figure 35).

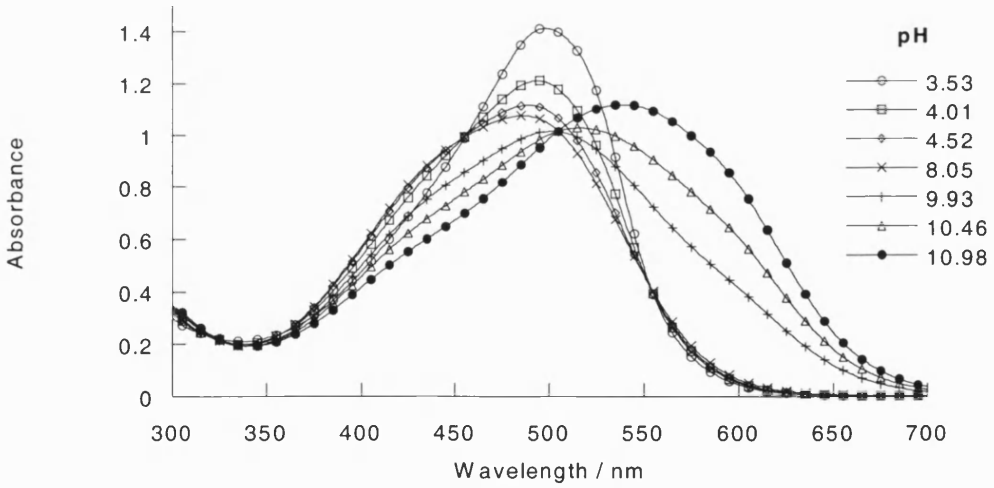

Figure 34: Absorption-pH spectral changes of dye **3** (5.66×10^{-5} mol dm^{-3})

Figure 35 shows that at high pH, in the presence of D-fructose, dye **3**'s absorption maxima do not shift to as long a wavelength as when the saccharide is absent (Figure 34). The spectral shift is actually large enough (55 nm) to give a visible colour change

from dark purple to red, upon the binding of D-fructose at high pH. This appears to indicate that a new species is formed upon saccharide binding at high pH, which is electronically different from the unbound dye. To investigate this phenomenon further it was decided to perform saccharide titrations at high pH with dye **3**.

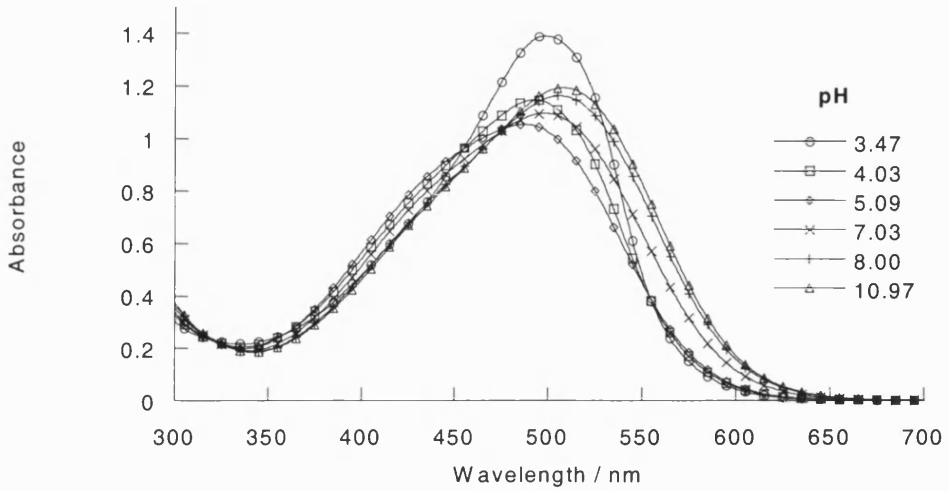

Figure 35: Absorption-pH spectral changes of dye **3** (5.66×10^{-5} mol dm^{-3}) with 0.05 mol dm^{-3} D-fructose

2.3.2 Absorption-Saccharide Titrations with Boronic Acid Azo Dyes

UV-VIS absorbance titrations of **3** with D-fructose, D-glucose and ethylene glycol were performed in a pH 11.32 aqueous methanolic buffer solution [52.1wt% methanol (KCl, 0.01000 mol dm^{-3}; $NaHCO_3$, 0.002771 mol dm^{-3}; Na_2CO_3, 0.002771 mol dm^{-3})].[144] The pH was chosen so that it was above the pK_a of the free dye, 10.19 (Table 2). This meant that at the start of each titration, the majority of unbound dye was in the form of the tetrahedral boronate anion (species **D** in Scheme 11). As the concentration of saccharide or diol was increased, a visible colour change from purple to red was observed. The colour-absorbance changes upon addition of D-glucose to **3** are shown in Figure 36. The absorbance of free dye at 564 nm decreases as binding occurs, and a new absorbance at 509 nm appears, a wavelength shift of 55 nm. The absorption spectra of the D-glucose

titration are shown in Figure 37 and those for D-fructose and ethylene glycol can be found in the Appendix. The spectral shift upon complexation occurs in all three cases. The concentration of the guest required to produce the change is different in each case and is due to the different stability constants (K) of the binding species with the boronic acid. The wavelength shift obtained upon addition of saccharide with dye **3** is the largest achieved to date in such a system.[145]

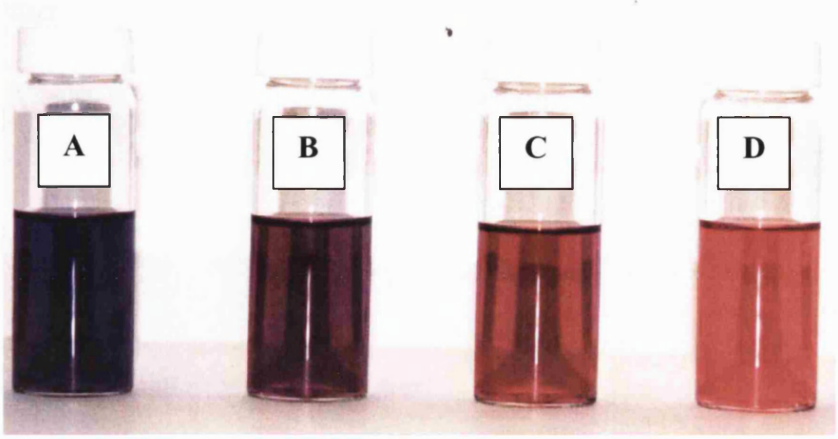

Figure 36: Colour-absorbance changes upon addition of D-glucose to dye 3 at pH 11.32; A: with no saccharide; B: with 0.339 x 10^{-2} mol dm^{-3} D-glucose; C: with 1.66 x 10^{-2} mol dm^{-3} D-glucose; D: with 22.7 x 10^{-2} mol dm^{-3} D-glucose

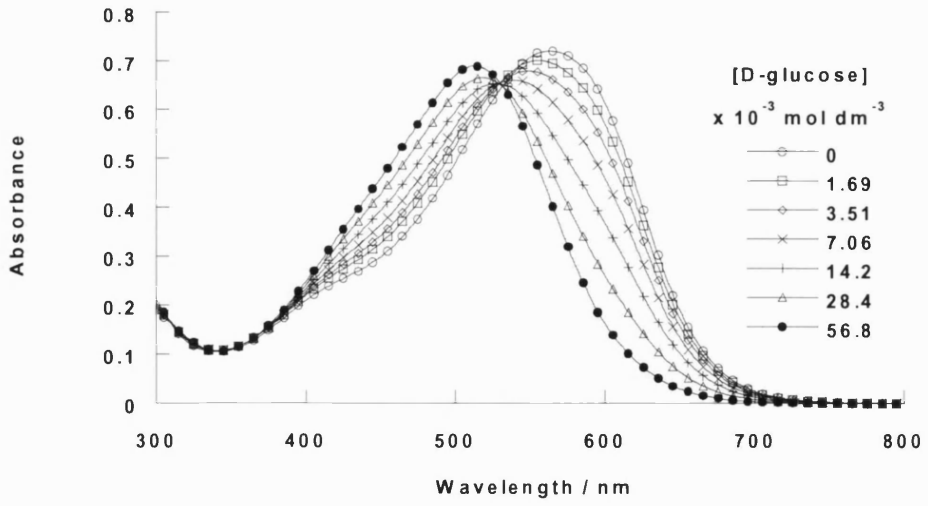

Figure 37: Absorption-spectral changes of dye **3** (2.83 x 10^{-5} mol dm^{-3}) with increasing concentration of D-glucose at pH 11.32

D-fructose and D-glucose titrations at pH 11.32 were also performed on dyes **4-7**, **10** and **17**. Dyes **4-7** all showed colour changes and spectral shifts upon saccharide binding (see Appendix for absorption-spectral changes). However, none gave as large a spectral shift as dye **3**. The slightly structurally different dyes **10** (*N*-methylated dye) and **17** (aminonaphthalene dye) both showed no change in absorbance and consequently no colour change upon saccharide binding at this pH (see Figure 38 and Figure 39 respectively). This observation will be discussed later.

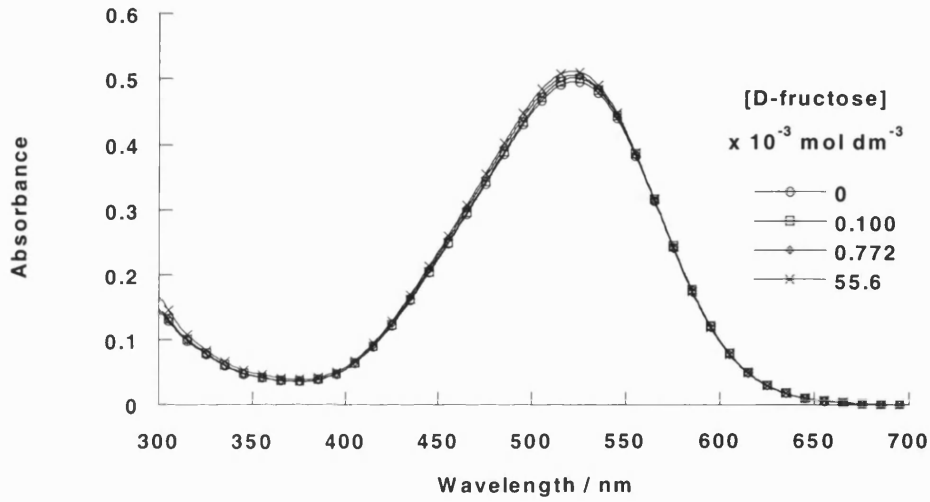

Figure 38: Absorption-spectral changes of dye **10** (2.09 x 10^{-5} mol dm^{-3}) with increasing concentration of D-fructose at pH 11.32

The stability constants (*K*) of the boronic acid dye-saccharide complexes can be calculated using Equation 2, assuming a 1:1 boronic acid-saccharide binding event.[44, 143] The stability constant curves were analysed in KaleidaGraph using the method previously employed for Equation 1. Figure 40 shows an example curve fit using Equation 2 for dye **3**'s interaction with D-glucose. Curve fits for the other dyes can be found in the Appendix. Table 3 gives the results of these calculations for all of the boronic acid azo dyes.

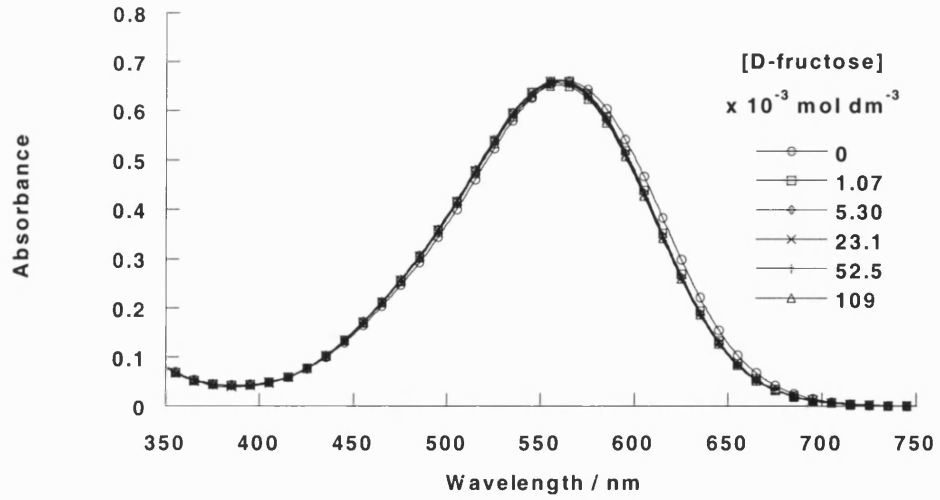

Figure 39: Absorption spectral changes of dye **17** (1.76 x 10^{-5} mol dm^{-3}) with increasing concentration of D-fructose at pH 11.32

$$A = (A_0 + A_{lim} K\,[\text{guest}])/(1 + K\,[\text{guest}])$$

Equation 2: A is the absorbance for a particular concentration of guest; A_0 is the initial absorbance; A_{lim} is the limiting (final) absorbance; K is the stability constant of the receptor with the guest; [guest] is the concentration of of the guest.

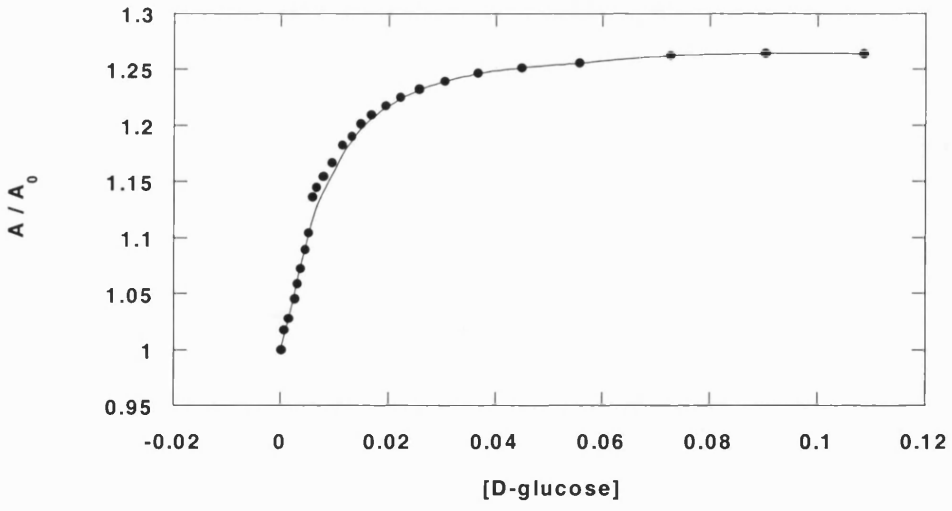

Figure 40: Curve fit to determine the stability constant at 509 nm of dye **3** with D-glucose

The results show that dye **3**, which gives the largest spectral change, has the lowest binding constant with D-fructose, compared to the other dyes. As mentioned earlier, dyes **10** and **17** did not show a spectral shift and, as a result, stability constants could not be calculated for them. The coefficient of determination (r^2) values for all of the dyes show very good fits ($r^2 > 0.98$), implying that the assumption of a 1:1 binding event is valid. The results also agree with the accepted order of selectivity for saccharide by mono-boronic acids; D-fructose binds more strongly than D-glucose.[27]

Dye	Polyol	K / dm^3 mol^{-1}	r^2	σ-value[146]
3	D-fructose	2550 ± 250	0.991	0.78
3	D-glucose	123 ± 9	0.983	0.78
3	Ethylene glycol	5.1 ± 0.1	0.999	0.78
4	D-fructose	3630 ± 274	0.995	0.38 [a]
4	D-glucose	184 ± 40	0.982	0.38 [a]
5	D-fructose	4160 ± 352	0.992	0.13 [b]
5	D-glucose	121 ± 9	0.997	0.13 [b]
6	D-fructose	5180 ± 229	0.998	-0.27
6	D-glucose	163 ± 16	0.993	-0.27
7	D-fructose	5590 ± 201	0.999	0.10 [b]
7	D-glucose	198 ± 20	0.993	0.10 [b]
10	D-fructose	- [c]	-	0.78
10	D-glucose	- [c]	-	0.78
17	D-fructose	- [c]	-	0.78

Table 3: Stability constants (K) for polyol-boronic acid azo dye complexes at pH 11.32; [a] - value for SO_3^-, [b] - value for CO_2^-, [c] - could not be determined from absorbance data

A number of different linear free-energy relationships (LFERs), notably the most widely used Hammett relationship,[147] have been applied to investigate substituent effects in benzenoid systems. If a comparison is made between the stability constants (*K*) and the relevant Hammett σ-values for the phenylazo ring substituents (Table 3), a trend is apparent for the *para*-substituted dyes. The stability constant is seen to increase as the σ-value becomes less positive, i.e. the ring substituent becomes less electron-withdrawing in nature. Dye **7** shows the highest binding constant. Dye **7** is the only *meta*-substituted dye in the series and, as such, will have an inductive effect on the chromophoric system, rather than the conjugative resonance influence of the *para*-substituted dyes. Direct comparison between the stability constants of the *para*- and *meta*-substituted dyes is therefore not really applicable.

If the effect of the phenylazo ring *para*-substituent on the boron-nitrogen interaction is considered, it may help to explain why there is a decrease in the value of the boronic acid-saccharide stability constant with the increase in electron-withdrawing character of the substituent. A strong electron-withdrawing substituent, such as the nitro group, will decrease the electron density on the anilinic nitrogen. This will reduce the strength of the boron-nitrogen interaction compared to a weaker electron-withdrawing substituent, such as the carboxyl group. This will also be reflected in the saccharide-binding event, as the boron-nitrogen interaction is strengthened upon complexation. It follows that the stronger the initial boron-nitrogen interaction, the stronger the bound interaction will be and hence the easier the saccharide will bind. Accordingly, this results in a higher stability constant for electron-donating substituents, including dye **6**'s methoxy group.

It was decided to carry out some saccharide titrations at near neutral pH to investigate further the effect of pH on the equilibria. UV-VIS absorbance titrations of dyes **3**, **10**

and **17** with D-fructose and D-glucose were performed in a pH 8.21 aqueous methanolic buffer solution [52.1wt% methanol (KCl, 0.01000 mol dm^{-3}; KH_2PO_4, 0.002752 mol dm^{-3}; Na_2HPO_4, 0.002757 mol dm^{-3})].[144] The pH of the buffer was chosen so that it was below the pK_a's of the unbound dyes, which are typically around 10 (Table 2). This should mean that, at the beginning of the titrations, the major solution dye species should be that containing the boron-nitrogen interaction (**C** in Scheme 11).

In all three cases, as the concentration of saccharide was increased, a spectral shift to longer wavelength was observed (see Figure 41, Figure 42, Figure 43 and Appendix). The shifts, and subsequent colour changes (Figure 44), were not as pronounced (< 20 nm) as the high pH titrations with dyes **3-7**. The stability constants (K) of the boronic acid dye-saccharide complexes can again be calculated using Equation 2, assuming a 1:1 boronic acid-saccharide binding event. Curve fits for dyes **3**, **10** and **17** with D-fructose and D-glucose can be found in the Appendix. Table 4 shows the results of these calculations for the three dyes.

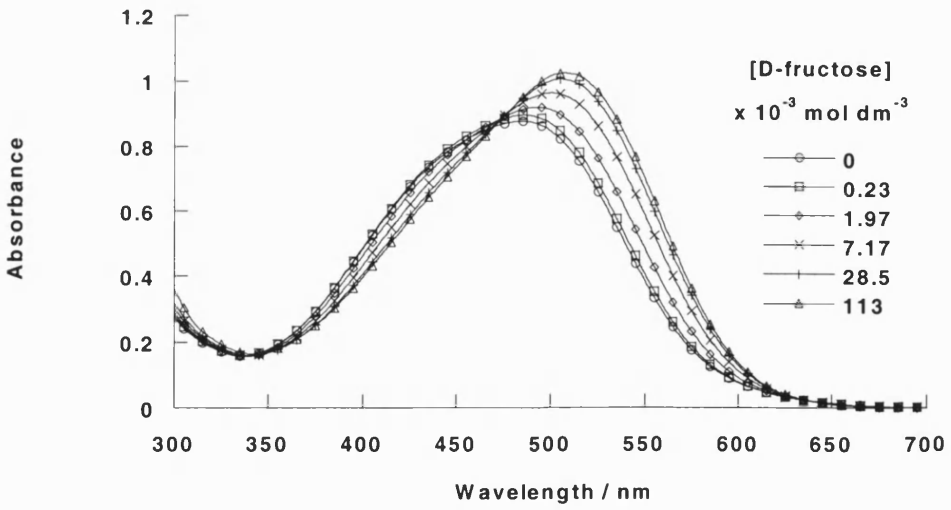

Figure 41: Absorption-spectral changes of dye **3** (2.83 x 10^{-5} mol dm^{-3}) with increasing concentration of D-fructose at pH 8.21

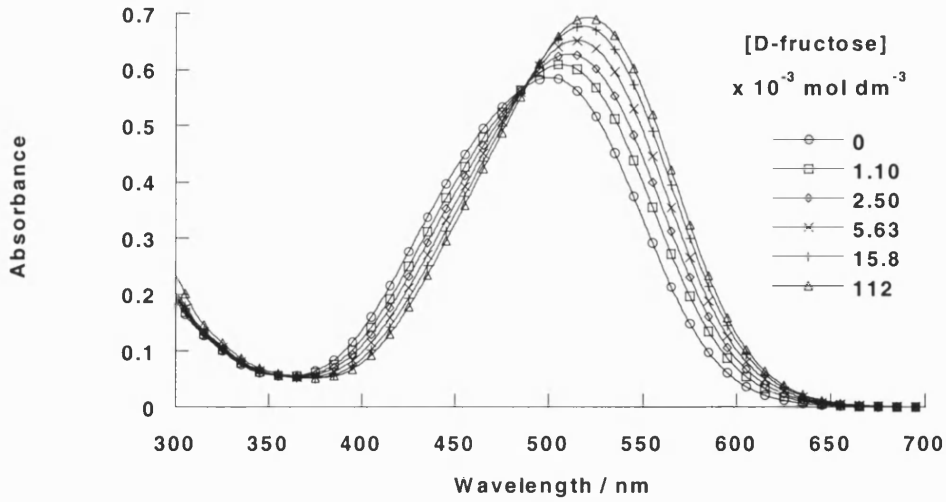

Figure 42: Absorption-spectral changes of dye **10** (2.00 x 10^{-5} mol dm^{-3}) with increasing concentration of D-fructose at pH 8.21

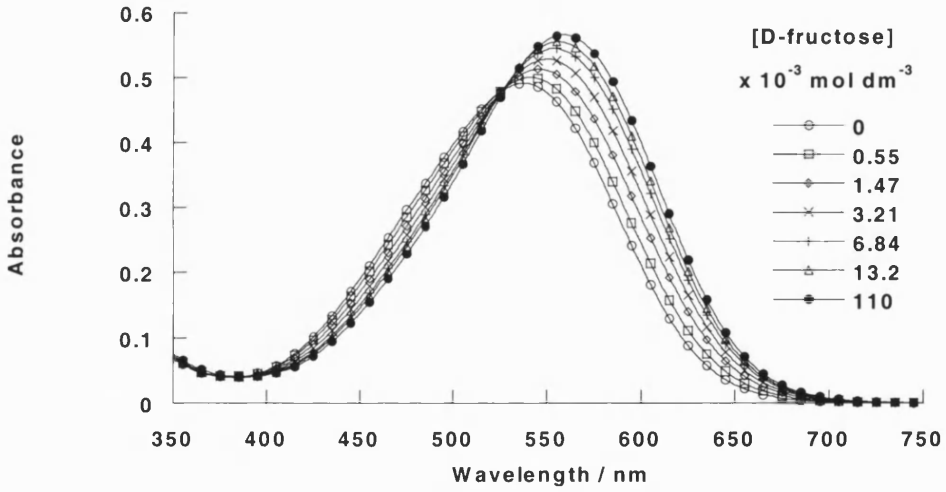

Figure 43: Absorption spectral changes of dye **17** (1.76 x 10^{-5} mol dm^{-3}) with increasing concentration of D-fructose at pH 8.21

Dye **3**'s spectral shift was also in the opposite direction to that seen at pH 11.32. However, what is apparent is that when dye **3** is complexed to saccharide, it does not matter what the starting pH is, the final solution saccharide-bound species is always the same, with an absorbance maximum at 509 nm. In contrast, both dyes **10** and **17**, have only one high pH species, no matter if it is saccharide-bound or not. This is shown in

Figure 38 and Figure 42 for dye **10**, where the absorbance maximum of the high pH species is at 521 nm in both instances. The equilibria involved with these dyes will be discussed in the following section.

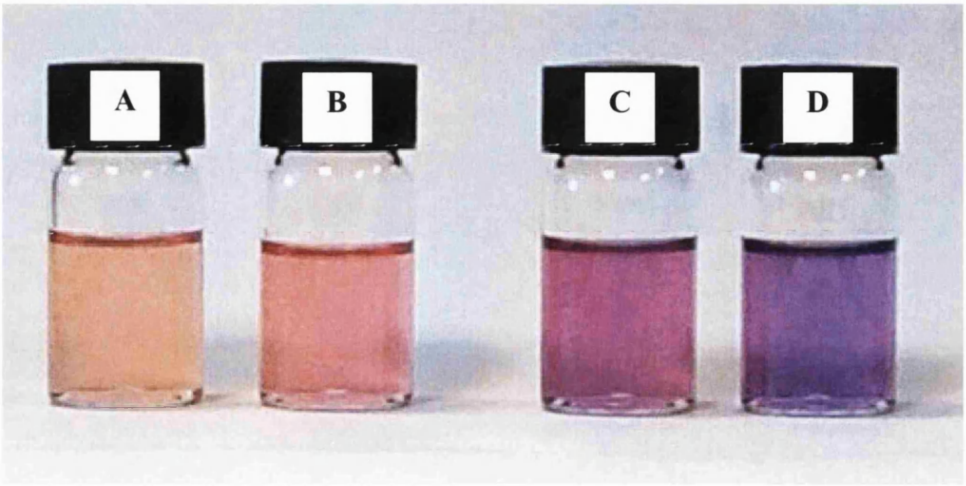

Figure 44: Colour-absorbance changes upon addition of D-frucose to dyes **3** and **17** (both 2.00 x 10^{-5} mol dm^{-3}) at pH 8.21; **A**: dye **3** with no saccharide; **B**: with 0.05 mol dm^{-3} D-fructose; **C**: dye **17** with no saccharide; **D** dye **17** with 0.05 mol dm^{-3} D-fructose

Dye	Polyol	K / dm^3 mol^{-1}	r^2
3	D-fructose	291 ± 24	0.994
3	D-glucose	26 ± 6	0.981
10	D-fructose	371 ± 7	0.999
10	D-glucose	23 ± 1	0.998
17	D-fructose	431 ± 16	0.999
17	D-glucose	17 ± 1	0.999

Table 4: Stability constants (K) for polyol-boronic acid azo dye complexes at pH 8.21

An interesting point to note about the stability constants at pH 8.21 (Table 4) is that they are approximately a factor of ten smaller than those at pH 11.32 (Table 3). As discussed

earlier in reference to Scheme 12, the possibility of neutral boronic acid binding to saccharides (K_a') rather than anionic binding (K_a), cannot be ruled out. It is known that stability constants measured at near neutral pH are lower than the corresponding anionic stability constants at higher pH.[82, 141] At pH 8.21, the free boronic acid azo dyes are below their pK_a (~10), so it is likely that some neutral binding is occurring in this case.

2.3.3 Saccharide-Boronic Acid Azo Dye Equilibria

This section will attempt to explain the observations made in the preceding absorption experiments for the various dyes and their interaction with saccharide. This will be accomplished by considering the free and saccharide bound boronic acid equilibrium species at different pH.

At intermediate pH values Shinkai has proposed that a boron-nitrogen interaction is prevalent in his *N*-methylated boronic acid azo dye, whereas at high and low pH this bond is broken.[72] Species **A**, **B** and **C** in Scheme 14 show this interpretation for unbound dye **3**. What makes dyes **3-7**'s equilibria more interesting is the presence of the anilinic hydrogen, which gives rise to different species at high pH, compared to *N*-methylated analogues, including dye **10**. This apparently simple modification in the molecular structure is responsible for the enhanced response of these dyes relative to those previously reported. Scheme 14 shows the proposed equilibrium species for dye **3** responsible for the observed colour change, consistent with the experimental results to date.

In the absence of saccharide, at pH 11.32, the observed colour is purple and in the presence of saccharide the colour is red (Figure 36). From previous work it is known that when saccharides form cyclic boronate esters with boronic acids, the Lewis acidity

of the boronic acid is enhanced and therefore the Lewis acid-base interaction between the boronic acid and the amine is strengthened. This stronger boron-nitrogen interaction will favour the red species over the equivalent saccharide bound purple species. The reason for this can be understood by considering species **B** and **D** in Scheme 14. In the presence of saccharide the boron-nitrogen interaction in species **D** is stronger than that in species **B**. The increased boron-nitrogen interaction of species **D** will make the anilinic proton of species **D** more acidic than in the corresponding unbound species **B**. Therefore, at higher pH, species **D** will deprotonate to form the red species **F** rather than the tetrahedral boronate anion (species **E**), whereas the weaker boron-nitrogen bond in species **B** is broken by hydroxide ion to form the purple coloured species **C**.

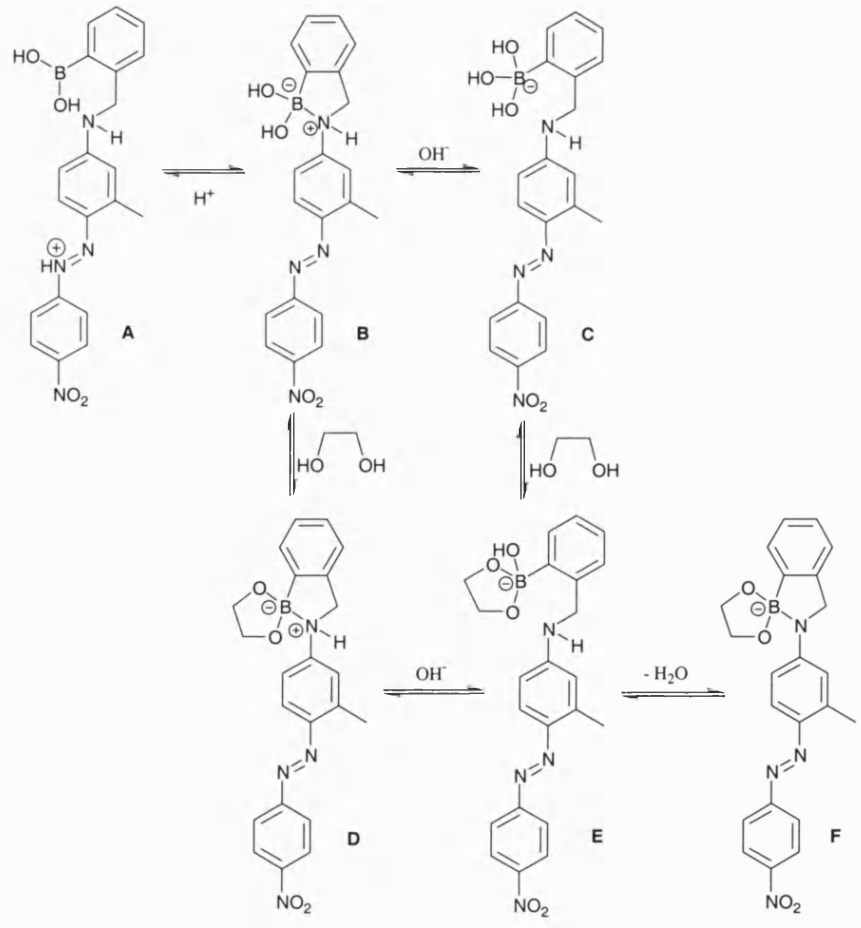

Scheme 14: Proposed pH and saccharide dependent equilibria species for dye **3**

In the pH 8.21 buffer solution, a small shift to longer wavelength is observed (Figure 41). This shift can be explained by reference to Scheme 14. The free boronic acid in the neutral pH range (species **B**) obviously binds to saccharide to form the deprotonated boron-nitrogen species **F**. Because there is only a small electronic differentiation between species **B** and **F**, i.e. loss of a single proton, this manifests itself in a small spectral shift in comparison to the higher pH change (species **C** to **F**).

The colour change arises from the different electronic environment of the anilinic nitrogen. As mentioned earlier, the anilinic nitrogen is conjugated to the azo chromophore. A change in the environment of this nitrogen leads to changes in the energy levels of the n and π^* orbitals of the azo chromophore and hence to a change in the absorption energy and wavelength. The substituent on the phenyl azo ring will also play a part in this. The stronger the electron-withdrawing group on this ring, the more acidic the anilinic proton will be, and consequently the easier the high pH boron-nitrogen species can form. This probably explains why dye **3**, with its highly electron-withdrawing nitro group, gives a larger spectral shift than dyes **4-7**, which have weaker electron-withdrawing functionalities and, consequently, less acidic anilinic protons.

It must be stressed that the equilibria discussed here for dye **3** and its derivatives are only proposals that fit the experimental data. Electrospray Ionisation Mass Spectrometry (ESIMS) was used to see if any of the proposed equilibrium species could be observed. The fructose-bound dye **3** high pH red species (*m/z* 533), **F** in Scheme 14, was detected by negative ion ESIMS.

The proposal of these equilibrium species also explains why dye **10** did not give a visible spectral shift on saccharide binding at high pH. Because the anilinic nitrogen is

tertiary in nature rather than secondary, there is no possibility of deprotonation, so the high pH boron-nitrogen bond cannot form (Scheme 15). Hence there is no electronic differentiation between the equilibrium species at high pH (**I** and **K** in Scheme 15) and as a result no spectral shift is observed. The small spectral shift observed in the pH 8.21 buffer solution must be caused by the breaking of the boron-nitrogen bond in species **H** (Scheme 15), to form the saccharide bound boronate anion (species **K** in Scheme 15).

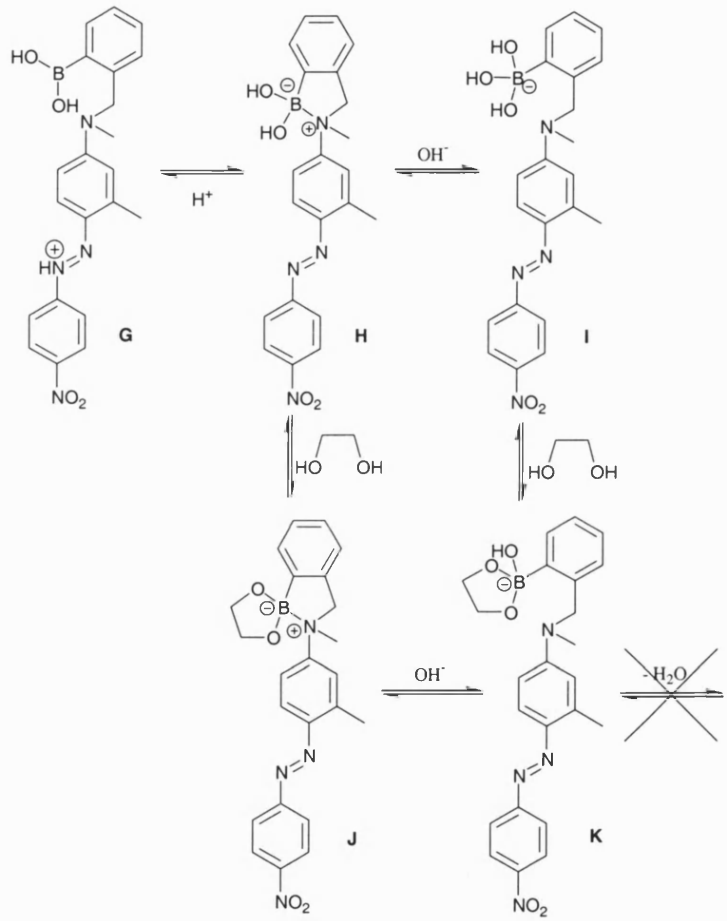

Scheme 15: Proposed pH and saccharide dependent equilibria species for dye **10**

So why does dye **17**, which has an anilinic proton, not behave in the same way as dye **3**, but show similar behaviour to dye **10**? The answer is probably due to steric interactions involving the proton in the 8-position of the naphthalene ring. At neutral pH unbound dye **17** forms the usual boron-nitrogen bond (species **M** in Scheme 16), which is broken

by hydroxide ion to form species **N**. If the boron-nitrogen interaction is to be maintained upon saccharide binding at neutral pH, including in the pH 8.21 buffer, the naphthalene 8-proton would experience an unfavourable steric interaction with either the dye's benzylic protons (species **O'**) or the bound saccharide (species **O**). This must force the saccharide bound dye to adopt the less sterically crowded boronate anion structure (species **P**). Likewise, the deprotonated boron-nitrogen species **Q** does not form because of the same steric interaction that would occur in species **O** and **O'**.

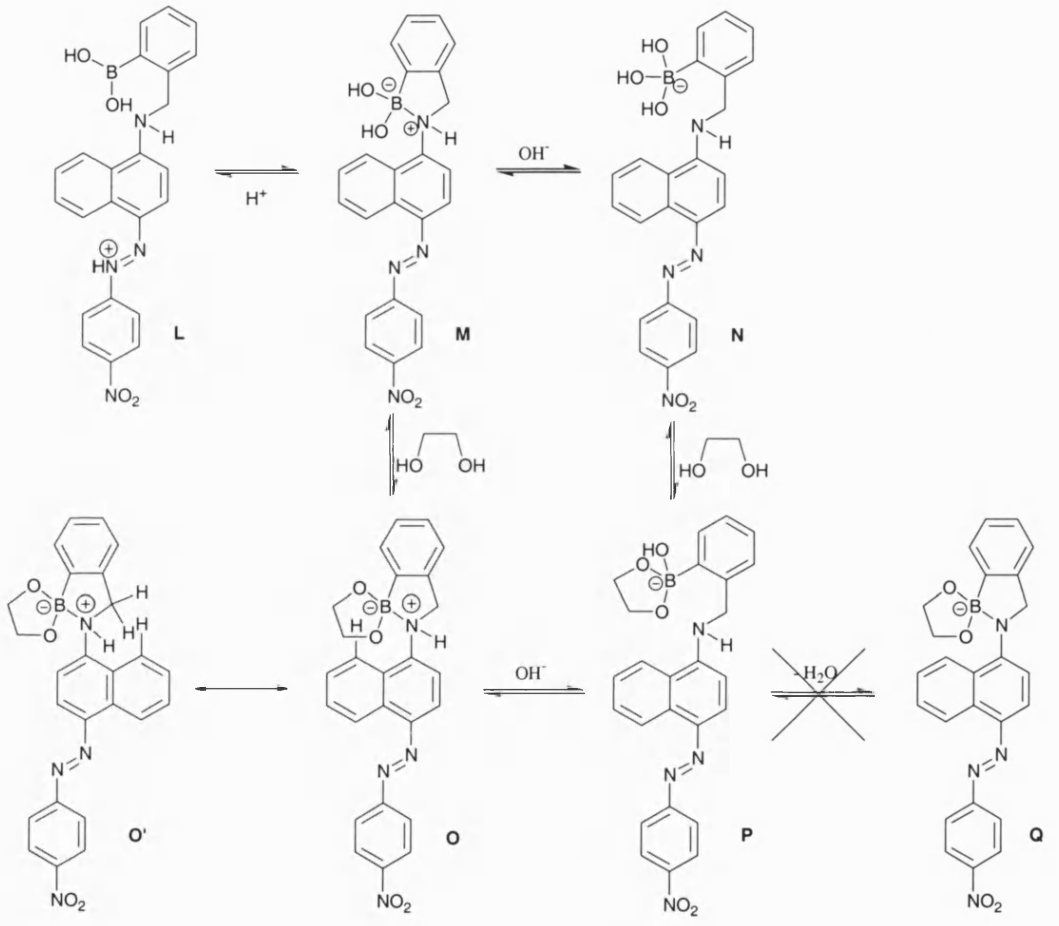

Scheme 16: Proposed pH and saccharide dependent equilibria species for dye **17**

Consequently, at whatever pH saccharide binds to dye **17**, species **P** always forms. With regards to the azo chromophore, species **P** is electronically indistinguishable from

species **N**. This accounts for the lack of a spectral shift at pH 11.32 (Figure 39), as species **N** goes to species **P** under these conditions.

2.3.4 Absorption Titrations with a Boronic Acid Tricyanovinyl Dye

The earlier investigation of boronic acid azo dyes has given an insight into the dyes' interaction with saccharide at different pH. The obvious progression of this work was to see what effect changing the chromophore away from the azo group would have on the dye-saccharide equilibria. The tricyanovinyl dye **14**, synthesised earlier, was chosen to examine this feature.

Absorbance-pH titrations, from pH 2 to 12, with boronic acid dye **14** were performed in aqueous methanolic solutions containing 0.05 mol dm^{-3} sodium chloride, with and without D-fructose. The absorbance spectra from both of these titrations are shown in Figure 45 and Figure 46.

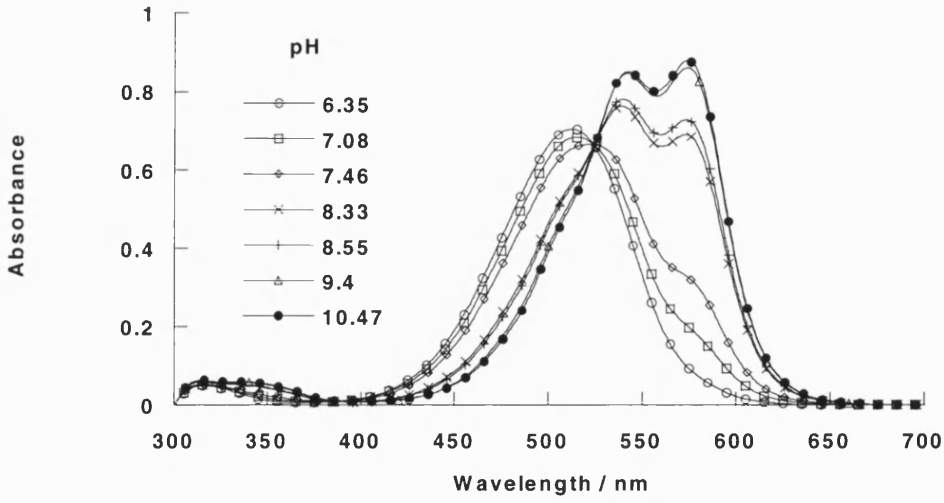

Figure 45: Absorption-pH spectral changes of dye **14** (3.14 x 10^{-5} mol dm^{-3})

The two sets of spectra show the same absorption at 512 nm at a pH of below 7, but show a marked difference above this pH. As the pH is raised above 7, the unbound dye **14** shows a spectral shift to around 560 nm with an increasing amount of structure to the spectra. In contrast, when bound with saccharide, dye **14**'s higher pH spectra only shift to a single peak at 530 nm. The response of dye **14** to pH, both with and without saccharide, is comparable to that of dye **3**.

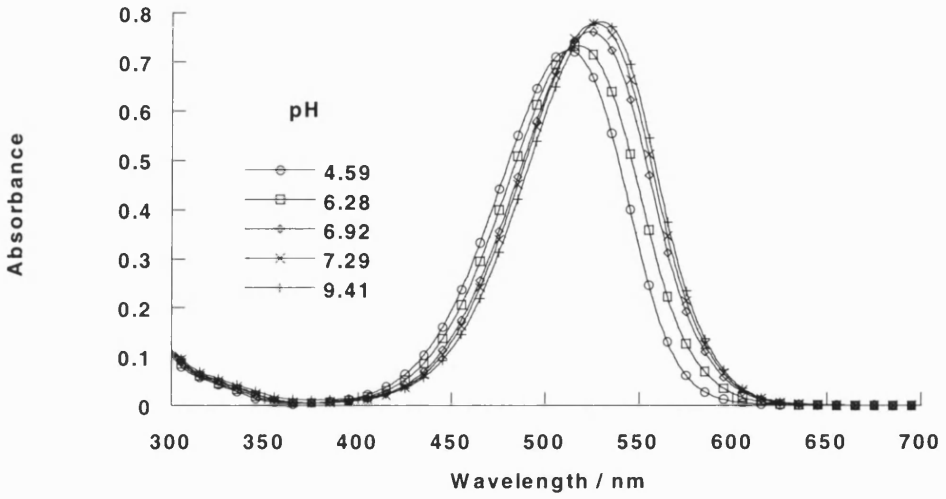

Figure 46: Absorption-pH spectral changes of dye **14** (3.14×10^{-5} mol dm^{-3}) in the presence of 0.05 mol dm^{-3} D-fructose

Dye	Without D-fructose		With D-fructose		ΔpK_a
	pK_a	r^2	pK_a'	r^2	
14	7.81 ± 0.02	0.999	6.47 ± 0.04	0.997	1.34

Table 5: pK_a values and coefficients of determination (r^2) for boronic acid tricyanovinyl dye **14**

Figure 47 shows the absorption-pH profile of dye **14**, with and without the presence of D-fructose. The plot shows the expected shift in the pK_a of the boronic acid upon the addition of D-fructose. The pK_a of this interaction was calculated from the absorption

data using Equation 1.[44, 143] The curves shown in Figure 47 were fitted using this method. Table 5 shows the results of this calculation for dye **14**.

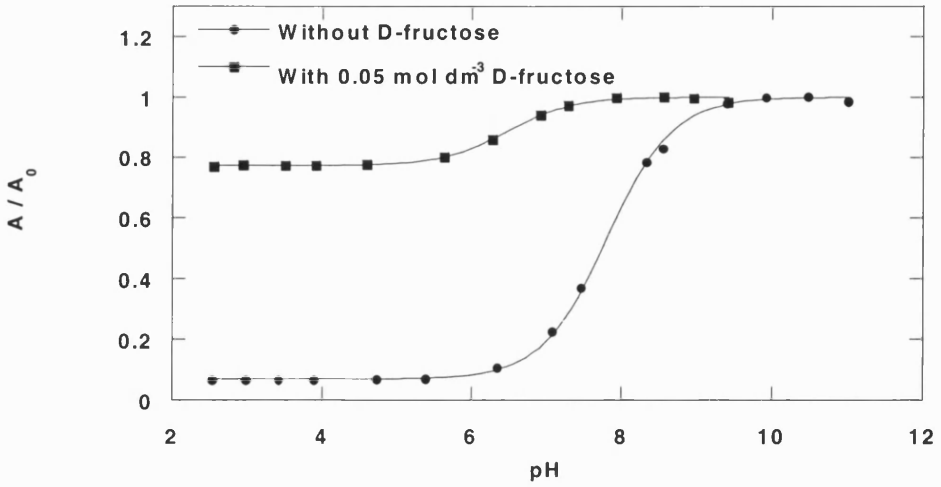

Figure 47: Absorption-pH profile of dye **14** with (575 nm) and without D-fructose (530 nm)

The pK_a of free dye **14** is approximately 2.5 pK_a units lower than that of the related boronic acid azo dyes studied earlier. Accordingly, the ΔpK_a shift is not as great with dye **14** when saccharide is added. The change in the chromophore to the highly electron-withdrawing tricyanovinyl group is almost certainly the reason for the lower pK_a value of dye **14**. The tricyanovinyl group is in conjugation with the anilinic nitrogen in a similar manner to how the azo chromophore was. The boron-nitrogen interaction will be weaker with the tricyanovinyl chromophore, as the lone pair of electrons is less available than in the azo derivatives. In other words the tricyanovinyl group makes the anilinic nitrogen less basic, and hence the boron-nitrogen bond is broken at a lower pH. In fact the anilinic nitrogen is not basic enough to be protonated, even at low pH. The pH spectra in Figure 45 and Figure 46 show that the near neutral pH species is the same as the low pH species, as there is no spectral shift observed upon lowering the pH.

Absorption-saccharide titrations were performed on dye **14** in the previously used pH 8.21 aqueous methanolic buffer solution.[144] Titrations in buffers above pH 10 could not be carried out because the tricyanovinyl group is very unstable towards base at these concentrations, and would quickly decompose. Figure 48 shows the absorption spectra for the titration with D-fructose and Figure 49 shows the visible colour change associated with this.

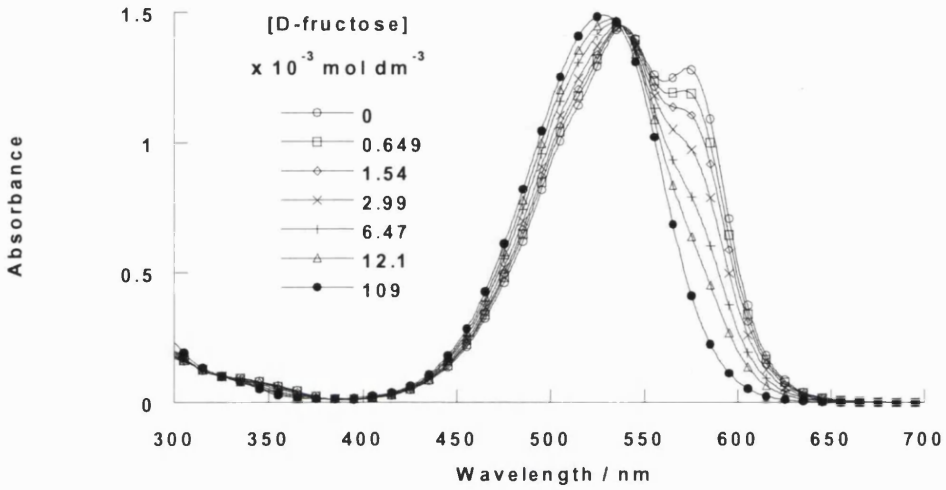

Figure 48: Absorption spectral changes of dye **14** (3.14 x 10^{-5} mol dm^{-3}) with increasing concentration of D-fructose at pH 8.21

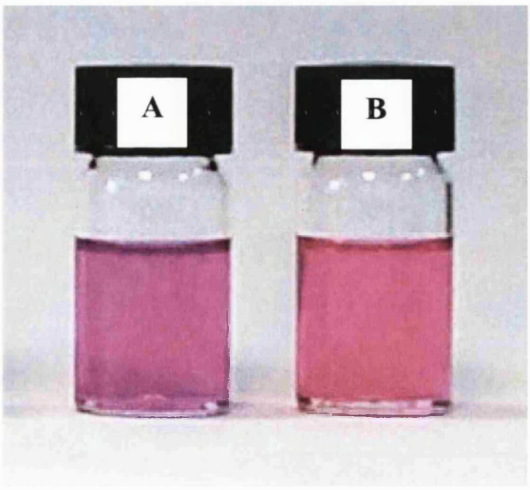

Figure 49: Colour-absorbance changes upon addition of D-frucose to dye **14** (2.00 x 10^{-5} mol dm^{-3}) at pH 8.21; **A**: dye **14** with no saccharide; **B**: with 0.05 mol dm^{-3} D-fructose

The stability constants (*K*) of the boronic acid dye-saccharide complexes can again be calculated using Equation 2, assuming a 1:1 boronic acid-saccharide binding event. The curve fits for dye **14** with D-fructose and D-glucose can be found in the Appendix. The results of the calculations are presented in Table 6. The stability constants are lower than the corresponding values for the boronic acid azo dyes. This is probably because the boron-nitrogen interaction is weaker in dye **14** due to the highly electron-withdrawing nature of the tricyanovinyl group.

Dye	Polyol	K / dm^3 mol^{-1}	r^2
14	D-fructose	170 ± 6	0.999
14	D-glucose	8 ± 0.3	0.999

Table 6: Stability constants (*K*) for saccharide-boronic acid dye **14** complexes at pH 8.21

Figure 48 shows that, as D-fructose binds to dye **14**, a significant spectral shift to lower wavelength occurs. Figure 49 shows the colour dependence of dye **14** with added D-fructose. The dye changes colour from purple to pink. This is very similar behaviour to that of azo dye **3** at pH 11.32. It is, therefore, not unfeasible to suggest that equivalent equilibria species are involved in the case of the tricyanovinyl dye (Scheme 17). Another point to note is that that the pH at which this spectral change occurs is now approaching the biologically acceptable range, compared to the highly basic pH used with dye **3**. This means that derivatives of dye **14** could possibly be used for sensing saccharides in blood and other biological samples.

Unbound dye **14** at lower pH contains a weak boron-nitrogen interaction (species **A** in Scheme 17), which is broken by hydroxide ion to form species **B**. Upon saccharide binding this interaction is strengthened, as previously discussed. This stronger boron-nitrogen interaction will favour the pink species **E** over the equivalent saccharide bound purple species **D**. The reason for this can be understood by considering species **A** and **C** in Scheme 17.

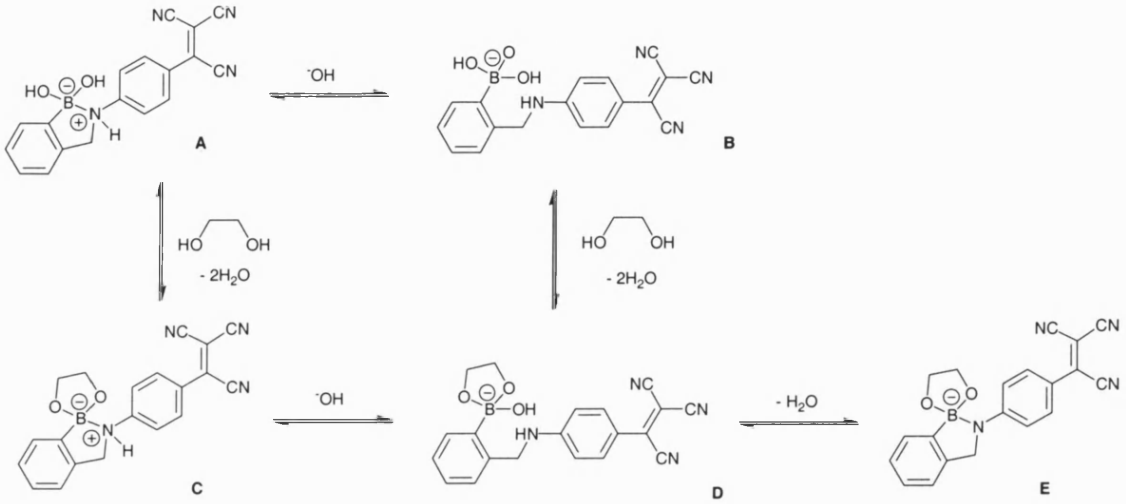

Scheme 17: Proposed pH and saccharide dependent equilibria species for dye **14**

In the presence of saccharide the boron-nitrogen interaction in species **C** is stronger than that in species **A**. The increased boron-nitrogen interaction of species **C** will make the anilinic proton of species **C** more acidic than in the corresponding unbound species **A**. Therefore, at higher pH, species **C** will deprotonate to form the pink species **E** rather than the tetrahedral boronate anion (species **D**), whereas the weaker boron-nitrogen bond in species **A** is broken by hydroxide ion to form the purple coloured species **B**. In the saccharide titration at pH 8.21, dye **14** is initially in the form of species **B**. As the saccharide concentration is increased, binding takes place to form the deprotonated boron-nitrogen species **E**.

2.3.4 Summary

- The interaction of saccharide with a series of boronic acid azo dyes and a boronic acid tricyanovinyl dye has been investigated using UV-VIS spectrophotometry.
- The pH dependence of this saccharide-dye interaction has also been evaluated.
- The well-known decrease in the pK_a value of the boronic acid is observed upon saccharide binding to the dyes.
- All of the dyes studied have shown a spectral response to saccharide, although the pH at which this occurs varies.
- Boronic acid azo dyes containing a secondary anilinic nitrogen centre have all shown significant spectral shifts upon addition of saccharide at high pH.
- The nitro-substituted azo dye **3**, at pH 11.32, has shown the largest spectral shift reported to date in such a system. A visible colour change from purple to red (55 nm) was observed upon binding to D-fructose.[145]
- A relationship between the Hammett substituent σ–value and the stability constant (K) of D-fructose binding to *para*-substituted azo dyes **3-6** has been identified.
- As the electron-withdrawing nature of the substituent increases, the boron-nitrogen interaction is weakened and the value of the stability constant subsequently decreases.
- The proposal of a high pH deprotonated boron-nitrogen bonded species has explained the enhanced response of the dyes with secondary anilinic nitrogens.
- The effect of saccharide on all of the boronic acid azo dyes at near neutral pH produces a small spectral shift to longer wavelengths.

- *N*-methylated boronic acid azo dye **10** shows a reduced spectral shift due to its inability to form a saccharide-bound high pH deprotonated boron-nitrogen bonded species.
- Boronic acid azo dye **17**, with a pendant naphthalene ring, cannot form saccharide bound species with a boron-nitrogen interaction, due to unfavourable steric effects of the naphthalene ring protons.
- Boronic acid tricyanovinyl dye **14** has shown similar spectral behaviour to that of dye **3**. Equivalent equilibria, including that of the saccharide-bound deprotonated anilinic nitrogen species, are proposed to explain dye **14**'s performance.
- The large spectral shift of dye **14** is observed at the biologically acceptable pH of 8.21. The decrease in the pH of this interaction is accounted for by the increased electron-withdrawing nature of the tricyanovinyl group.

2.4 Interaction of Boronic Acid Dyes with Fluoride

This section will examine the interaction of the fluoride anion with some of the boronic acid dye molecules that were used in the saccharide studies. Standard Ultraviolet-Visible (UV-VIS) spectrophotometry techniques were used to study the binding of the dyes to potassium fluoride. The effect of other potassium halides on the dyes was also investigated for comparison purposes. The aim of the research was to see whether a spectral shift (colour change) would actually occur upon a fluoride-binding event. There is interest in following the uptake and metabolism of fluoride in both plants and animals, as well as in the analysis of drinking water. Coloured sensor systems for fluoride could have applications in these areas. Colorimetric assays for fluoride have been well documented.[92] However, the use of designed receptors for colorimetric fluoride detection is a more recent advance.[86] The use of boronic acid receptors in this field has been limited to a few systems based on electrochemical[112, 116, 122] or fluorescent detection.[115]

Previous boronic acid systems have been based on the Lewis acid-base interaction between boron and anions. The systems have shown an exclusive selectivity for fluoride over other halide ions. When boron binds to certain anions, including fluoride, the hybridisation of the boron centre changes from sp^2 to sp^3 (Scheme 18).[148] Multiple binding of fluoride to the boron centre is possible (Scheme 18). The tri-fluoro adduct has been shown to be the favoured species in simple boronic acids such as phenylboronic acid and 2-naphthylboronic acid.[115, 117] A mono-fluoride adduct has been observed and is thought to be stabilised by hydrogen bonding to a protonated amine (Figure 50).[115]

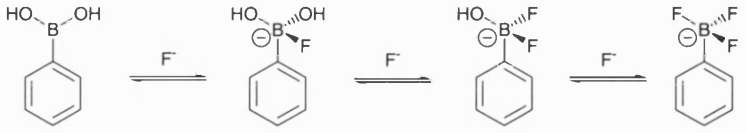

Scheme 18: Interaction of fluoride with simple boronic acids

Figure 50: Formation of a hydrogen bonded stabilised mono-fluoride adduct

There have been no studies made on the effect of fluoride on boronic acid appended dyes. The following UV-VIS titrations were designed to probe this interaction and to explore the equilibria involved.

2.4.1 Absorption-Halide Titrations with Boronic Acid Dyes

Initial investigations began with boronic acid azo dye **3** (Scheme 2) and model azo dye **12** (Scheme 6). UV-VIS absorption titrations of dyes **3** and **12** with solid potassium fluoride were performed in a methanolic solution. HPLC methanol was chosen as the solvent to offset any effects of water on the system. Figure 51 and Figure 52 show the respective absorbance spectra for the titrations with dyes **3** and **12**.

When dye **3** is titrated with fluoride the colour of solution changes from orange (450 nm) to claret (563 nm), a spectral shift of 113 nm. Figure 53 shows the observed colour change upon fluoride addition. In contrast, dye **12** shows no colour change upon addition of fluoride (Figure 54), only an increase in the intensity of absorption. This result shows that fluoride must be binding to the boronic acid centre in dye **3** and that

the spectral shift is not an effect of fluoride attack on the azo group, as revealed by the lack of a colour change in dye **12**.

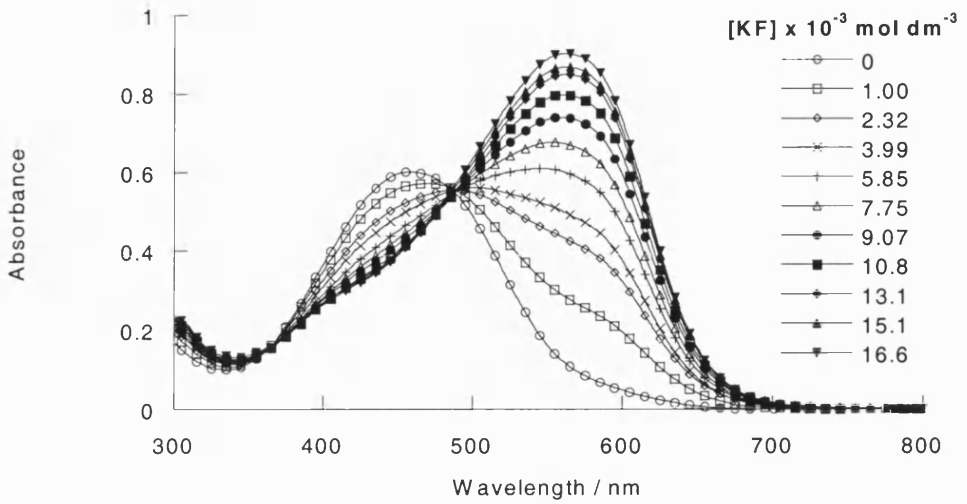

Figure 51: Absorption spectral changes of dye **3** (3.16 x 10^{-5} mol dm^{-3}) with increasing concentration of potassium fluoride in methanol

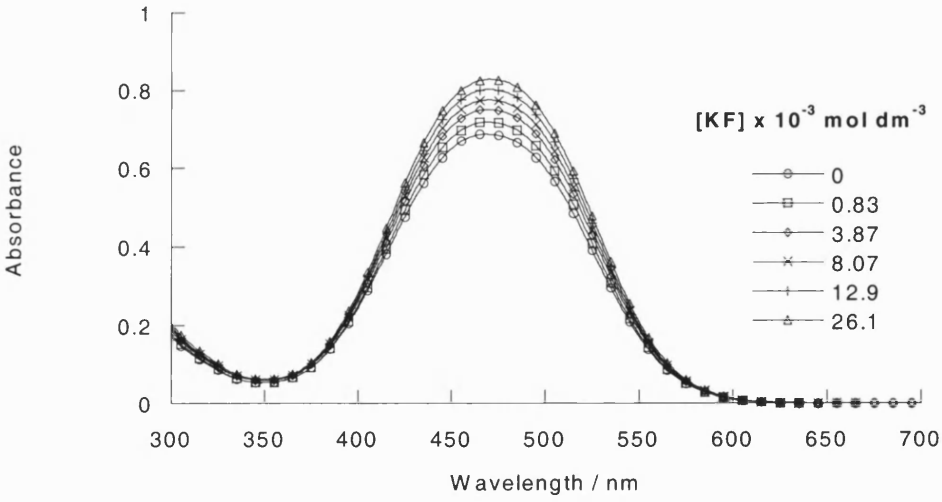

Figure 52: Absorption spectral changes of dye **12** (2.89 x 10^{-5} mol dm^{-3}) with increasing concentration of potassium fluoride in methanol

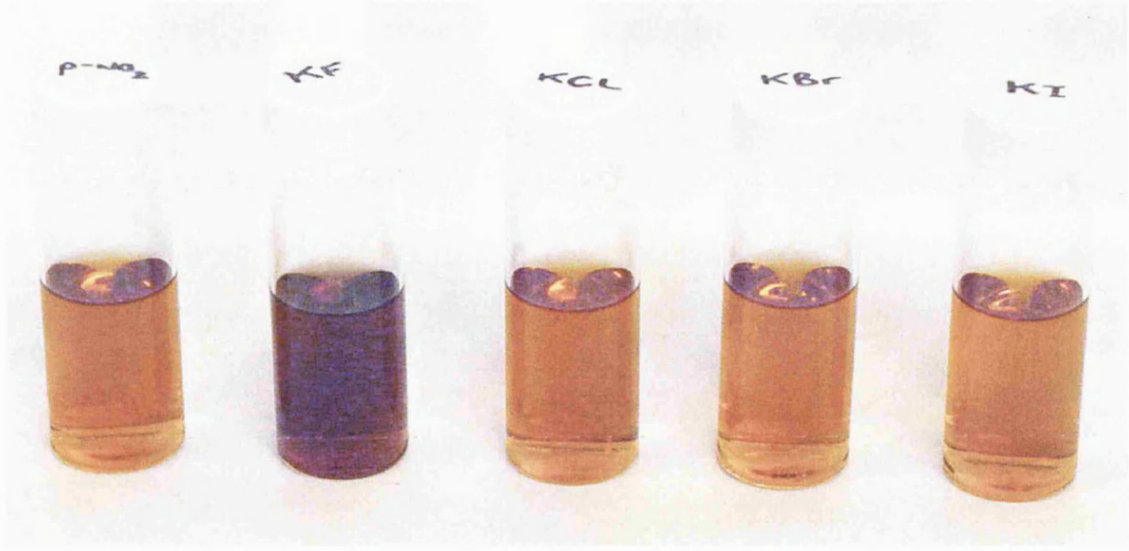

Figure 53: Colour of dye **3** (3.48 x 10^{-5} mol dm^{-3}) in methanol with and without 0.01 mol dm^{-3} KX. From left to right: free **3**; **3** with KF; **3** with KCl; **3** with KBr; **3** with KI.

Figure 54: Colour of dye **12** (3.48 x 10^{-5} mol dm^{-3}) in methanol with and without 0.01 mol dm^{-3} KF. From left to right: free **12**; **12** with KF.

When the titration of dye **3** was repeated separately with potassium chloride, bromide and iodide, a similar phenomenon to that of dye **12**'s titration with fluoride was observed. Again there is no spectral shift, only an absorbance increase at 450 nm (see Figure 55 and Appendix for absorbance spectra). The colour of the dye remains orange throughout the halide addition (Figure 53). These titrations show that boronic acid dye **3** binds selectively to fluoride. In all of the titrations, an increase in the intensity of absorbance occurs upon adding potassium halide. This can be attributed to an increase

in the dielectric constant of the solution. As all of the titrations are performed in unbuffered methanol, adding halide salt will change the polarity of the solvent. It is well documented that changes in solvent polarity can affect the intensity of absorbance of azo dye molecules.[149]

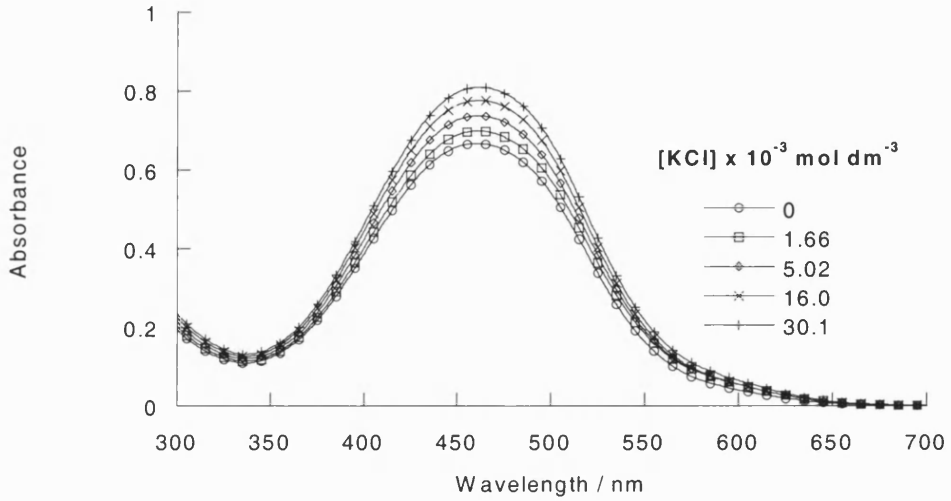

Figure 55: Absorption spectral changes of dye **3** (3.16 x 10^{-5} mol dm^{-3}) with increasing concentration of potassium chloride in methanol

Further potassium halide titrations were performed on boronic acid dyes **10** (Scheme 5), **14** (Scheme 9) and **17** (Scheme 7) using the same conditions. The absorbance spectra for each of the respective dyes interaction with potassium fluoride are shown in Figure 56, Figure 57 and Figure 58. Those for the other potassium halide titrations can be found in the Appendix. All of the dyes show a spectral shift to longer wavelength upon addition of fluoride in a similar manner to that of dye **3**. Again the dyes experience no spectral change upon addition of other halides, signifying that they are fluoride selective.

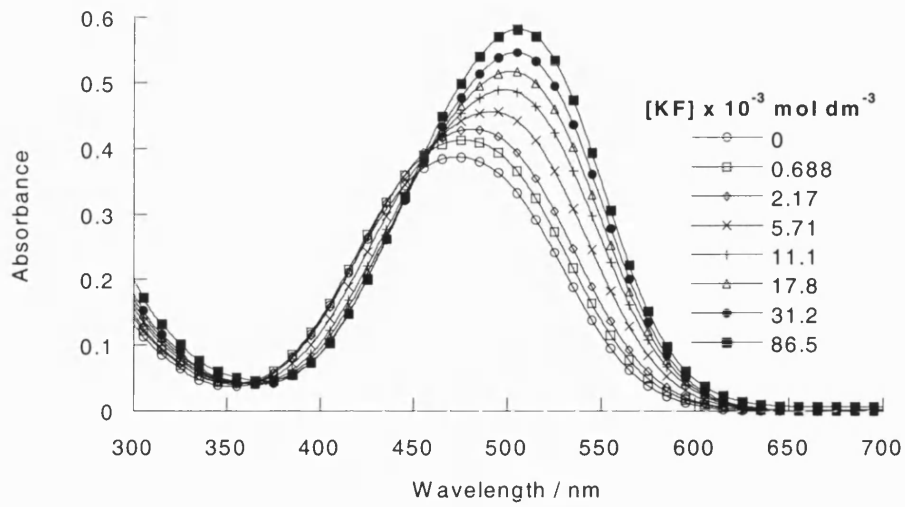

Figure 56: Absorption spectral changes of dye **10** (2.93 x 10^{-5} mol dm^{-3}) with increasing concentration of potassium fluoride in methanol

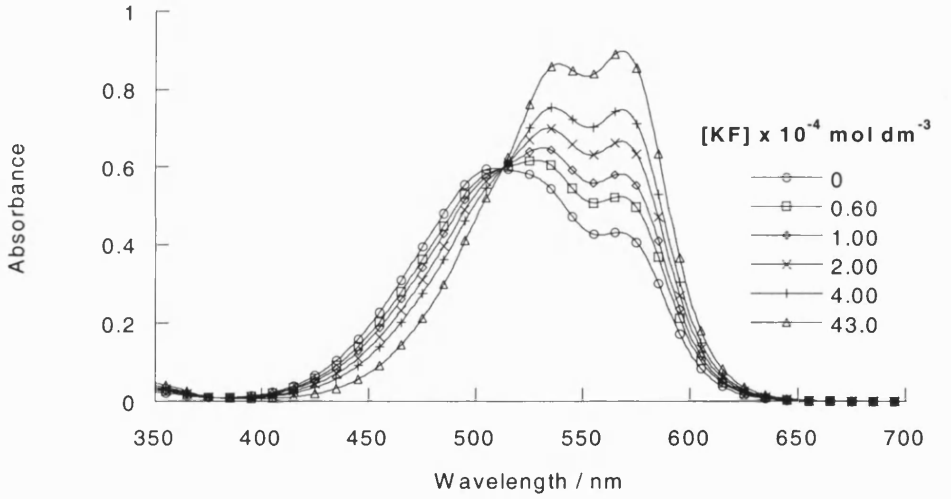

Figure 57: Absorption spectral changes of dye **14** (1.57 x 10^{-5} mol dm^{-3}) with increasing concentration of potassium fluoride in methanol

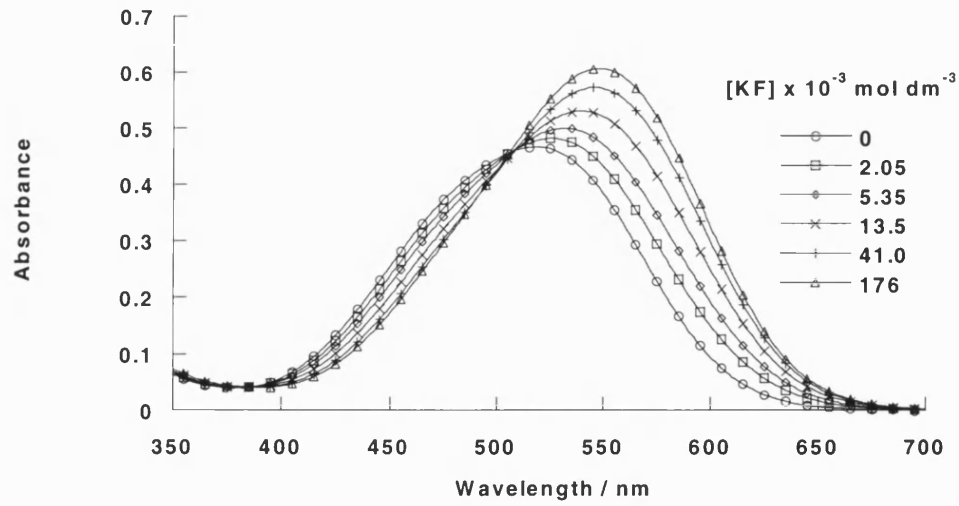

Figure 58: Absorption spectral changes of dye **17** (1.76 x 10^{-5} mol dm^{-3}) with increasing concentration of potassium fluoride in methanol

The stability constants (*K*) of the boronic acid dye-fluoride complexes can be calculated using Equation 2.[44, 143] The stability constant curves were analysed in KaleidaGraph as before. Figure 59 shows an example curve fit using Equation 2 for dye **3**'s interaction with fluoride. Curve fits for the other dyes can be found in the Appendix. Table 7 gives the results of these calculations for all of the boronic acid dyes studied.

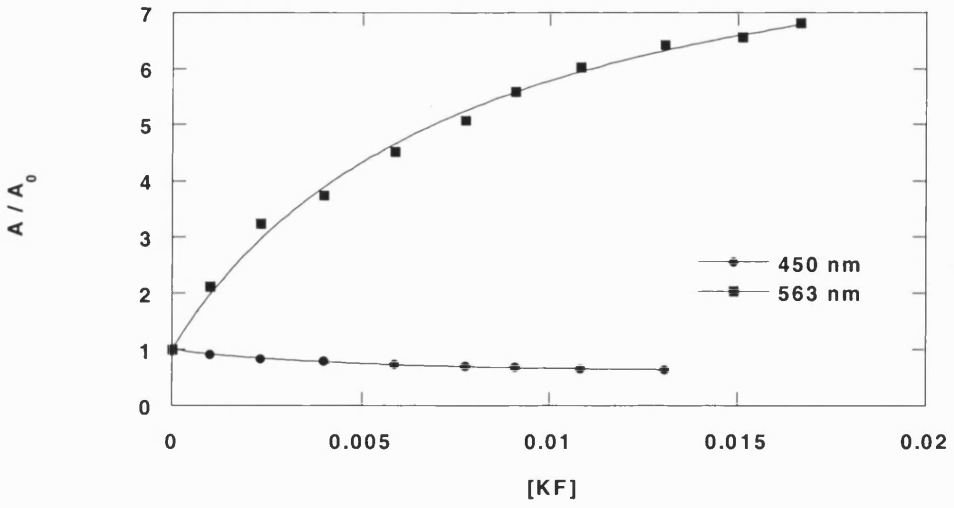

Figure 59: Curve fits to determine the stability constant of dye **3** with potassium fluoride at 450 nm and 563 nm

Dye	*K* (High λ) / dm^3 mol^{-1}	r^2	*K* (Low λ) / dm^3 mol^{-1}	r^2
3	130 ± 13	0.995	195 ± 18	0.996
10	124 ± 5	0.997	- [a]	-
14	9560 ± 490	0.997	- [a]	-
17	120 ± 8	0.995	- [a]	-

Table 7: Stability constants (*K*) for fluoride-boronic acid dye complexes in methanol; [a] – overall wavelength shift not large enough to obtain accuarate low wavelength *K*-value

All dyes show an excellent fit to a 1:1 fluoride-dye binding model as evident by the values of the coefficients of determination (r^2) in Table 7. The boronic acid azo dyes **3**, **10** and **17** all show comparable values of stability constants. In contrast, the tricyanovinyl dye **14** has a very much larger *K*-value. In fact, dye **14** shows nearly a 100-fold increase in sensitivity to fluoride than the corresponding azo dyes. The reason for this difference will be discussed in the next section.

2.4.2 Fluoride-Boronic Acid Dye Equilibria

The spectral shifts and related colour changes observed upon adding potassium fluoride to all of the boronic acid dyes studied above, are all very similar to those observed for the relevant pH titrations (see Section 2.3.1). The colour change with pH is associated with the formation of a tetrahedral boronate anion. Therefore, the addition of potassium fluoride to a solution of any of the boronic acid dye molecules in methanol must also be producing a tetrahedral boronate anion. Formation of a boronate anion can only be achieved if the boron-nitrogen interaction, which is prevalent in the free dyes in methanol, is broken by fluoride. Scheme 19 shows this explanation using dye **3** as a

general example. This is essentially the same process as adding hydroxide to the dye solution in the pH titrations.

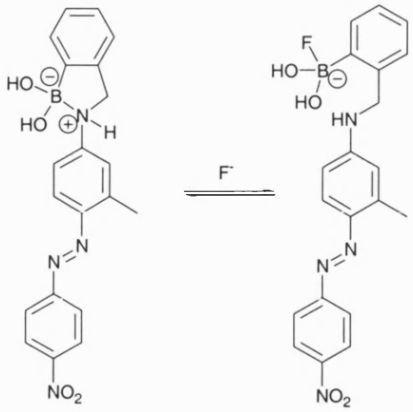

Scheme 19: The breaking of the boron-nitrogen bond in dye **3** by fluoride

The breaking of the boron-nitrogen bond by fluoride requires only one equivalent of fluoride. This agrees with the stability constant data described earlier, which shows a 1:1 relationship between dye and fluoride. The nature of the absorbance experiment means that only the fluoride ion that breaks the boron-nitrogen bond is observed spectroscopically. Therefore, it cannot be ruled out that further fluoride binding to the boronic acid centre occurs after this initial binding event (Scheme 20).

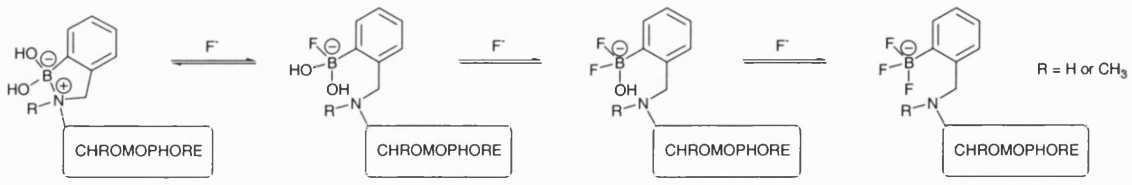

Scheme 20: Fluoride binding to boronic acid dyes

The proposal that the breaking of the boron-nitrogen bond in the boronic acid dyes is the key to the spectroscopic change, also explains why the tricyanovinyl dye **14** has a larger stability constant with fluoride than the azo dye derivatives. Boronic acid azo dyes **3**, **10** and **17** all have the same nitro-substituted azo chromophore. Consequently,

the boron-nitrogen interaction formed in these molecules will be very much alike and hence the binding with fluoride will be similar when this bond is broken. In contrast, the highly electron-withdrawing tricyanovinyl group weakens the boron-nitrogen interaction relative to that in the azo systems. This means the bond is easily broken by fluoride. This sensitivity to fluoride is reflected in the higher stability constant. This phenomenon is also related to the pK_a values of the dyes, i.e. how easy it is to break the boron-nitrogen bond with hydroxide ion. Dyes **3**, **10** and **17** all have similar pK_a values (around 10), whereas dye **14**'s value is significantly lower (approximately 7). In other words, it takes a lower concentration of hydroxide ions to break the boron-nitrogen bond in dye **14** than it does with the other dyes, and hence the difference in the stability constants with fluoride between the two chromophores.

2.4.3 Summary

- The interaction of potassium halides with a number of boronic acid dyes and a non-boronic acid model azo dye has been investigated using UV-VIS spectrophotometry.
- All of the boronic acid dyes studied have shown spectral changes upon addition of potassium fluoride in methanol. The non-boronic acid model dye shows no such spectral shift.
- The interaction of other potassium halides with the boronic acid dyes has shown that they are all fluoride selective.
- Boronic acid azo dye **3** has shown the largest spectral shift. A visible colour change from orange to claret (113 nm) was observed upon binding to fluoride.[150]
- The greatest fluoride sensitivity is exhibited by the boronic acid tricyanovinyl dye **14** – a 100-fold increase over the corresponding azo dyes.
- The dyes' spectral behaviour with fluoride shows similarities to their pH spectra.

- It is proposed that the breaking of the boron-nitrogen bond in the dye by fluoride causes the spectral change.
- The dyes all show curve fits illustrating the formation of a mono-fluoride adduct. This is reasonable since only the fluoride ion that breaks the boron-nitrogen bond is observed spectroscopically.

2.5 Colour Sensors for Boronic Acids

In the past decade there has been an explosion in the use and applications of boronic acids in chemical and biological environments. Boronic acids have been used in the development of various sensor systems for saccharides;[1, 2] as intermediates in the synthetically important Suzuki cross-coupling reaction;[3] as selective transporters of saccharides, nucleosides and nucleotides;[62, 151] and as reagents in boron neutron capture therapy (BNCT) for the treatment of brain tumours.[152] Therefore, sensor systems for the detection and analysis of boronic acids could prove to be an invaluable tool across these fields.

The aim with this research was to develop a colorimetric sensor for boronic acids. This is a reversal of our previous work in which we used boronic acid appended chromophores for saccharide and fluoride detection. Such a detection system for boronic acids would make it possible to develop an independent (of saccharide) scale for boronic acid binding efficiency. We believe that such a scale would help in the development of new saccharide receptors. The development of universal methods for the colorimetric analysis of small and medium sized analytes in solution has attracted widespread attention.[86, 153, 154] These systems are very attractive since immediate visual inspection can provide qualitative information, while absorption spectroscopy yields quantitative data.

2.5.1 Applications of the Diethanolamine Building Block

Wang has suggested the use of fluorescent systems bearing the diethanolamine moiety for binding to boric and boronic acids (species **A** in Figure 60).[125] The complexation

occurs through boronate formation and a boron-nitrogen interaction (species **B** in Figure 60). This interaction between boronic acids and the diethanolamine moiety has previously been used in a number of solid phase supports.[155-158]

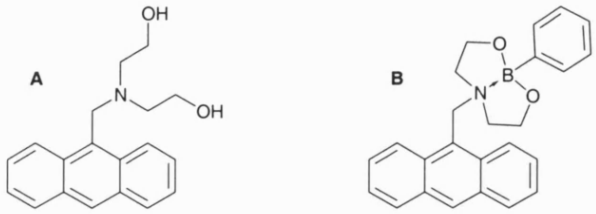

Figure 60: The diethanolamine unit and its binding affinity for boronic acids

It was decided to synthesise an azo dye derivative of the Wang system to test its feasibility as a colour sensor for boronic acids. Commercially available *m*-tolyldiethanolamine was reacted with the diazonium salt of 4-nitroaniline under standard azo coupling conditions to afford compound **24** in 89% yield (Scheme 21).

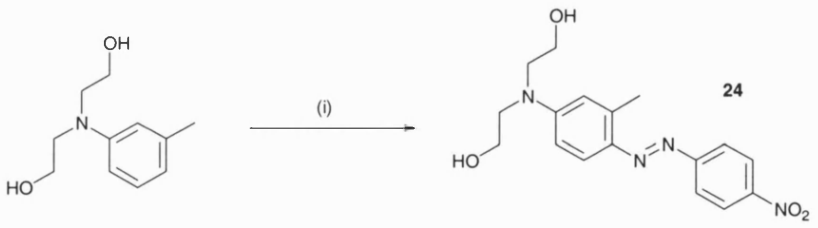

Scheme 21: Synthetic procedure for a diethanolamine-appended azo dye; (i) $O_2N\text{-}C_6H_4N_2^+Cl^-$, pH 4, 0-5 °C, 2 hr.

Absorbance-pH titrations with dye **24** were performed in a methanolic aqueous solution containing sodium chloride (0.05 mol dm^{-3}), with and without the presence of 0.005 mol dm^{-3} phenylboronic acid (PBA). The absorption spectra for the two titrations are shown in Figure 61 and Figure 62. In both instances, only one pK_a was observed, at low pH, corresponding to protonation of the azo group (Figure 63). The pK_a values were calculated using Equation 1 by fitting the absorbance at 432 nm versus proton

concentration. The calculated pK_a's are 2.51 ± 0.03 and 2.13 ± 0.04, without and with PBA respectively.

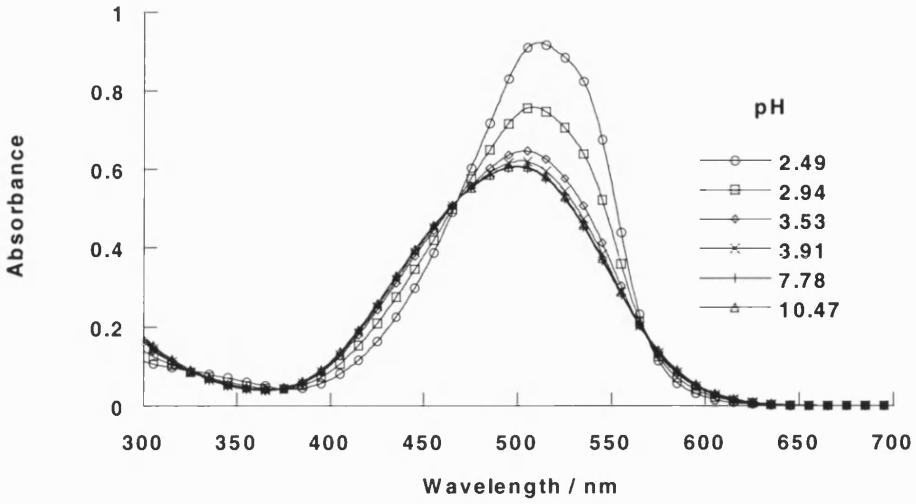

Figure 61: Absorption-pH spectral changes of dye **24** (1.92 x 10^{-5} mol dm^{-3})

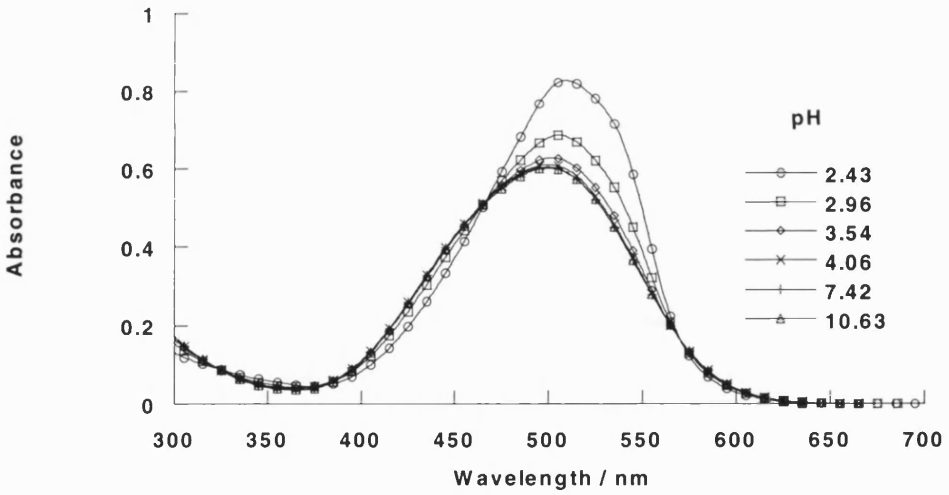

Figure 62: Absorption-pH spectral changes of dye **24** (1.92 x 10^{-5} mol dm^{-3}) with 0.005 mol dm^{-3} phenylboronic acid

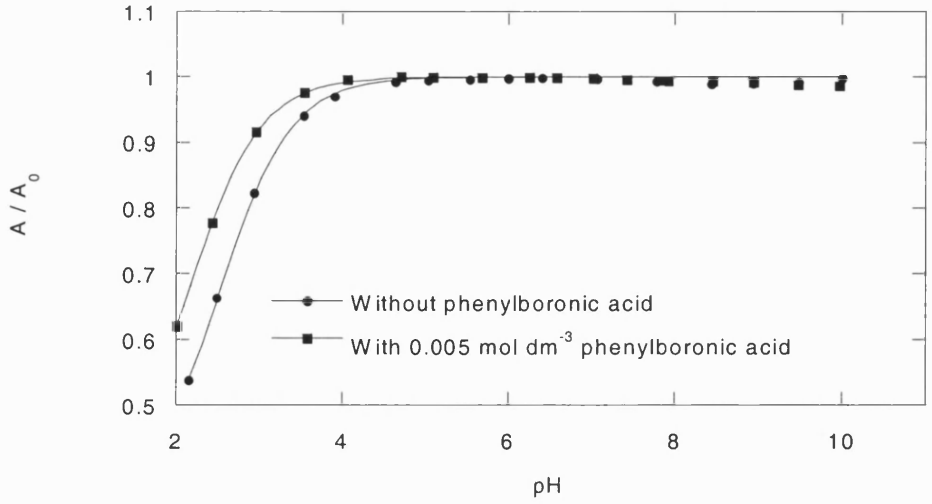

Figure 63: Absorption-pH profile of dye **24** with and without phenylboronic acid at 432 nm

Titrations of dye **24** with PBA in a number of different methanolic aqueous pH buffers showed no evidence of a spectral change. There is no evidence to suggest that PBA binds to the diethanolamine under these experimental conditions. The anilinic nitrogen lone electron pair is available to form a boron-nitrogen bond and is also directly conjugated to the azo chromophore. Hence, if PBA was to bind, there would be a perturbation in the electronic configuration of the anilinic lone electron pair, which would lead to a spectral change in the azo chromophore.

A recent re-investigation of Wang's fluorescent sensor has revealed that the solution binding of PBA to the diethanolamine, in methanolic conditions, is extremely weak.[159] The spectral change that was observed by Wang has now been shown to be nothing more than a protonation event and not, as first thought, due to boronic acid binding. The diethanolamine moiety has been used in a number of solid phase supports for binding boronic acids, where it has shown high affinity for boronate ester formation when used in non-competitive aprotic solvents, such as tetrahydrofuran.[155-158] It seems that the

diethanolamine unit is not a good receptor for boronic acids in competitive solvents like methanol.

Repeat titrations of dye **24** with PBA in the non-competitive chloroform and tetrahydrofuran also showed no spectral shift. The anilinic nitrogen in dye **24** must not be basic enough to form a boron-nitrogen bond with boronic acids, even in non-competitive solvents. Therefore, there can be no electronic change transmitted through the anilinic nitrogen to the azo chromophore upon addition of boronic acid, and no subsequent spectral change. The nitrogen used in the Wang system is a benzylamine and is more basic than the anilinic nitrogen in dye **24**. As such it can form a boron-nitrogen interaction in non-competitive solvents.[159]

2.5.2 Alizarin – Teaching an Old Indicator More Tricks[81]

Undeterred by the results with diethanolamine, it was decided to examine some previous colorimetric chemosensors. Anslyn has developed a colorimetric assay for the tartrate anion using a single boronic acid group and two guanidinium groups preorganised to create a cavity for tartrate (compound **A** in Figure 64).[81] Anslyn used the coloured alizarin complexone (compound **B** in Figure 64) to bind to the receptor. Alizarin complexone has been previously used as an indicator for pH, fluoride and lanthanides.[153] The boronic acid group covalently binds to the dihydroxy groups of compound **B**, while the carboxyl groups bind electrostatically to the guanidinium moieties. Upon adding tartrate, the bound alizarin complexone is replaced with tartrate and the dye changes colour.

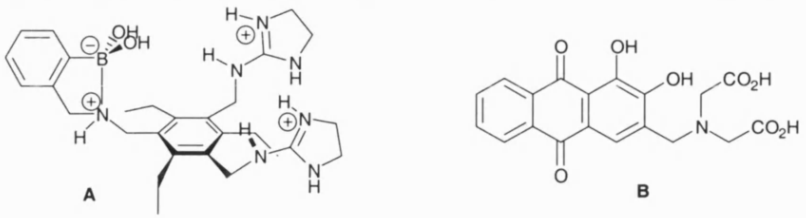

Figure 64: Anslyn's tartrate receptor (**A**) and alizarin complexone (**B**)

From Anslyn's result it was thought that the commercially available Alizarin Red S, compound **25** in Figure 65, without the carboxylic acid binding sites, should act as a colour sensor for simple boronic acids. In fact Alizarin Red S (the sodium salt of 1,2-dihydroxyanathraquinone-3-sulfonic acid) has been used as a fluorescent sensor for boric acid since 1936.[160] It has recently been used in several spectrofluorimetric methods for inorganic boron in the form of borate anion.[126, 127] However, it seems that there have not been any colorimetric studies performed with Alizarin Red S and its interaction with boronic acids.[†]

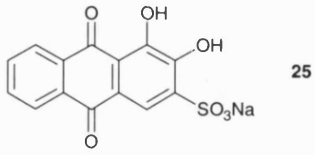

Figure 65: Alizarin Red S

Absorbance-pH titrations with compound **25** were performed in a 50wt% methanol aqueous solution (sodium chloride 0.05 mol dm^{-3}), with and without the presence of 0.005 mol dm^{-3} phenylboronic acid (PBA). Figure 66 and Figure 67 show the absorbance-spectral changes of these titrations. The spectra show that, in both cases, there are three different species as the pH is increased – one at low pH, one at

[†] Since the development of this research, Springsteen and Wang have published their own results on the use of Alizarin Red S as a general optical reporter for studying the binding of boronic acids with carbohydrates (G. Springsteen, and B. Wang, *Chem. Commun.*, 2001, 1608).

intermediate pH, and one with structured spectra at high pH. However, there is a difference in the intermediate pH spectra between the two titrations.

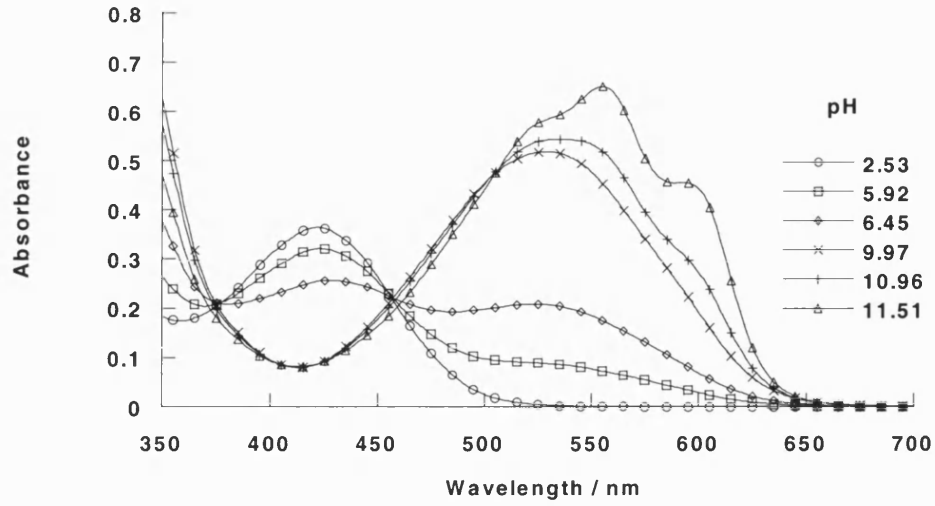

Figure 66: Absorption-pH spectral changes of dye **25** (7.40 x 10^{-5} mol dm^{-3})

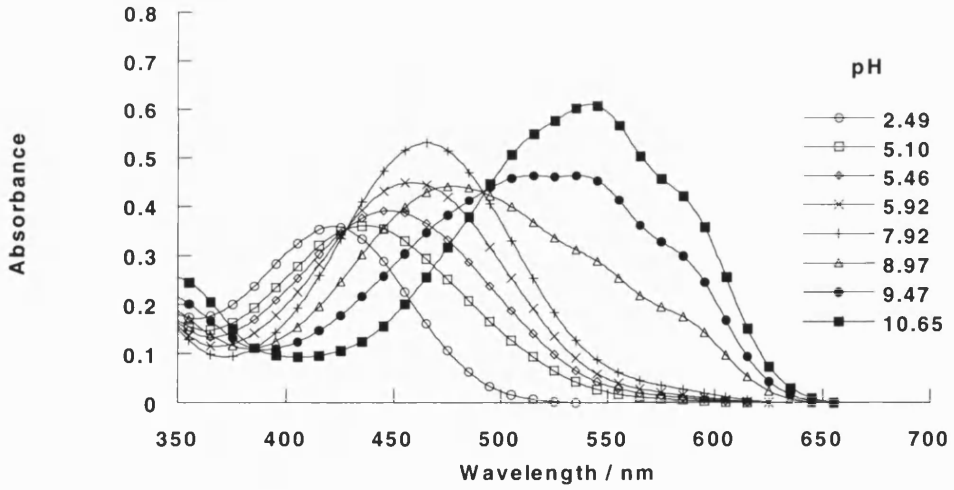

Figure 67: Absorption-pH spectral changes of dye **25** (7.40 x 10^{-5} mol dm^{-3}) with 0.005 mol dm^{-3} phenylboronic acid

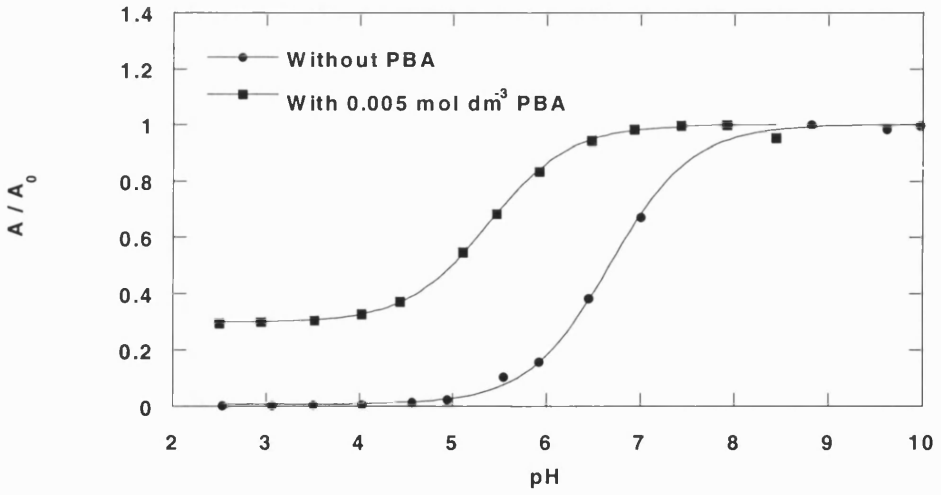

Figure 68: Absorption-pH profile of dye **25** with (466 nm) and without (558 nm) phenylboronic acid

A substantial shift in the pK_a of **25** is observed upon addition of PBA (Figure 68). The higher pH pK_a values were calculated using Equation 1, and are 6.68 ± 0.02 for free **25** and 5.38 ± 0.03 for **25** with added PBA. The shift is indicative of the boronic acid binding to the catechol-like hydroxyl groups of the alizarin. Lorand and Edwards' early studies of phenylboronic acid binding showed strong binding to catechol.[27] In fact the binding to catechol was shown to be approximately ten times greater than with D-fructose.

To investigate this further, an UV-VIS absorbance titration of **25** with PBA was performed in pH 8.21 aqueous methanolic buffer solution [52.1wt% methanol (KCl, 0.01000 mol dm^{-3}; KH_2PO_4, 0.002752 mol dm^{-3}; Na_2HPO_4, 0.002757 mol dm^{-3})].[144] As the concentration of PBA increased, a visible colour change from burgundy to yellow-orange was observed (Figure 70). Figure 69 shows the absorption changes with added PBA. The absorbance of the free dye at 530 nm decreases as PBA is added, and a new absorbance at 464 nm appears, a wavelength shift of 66 nm.

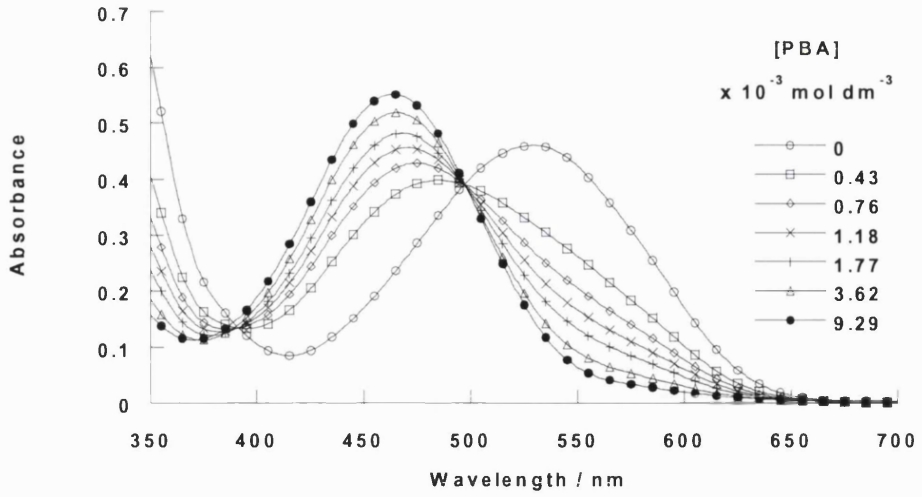

Figure 69: Absorption-spectral changes of dye **25** (9.60 x 10^{-5} mol dm^{-3}) with increasing concentration of phenylboronic acid at pH 8.21

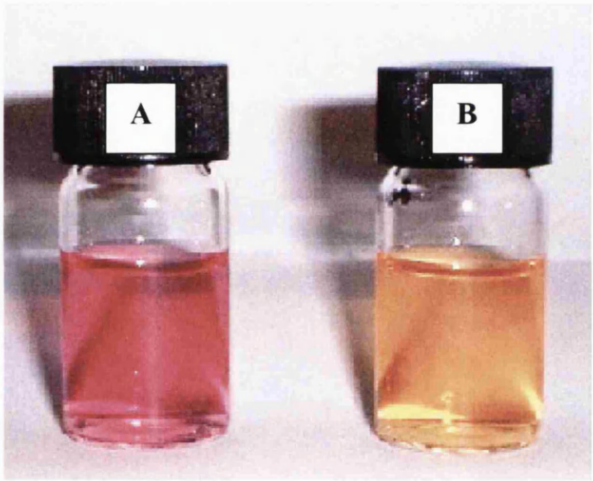

Figure 70: Colour-absorbance changes upon addition of boronic acid to dye **25** (1.00 x 10^{-4} mol dm^{-3}) at pH 8.21; **A**: dye **25** with no boronic acid; **B**: with 0.004 mol dm^{-3} phenylboronic acid

The titration at pH 8.21 was repeated with a number of simple boronic acids and similar absorbance shifts were observed in all cases (see Appendix for absorbance spectra). The stability constants (*K*) of **25** with the boronic acids were calculated by fitting the absorbance at 530 nm versus the boronic acid concentration using Equation 2. The fit for **25** with PBA is shown in Figure 71. The calculated *K* values are shown in Table 8.

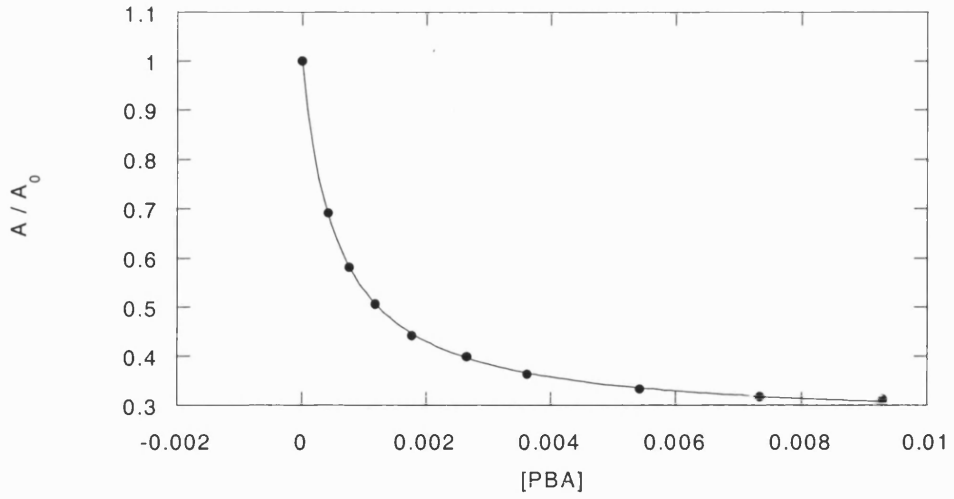

Figure 71: Curve fit to determine the stability constant at 530 nm of dye **25** with phenylboronic acid

Boronic Acid	K / dm^3 mol^{-1}	r^2
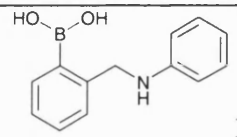 **13**	1547 ± 89	0.998
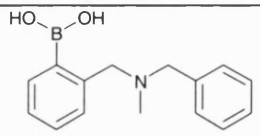 **BBMA**[115, 161]	1581 ± 74	0.999
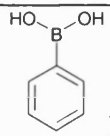 **PBA**	1719 ± 22	0.999
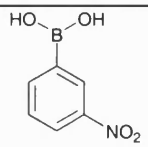 **3-NPBA**	5615 ± 269	0.998

Table 8: Stability constants (K) for boronic acid complexes with **25** at pH 8.21

Compound **13** (synthesised earlier) and benzyl-(2-boronobenzyl)-methylamine (**BBMA**)[115, 161] show very similar binding constants to phenylboronic acid (**PBA**),

whereas the value for 3-nitrophenylboronic acid (**3-NPBA**) is significantly higher. These results seem to indicate that the neighbouring amino nitrogen has no effect on the boronic acid binding-site with the alizarin, other than the well-known phenomenon of lowering the pH at which the boronic acid can bind to diols.[1, 142] It appears that changing the electronics of the boronic acid ring system, for example by adding the electron withdrawing nitro group, has a substantial effect on the binding strength of the boronic acid centre.

In conclusion, it has been shown that Alizarin Red S undergoes a large visible colour change upon complexation with a variety of simple boronic acids. This could prove to be a very useful colorimetric detection method for the many researchers working with boronic acids. It should be stressed that the system should also work as a fluorescent sensor. Further work is needed to develop this colorimetric system towards an independent scale of boronic acid binding affinity to diols.

2.5.3 Summary

- An anilinic diethanolamine appended azo dye **24** has been synthesised for use as a potential colour sensor for boronic acids.
- However, it has been shown that upon addition of boronic acid to the dye, if a boron-nitrogen interaction is formed binding, it is too weak to induce a spectral shift in the azo chromophore.
- Alizarin Red S (dye **25**) has been investigated for its application as a colorimetric system for detecting boronic acids.
- A large visible colour change from burgundy to yellow-orange (66 nm) is observed upon binding of boronic acid to the alizarin.

- Within the limited range of boronic acids studied, it seems that binding to the alizarin is only affected by the electronic environment of the boronic acid ring system, and not by a boron-nitrogen interaction that may be present.

3 Experimental

"What is now proved was once only imagined."

William Blake, 1757-1827

3.1 General Procedures

^{1}H and ^{13}C NMR spectra were recorded on Bruker AC-300 and Bruker AC-400 spectrometers. All spectral data is reported relative to tetramethylsilane as the internal standard using the δ scale. The multiplicities of the spectroscopic data are presented in the following manner: s-singlet, d-doublet, m-multiplet, t-triplet, br-broad. *J*-values are given in Hertz. Due to quadrapolar relaxation, the aryl carbon atoms attached directly to the boronic acid boron atoms are not observed by ^{13}C NMR.

Infrared spectra were recorded on a Perkin-Elmer Paragon 1000 FT-IR spectrometer and a Perkin-Elmer 1600 Series FT-IR spectrometer. Samples were run either as a Nujol mull or as pressed KBr disks.

Electron Impact (EI) mass spectra were recorded on a VG ProSpec mass spectrometer. Liquid Secondary Ion (LSI) mass spectra were recorded on a VG ZabSpec instrument. A Micromass LCT mass spectrometer was used for Electrospray Ionisation (ESI) mass spectra. Fast Atom Bombardment (FAB) and EI mass spectra were also recorded on a double focussing, magnetic sector Micromass Autospec instrument, using a DEC Alpha data system running Opus V3.4X software, overlaid on an Open VMS operating system. High Resolution Mass Spectra (HRMS) were obtained from all of the above instruments.

Elemental analyses were performed at the University of North London, the University of Birmingham and the University of Bath. Melting points were measured on Gallenkamp and Büchi 535 melting point apparatus and are uncorrected.

UV-Visible absorption measurements used Sigma Spectrophotometer Silica (Quartz) Cuvets with 10 mm path lengths and were recorded on a Perkin-Elmer Lambda 20 UV/VIS Spectrophotometer. Data was collected *via* the Perkin-Elmer UV Winlab software package on a PC running Microsoft NT v4. All pH measurements were recorded on a Hanna Instruments HI 9321 Microprocessor pH Meter that was calibrated using Fisher Chemicals standard buffer solutions (pH 4.0 - phthalate, 7.0 – phosphate, and 10.0 - borate).

Thin-layer chromatography (TLC) was performed on pre-coated aluminium-backed silica gel plates supplied by Merck Ltd. (Silica Gel 60 F_{254}, thickness 0.2 mm, Art. 5554). Visualisation was achieved by UV light (254 nm).

Acetonitrile was dried by refluxing with calcium hydride. It was subsequently distilled and collected by dry syringe as required. Prior to use, tetrahydrofuran and diethyl ether were distilled from sodium benzophenone ketyl under a nitrogen atmosphere. All other reagents and solvents were used as supplied by the Aldrich Chemical Co. Ltd., Lancaster Synthesis Ltd., Fisher Scientific Ltd., Acros Organics, Tokyo Kasei Kogyo (TCI) Co. Ltd., Merck Ltd. and Frontier Scientific Europe Ltd.

3.2 Synthesis and Characterisation

(2-boronobenzylidene)-*m*-tolylamine (1)

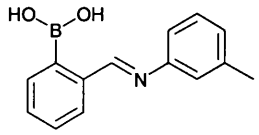

m-toluidine (0.72 g, 6.67 mmol) and 2-formylbenzeneboronic acid (1.00 g, 6.67 mmol) were mixed in absolute ethanol (45 ml) and toluene (5 ml). A Dean and Stark trap was fitted to permit the azeotropic removal of water, and the reaction mixture heated at reflux overnight (18 hours). After cooling, the solvent was removed *in vacuo* to obtain **1** (1.35 g, 92%) as a cream coloured solid: mp 170-172 °C (dec.); ν_{max}(Nujol)/cm^{-1} 1732 (CH=N); δ_H(300 MHz; CD_3OD; Me_4Si) 2.41 (3 H, s, Ar-C*H*$_3$), 7.24 (1 H, d, *J* 6.0, Ar-*H*), 7.34-7.46 (2 H, m, Ar-*H*), 7.51-7.66 (4 H, m, Ar-*H*), 7.70 (1 H, d, *J* 6.0, Ar-*H*), 9.12 (1 H, s, ArN=C*H*Ar); δ_C(75 MHz; CD_3OD; Me_4Si) 21.9, 120.3, 123.8, 129.6, 129.9, 130.9, 131.1, 131.5, 134.9, 135.1, 140.0, 141.1, 143.9, 166.6; *m/z* (LSIMS) 509 ([M – 2 H_2O + 2 NOBA]$^+$, 22%), 357 ([M + 1 NOBA – H_2O]$^+$, 100) and 222 ([M – H_2O]$^+$, 17).

(2-boronobenzyl)-*m*-tolylamine (2)

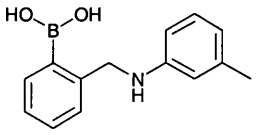

Sodium borohydride (0.79 g, 20.9 mmol, 5 equiv.) was added slowly to **1** (1.00 g, 4.18 mmol) in dry methanol (50 ml). The reaction was left to stir at room temperature for 2 hours and then poured into ice-water (20 ml). Hydrochloric acid (1 M, 10 ml) was added slowly and the mixture left to stir for 30 minutes, whereupon the precipitate formed was collected by suction filtration to afford **2** (0.82 g, 81%) as a white solid: (Found: C, 69.6; H, 6.4; N, 5.8. $C_{14}H_{16}BNO_2$ requires C, 69.7; H, 6.7; N, 5.8%); mp 72-

73 °C (dec.); δ_H(300 MHz; CD_3OD; Me_4Si) 2.20 (3 H, s, Ar-C*H*$_3$), 4.29 (2 H, s, ArC*H*$_2$-NHAr), 6.54-6.66 (4 H, m, Ar-*H*), 6.99 (1 H, t, *J* 7.5, Ar-*H*), 7.15-7.32 (4 H, m, Ar-*H*); δ_C(75 MHz; CD_3OD; Me_4Si) 22.3, 52.2, 115.1, 118.6, 122.9, 127.1, 128.2, 130.0, 130.3, 133.0, 140.3, 146.1, 149.0; *m/z* (LSIMS) 241 ($[M]^+$, 40%), 223 ($[M\text{-}H_2O]^+$, 100).

(2-boronobenzyl)-[3-methyl-4-(4-nitrophenylazo)-phenyl]-amine (3)

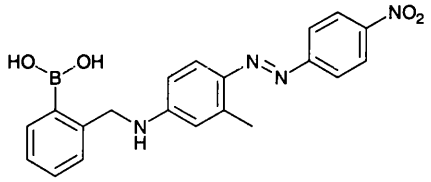

4-nitroaniline (0.10 g, 0.70 mmol) was mixed in water (1 ml), methanol (1 ml) and hydrochloric acid (1 ml, 5.0 M) and then cooled to 0-5 °C on an ice-bath. A chilled solution of sodium nitrite (0.06 g, 0.84 mmol, 0.2 M) was added dropwise. Excess nitrite was destroyed by the addition of sulphamic acid after stirring for 5 minutes. (2-borono-benzyl)-*m*-tolylamine (0.16 g, 0.66 mmol) was dissolved in methanol (2 ml) and dilute hydrochloric acid (1 ml, 1 M) then added dropwise to the reaction mixture, which quickly turned a red colour. Sodium acetate was added to raise the pH of the solution to 4 and this was then left to stir at 0-5 °C for 3 hours. Sodium hydroxide (2 M) was slowly added to raise the pH to 7. The resulting precipitate was collected by suction filtration and dried in a dessicator overnight to afford **3** (0.19 g, 74%) as a dark red solid: (HRMS: Found 372.1381, $[M\text{-}H_2O]^+$. $C_{20}H_{17}BN_4O_3$ requires 372.1392); mp 120-122 °C (dec.); λ_{max}(pH 8.05, 0.05 mol dm^{-3} NaCl, 33% MeOH: 67% H_2O w/w)/nm 486 (ε/dm^3 mol^{-1} cm^{-1} 19000); ν_{max}(KBr disk)/cm^{-1} 1602 (N=N), 1518 and 1333 (NO_2); δ_H(300 MHz; CD_3OD; Me_4Si) 2.63 (3 H, m, Ar-C*H*$_3$), 4.45 (2 H, s, ArC*H*$_2$-NHAr), 6.52-6.58 (1 H, m, Ar-*H*), 6.99-7.04 (1 H, m, Ar-*H*), 7.18-7.40 (5 H, m, Ar-*H*), 7.63-7.72 (1 H, m, Ar-*H*), 7.87-7.93 (1 H, m, Ar-*H*), 8.21-8.36 (2 H, m, Ar-*H*); δ_C(125 MHz; CD_3OD; Me_4Si) 18.1, 49.7, 113.2, 114.7, 118.3, 122.7, 123.6, 125.7, 127.6, 128.1,

129.8, 130.2, 132.8, 144.3; *m/z* (EI) 373 ($[MH-H_2O]^+$, 66%), 222 ($[M-H_2O-N_2C_6H_4NO_2]^+$, 100).

4-[4-(2-boronobenzylamino)-2-methylphenylazo]-benzenesulfonic acid (4)

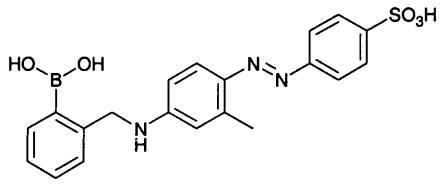

The above procedure was repeated with sulphanilic acid (0.08 g, 0.44 mmol) in place of *p*-anisidine (all other reagents were used in the same mole ratios), to afford **4** (0.05 g, 27%) as a dark red solid: (HRMS: Found 424.1142, $[M-H]^+$. $C_{20}H_{19}BN_3O_5S$ requires 424.1138); mp 219 °C (dec.); λ_{max}(pH 8.18, 0.05 mol dm^{-3} NaCl, 33% MeOH: 67% H_2O w/w)/nm 421 (ε/dm^3 mol^{-1} cm^{-1} 19300); ν_{max}(KBr disk)/cm^{-1} 1610 (N=N), 1350 and 1150 (SO_2); δ_H(300 MHz; CD_3OD; Me_4Si) 2.59 (3 H, m, Ar-C*H*$_3$), 4.41 (2 H, s, ArC*H*$_2$-NHAr), 6.49-6.59 (2 H, m, Ar-*H*), 7.19-7.41 (4 H, m, Ar-*H*), 7.59-7.66 (1 H, m, Ar-*H*), 7.81 (2 H, d, *J* 9.0, Ar-*H*), 7.92 (2 H, d, *J* 9.0, Ar-*H*); δ_C(125 MHz; CD_3OD; Me_4Si) 18.0, 49.7, 113.1, 113.7, 115.1, 117.9, 122.9, 127.5, 127.9, 129.8, 132.7, 146.6, 153.7, 155.7; *m/z* (ESI) 424 ($[M-H]^+$, 33%), 406 ($[M-H_3O]^+$, 100).

4-[4-(2-boronobenzylamino)-2-methylphenylazo]-benzoic acid (5)

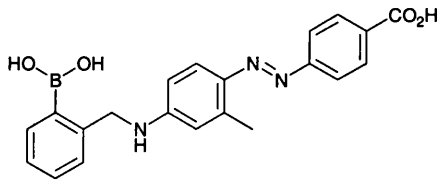

The above procedure was repeated using 4-aminobenzoic acid (0.11 g, 0.83 mmol) instead of 3-aminobenzoic acid (all other reagents were used in the same mole ratios), to afford **5** (0.10 g, 31%) as an orange-red solid: (Found: C, 64.8; H, 5.0; N, 10.7. $C_{21}H_{20}BN_3O_4$ requires C, 64.8; H, 5.2; N 10.8%); mp 208-210 °C (dec.); λ_{max}(pH 8.42,

0.05 mol dm^{-3} NaCl, 33% MeOH: 67% H_2O w/w)/nm 418 (ε/dm^3 mol^{-1} cm^{-1} 16000); ν_{max}(KBr disk)/cm^{-1} 1602 (N=N), 1684 (C=O); δ_H(300 MHz; CD_3OD; Me_4Si) 2.60 (3 H, m, Ar-C*H*$_3$), 4.42 (2 H, s, ArC*H*$_2$-NHAr), 6.50-6.61 (2 H, m, Ar-*H*), 7.18-7.41 (4 H, m, Ar-*H*), 7.61-7.68 (1 H, m, Ar-*H*), 7.82 (2 H, d, *J* 9.0 Ar-*H*), 8.11 (2 H, d, *J* 9.0 Ar-*H*); δ_C(125 MHz; CD_3OD; Me_4Si) 18.1, 49.6, 117.9, 122.8, 127.5, 131.6; *m/z* (LSIMS) 660 ([MH- $2H_2O$ + 2 NOBA]$^+$, 55%), 460 ([M- $2H_2O$ + $2CH_3OH$ + K]$^+$, 100).

(2-boronobenzyl)-[4-(4-methoxyphenylazo)- 3-methylphenyl]-amine (6)

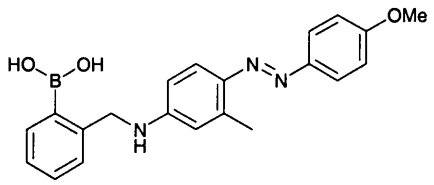

The previous experiment was repeated using *p*-anisidine (0.61 g, 4.98 mmol, 6 equivs.) instead of 4-aminobenzoic acid. Purification was performed by washing the product (in dichloromethane) with 10% sodium hydrogen carbonate solution (w/w) to remove residual acetic acid, to yield **6** (0.11 g, 35%) as a orange-brown solid: (Found: C, 67.3; H, 5.8; N, 10.2. $C_{21}H_{22}BN_3O_3$ requires C, 67.2; H, 5.9; N 11.2%); mp 102-103 °C (dec.); λ_{max}(pH 8.42, 0.05 mol dm^{-3} NaCl, 33% MeOH: 67% H_2O w/w)/nm 400 (ε/dm^3 mol^{-1} cm^{-1} 14600); ν_{max}(KBr disk)/cm^{-1} 1602 (N=N); δ_H(300 MHz; CD_3OD; Me_4Si) 2.56 (3 H, m, Ar-C*H*$_3$), 3.84 (3 H, s, Ar-OC*H*$_3$), 4.39 (2 H, s, ArC*H*$_2$-NHAr), 6.49-6.59 (2 H, m, Ar-*H*), 7.00 (2 H, d, *J* 9.0, Ar-*H*), 7.20-7.40 (4 H, m, Ar-*H*), 7.52-7.57 (1 H, m, Ar-*H*), 7.76 (2 H, d, *J* 9.0, Ar-*H*); δ_C(125 MHz; CD_3OD; Me_4Si) 18.0, 49.7, 56.0, 113.8, 115.2, 115.5, 117.5, 124.8, 127.5, 127.8, 129.7, 132.6, 141.3, 144.3, 145.0, 149.0, 152.5, 162.5; *m/z* (ESI) 376 ([MH]$^+$, 100%).

3-[4-(2-boronobenzylamino)-2-methylphenylazo]-benzoic acid (7)

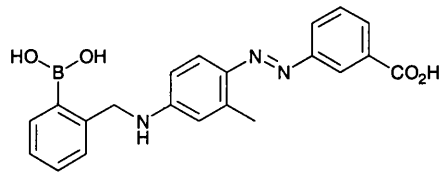

The previous experiment was repeated using 3-aminobenzoic acid (0.06 g, 0.41 mmol) instead of 4-nitroaniline (all other reagents were used in the same mole ratios), to yield **7** (0.10 g, 61%) as a red solid: (Found: C, 64.9; H, 5.2; N, 10.9. $C_{21}H_{20}BN_3O_4$ requires C, 64.8; H, 5.2; N 10.8%); mp 133-135 °C (dec.); λ_{max}(pH 8.48, 0.05 mol dm^{-3} NaCl, 33% MeOH: 67% H_2O w/w)/nm 406 (ε/dm^3 mol^{-1} cm^{-1} 19000); ν_{max}(KBr disk)/cm^{-1} 1603 (N=N); δ_H(300 MHz; CD_3OD; Me_4Si) 2.62 (3 H, m, Ar-C*H*$_3$), 4.40 (2 H, s, ArC*H*$_2$-NHAr), 6.50-6.60 (2 H, m, Ar-*H*), 7.18-7.42 (4 H, m, Ar-*H*), 7.52-7.66 (2 H, m, Ar-*H*), 7.94-8.05 (2 H, m, Ar-*H*), 8.37-8.41 (1 H, m, Ar-*H*); δ_C(125 MHz; CD_3OD; Me_4Si) 19.1, 52.5, 114.2, 118.9, 123.1, 125.4, 128.2, 128.6, 129.0, 130.8, 131.2, 132.2, 133.7, 133.7, 143.8, 145.1, 145.8, 154.6, 155.9, 170.9; *m/z* (ESI) 418 ([MH - $2H_2O$ + $2CH_3OH]^+$, 100%).

(2-bromobenzyl)-methyl-*m*-tolylamine (8)

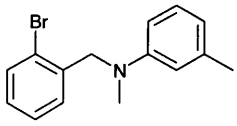

2-bromobenzyl bromide (10.0 g, 40.0 mmol) was mixed in distilled acetonitrile (100 ml) with potassium carbonate (16.6 g, 120 mmol, 3 equiv.). The system was evacuated and put under an argon atmosphere. *N*-methyl-*m*-toluidine (4.8 g, 40.0 mmol) was syringed into solution and the reaction mixture heated to reflux. After 4 hours, TLC analysis showed the reaction had gone to completion. The solvent was removed, after filtration, to yield **8** as a yellow oil (2.22 g, 98%); δ_H(300 MHz; $CDCl_3$; Me_4Si) 2.53 (3 H, m, Ar-C*H*$_3$), 3.19 (3 H, s, N-C*H*$_3$), 4.69 (2 H, s, ArC*H*$_2$-NMeAr), 6.60-6.72 (3 H, m,

Ar-*H*), 7.19-7.39 (4 H, m, Ar-*H*), 7.67-7.71 (1 H, m, Ar-*H*); δ_C(125 MHz; $CDCl_3$; Me_4Si) 22.1, 38.8, 57.5, 109.3, 112.7, 117.7, 122.8, 127.6, 128.0, 128.4, 129.2, 132.9, 137.6, 139.0, 149.4; *m/z* (EI) 289 ($[M]^+$, 39%), 91 ($[C_6H_5CH_2]^+$, 100).

(2-boronobenzyl)-methyl-*m*-tolylamine (9)

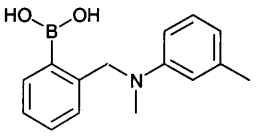

(2-bromobenzyl)-methyl-*m*-tolylamine (5.00g, 17.2 mmol) was mixed in distilled tetrahydrofuran (40 ml) under argon. The solution was cooled to –78 °C and then *n*-butyl lithium (10.3 ml, 2.5 M in THF, 25.8 mmol, 1.5 equiv.) was syringed slowly into the reaction mixture. After stirring at –78 °C for 1 hour, the lithiated solution was transferred drop wise, using a canula, into dry THF (40 ml) containing trimethylborate (8.9 g, 86.0 mmol, 5 equiv.) at –78 °C under argon. The reaction was allowed to warm to room temperature before adding hydrochloric acid (40 ml, 1 M). After stirring for 1 hour, water (50 ml) was added and the resulting aqueous layer washed with hexane (2 x 50 ml) and salted with sodium chloride. The aqueous phase was extracted with dichloromethane (3 x 50 ml) and the organic layers combined, dried over $MgSO_4$ and filtered. The solvent was removed *in vacuo* and **9** (1.08 g, 25%) was afforded by precipitation from chloroform with hexane as a white solid: (HRMS: Found 256.1501; $C_{15}H_{19}BNO_2$ requires 256.1509); mp 61-63 °C (dec.); δ_H(300 MHz; CD_3OD; Me_4Si) 2.41 (3 H, s, Ar-CH_3), 3.28 (3 H, s, Ar-CH_3), 4.90 (2 H, s, ArCH_2-NHAr), 7.26-7.49 (8 H, m, Ar-*H*); δ_C(125 MHz; CD_3OD; Me_4Si) 22.0, 45.7, 66.3, 120.3, 123.6, 131.0, 131.8, 132.1, 132.7, 134.4, 136.2, 137.2, 142.9, 143.3; *m/z* (ESI) 256 ($[MH]^+$, 100%).

(2-boronobenzyl)-methyl-[3-methyl-4-(4-nitrophenylazo)-phenyl]-amine (10)

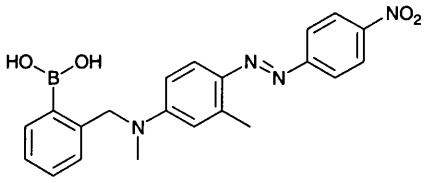

4-nitroaniline (0.05 g, 0.39 mmol) was mixed in water (1 ml), methanol (1 ml) and hydrochloric acid (1 ml, 10.0 M) and then cooled to 0-5 °C on an ice-bath. A chilled solution of sodium nitrite (0.03 g, 0.43 mmol, 0.2 M) was added drop wise. Excess nitrite was destroyed by the addition of sulphamic acid. (2-borono-benzyl)-methyl-*m*-tolyl-amine (0.10 g, 0.39 mmol) was dissolved in methanol (2 ml) and dilute hydrochloric acid (1 ml, 1 M), then added drop wise to the reaction mixture, which quickly turned a red colour. Sodium acetate was added to raise the pH of the solution to 4 and this was then left to stir at 0-5 °C for 3 hours. Sodium hydroxide (1 M) was slowly added to raise the pH to 7. The resulting precipitate was collected by suction filtration and dried in a dessicator overnight to afford **10** (0.13 g, 82%) as a dark red solid (Found: C, 62.8; H, 5.2; N, 13.1. $C_{21}H_{21}BN_4O_4$ requires C, 62.4; H, 5.2; N 13.8%); (HRMS: Found 405.1739, $[MH]^+$. $C_{21}H_{21}BN_4O_4$ requires 405.1734); mp 115-120 °C (dec.); λ_{max}(pH 8.21, 0.01 mol dm^{-3} KCl, 0.002752 mol dm^{-3} KH_2PO_4, 0.002757 mol dm^{-3} Na_2HPO_4, 52.1% MeOH: 47.9% H_2O w/w)/nm 501 (ε/dm^3 mol^{-1} cm^{-1} 29300); ν_{max}(KBr disk)/cm^{-1} 1599 (N=N), 1512 and 1333 (NO_2); δ_H(300 MHz; CD_3OD; Me_4Si) 2.68 (3 H, s, Ar-C*H*$_3$), 3.11 (3 H, s, Ar-C*H*$_3$), 4.66 (2 H, s, ArC*H*$_2$-NHAr), 6.72-6.79 (2 H, m, Ar-*H*), 7.19-7.40 (5 H, m, Ar-*H*), 7.70-7.76 (1 H, m, Ar-*H*), 7.91 (2 H, d, *J* 12.0, Ar-*H*), 8.32 (2 H, d, *J* 12.0, Ar-*H*); δ_C(125 MHz; CD_3OD; Me_4Si) 18.5, 40.2, 58.3, 113.0, 115.4, 118.3, 123.5, 125.7, 127.7, 127.9, 128.9, 130.1, 133.0, 142.8, 143.9, 148.8, 155.5, 158.1; *m/z* (ESI) 405 ($[MH]^+$, 100%).

Benzyl-*m*-tolylamine (11)

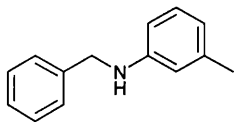

Benzaldehyde (1.04 g, 9.84 mmol) and *m*-toluidine (1.05 g, 9.84 mmol) were mixed in toluene (50 ml) and heated at reflux for 15 hours in a Dean-Stark apparatus. After cooling, the solvent was removed *in vacuo* to afford a yellow oil, which was used directly in the next reaction step without further purification. Sodium borohydride (0.74 g, 19.7 mmol) was added in small portions to a stirred solution of the imine from the previous step in methanol (40 ml) at room temperature. TLC showed completion of the reaction after 2 hours. The reaction mixture was poured on to ice (5 g) and concentrated hydrochloric acid (1 ml) and stirred for 30 minutes, before removing most of the solvent *in vacuo*. Water (30 ml) was added and then the aqueous layer was extracted with dichloromethane. The organic extracts were combined, dried ($MgSO_4$) and filtered. The solvent was removed *in vacuo* to yield **11** (1.87 g, 96%) as a brown oil: (HRMS: Found 197.1197. $C_{14}H_{15}N$ requires 197.1205); δ_H(300 MHz; $CDCl_3$; Me_4Si) 2.37 (3 H, s, Ar-C*H*$_3$), 4.04 (1 H, br. s, N*H*), 4.39 (2 H, s, ArC*H*2-NHAr), 6.49-6.70 (3 H, m, Ar-*H*), 7.16 (1 H, t, *J* 6.0, Ar-*H*), 7.33-7.50 (4 H, m, Ar-*H*); δ_C(75 MHz; $CDCl_3$; Me_4Si) 21.7, 48.3, 109.9, 113.7, 118.5, 127.18, 127.5, 128.6, 129.2, 139.0, 139.6, 148.2; *m/z* (EI) 197 ([M]$^+$, 60%), 91 ([$C_6H_5CH_2$]$^+$, 100).

Benzyl-[3-methyl-4-(4-nitrophenylazo)-phenyl]-amine (12)

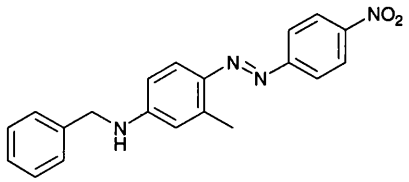

The procedure to form **10** was repeated using benzyl-*m*-tolylamine (0.20 g, 1.01 mmol) instead of (2-borono-benzyl)-*m*-tolyl-amine (all other reagents were used in the same mole ratios). Precipitation from chloroform with hexane afforded analytically pure **12** (0.08 g, 23%) as a dark red solid: (Found: C, 69.1; H, 5.4; N, 16.3. $C_{20}H_{18}N_4O_2$ requires C, 69.3; H 5.2; N 16.2%); mp 147-149 °C (dec.); ν_{max}(KBr)/cm^{-1} 1604 (N=N), 1507 and 1328 (NO_2); δ_H(300 MHz; $CDCl_3$; Me_4Si) 2.67 (3 H, m, Ar-C*H*$_3$), 4.43 (2 H, d, *J* 6.0 Hz, ArC*H*$_2$-NHAr), 4.71 (1 H, t, *J* 6.0 Hz, N*H*), 6.47-6.55 (2 H, m, Ar-*H*), 7.25-7.38 (5 H, m, Ar-*H*), 7.73-7.78 (1 H, m, Ar-*H*), 7.86-7.92 (2 H, m, Ar-*H*), 8.27-8.33 (2 H, m, Ar-*H*); δ_C(75 MHz; $CDCl_3$; Me_4Si) 18.3, 47.90, 111.5, 113.3, 117.9, 122.9, 124.9, 127.7, 127.9, 129.1, 138.3, 143.4, 143.7, 147.5, 152.2, 157.2; *m/z* (EI) 346 ([M]$^+$, 42%) 196 ([M–$N_2C_6H_4NO_2$]$^+$, 38), 91 ([$C_6H_5CH_2$]$^+$, 100).

2-boronobenzyl-phenylamine (13)

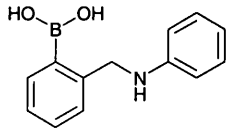

Aniline (0.62 g, 6.67 mmol) and 2-formylbenzeneboronic acid (1.00 g, 6.67 mmol) were mixed in absolute ethanol (45 ml) and toluene (5 ml). A Dean and Stark trap was fitted to permit the azeotropic removal of water, and the reaction mixture heated at reflux overnight (18 hours). After cooling, the solvent was removed *in vacuo* to afford a yellow oil. Sodium borohydride (0.50 g, 13.3 mmol, 2 equiv.) was added slowly to the oil in dry methanol (50 ml). The reaction was left to stir at room temperature for 2 hours

and then poured into ice-water (20 ml). The aqueous solution was extracted with dichloromethane (3 x 50 ml). The organic extracts were combined, dried over $MgSO_4$ and filtered. The solvent was removed *in vacuo* to afford **13** (1.26 g, 83%) as a white solid: (HRMS: Found 497.1779, $[M\text{-}2H_2O + 2\ NOBA]^+$. $C_{27}H_{24}BN_3O_6$ requires 497.1758); mp 125-129 °C (dec.); δ_H(300 MHz; CD_3OD; Me_4Si) 4.72 (2 H, s, ArCH_2-NHAr), 7.40-7.61 (9 H, m, Ar-*H*); δ_C(75 MHz; CD_3OD; Me_4Si) 58.6, 124.7, 130.8, 131.5, 132.0, 132.3, 132.4, 133.6, 137.5; *m/z* (FAB) 498 ($[M\text{-}2H_2O + 2\ NOBA]^+$, 100%).

2-[4-(2-boronobenzylamino)phenyl]-3-cyano-but-2-enedinitrile (14)

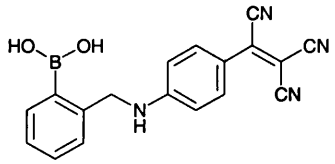

2-boronobenzyl-phenylamine (0.33 g, 1.2 mmol) was mixed in *N,N*-dimethylformamide (5 ml) and tetracyanoethylene (0.16 g, 1.2 mmol) was slowly added. The reaction mixture was heated to 55 °C for 1 hour. After cooling, the mixture was poured on to ice-water (10 ml) and the precipitate collected by filtration. This was recrystallised from acetic acid to yield **14** (0.25 g, 63 %) as a red solid: (Found: C, 66.0; H, 4.0; N, 17.1. Calc. for $C_{18}H_{13}BN_4O_2$: C, 65.9; H, 4.0; N, 17.1%); mp >115 °C (dec.); λ_{max}(pH 7.77, 0.01000 mol dm^{-3} KCl, 0.002642 mol dm^{-3} KH2PO4, 0.002642 mol dm^{-3} Na_2HPO_4, 33% MeOH-67% H_2O w/w)/nm 521 (ε/dm^3 mol^{-1} cm^{-1} 9380); ν_{max}(KBr)/cm-1 2216 (CN); δ_H(300 MHz; CD_3OD; Me_4Si) 4.53 (2 H, s, CH_2NH), 6.79 (2 H, d, *J* 9.0, Ar-*H*), 7.20-7.40 (4 H, m, Ar-*H*), 7.98 (2 H, d, *J* 9.0, Ar-*H*); δ_C(100 MHz; CD_3OD; Me_4Si) 50.68, 109.62, 115.00, 115.56, 116.15, 119.54, 119.80, 128.46, 129.15, 130.69, 133.60, 134.54, 142.86, 157.62; *m/z* (ESI) 379 ($[M - 2H_2O + 2MeOH + Na]^+$, 100%).

4-(4-nitrophenylazo)-naphthalen-1-ylamine (15)

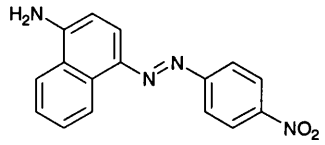

The procedure to form **10** was repeated using 1-aminonaphthalene (0.20 g, 1.40 mmol) instead of (2-borono-benzyl)-*m*-tolyl-amine (all other reagents were used in the same mole ratios), to afford a dark solid, **15,** (0.32 g, 79%): (HRMS: Found 292.0953. $C_{16}H_{12}N_4O_2$ requires 292.0960); mp >97 °C (dec.); ν_{max}(KBr)/cm^{-1} 1600 (N=N), 1507 and 1322 (NO_2); δ_H(300 MHz; $(CD_3)_2SO$; Me_4Si) 6.83 (1 H, d, *J* 9.0, Ar-*H*), 7.47-7.71 (2 H, m, Ar-*H*), 7.97 (2 H, d, *J* 9.0, Ar-*H*), 8.04-8.28 (2 H, m, Ar-*H*), 8.31 (2 H, d, *J* 9.0, Ar-*H*), 8.86 (1 H, d, *J* 9.0, Ar-*H*); δ_C(75 MHz; $(CD_3)_2SO$; Me_4Si) 121.3, 122.2, 123.1, 123.4, 124.9, 125.1, 125.4, 126.0, 128.7, 129.2, 134.5, 137.2, 146.2; *m/z* (EI) 292 ([M]$^+$, 16%), 42 ([CH_3CO]$^+$, 100).

2-(boronobenzyl)-naphthalen-1-yl-amine (16)

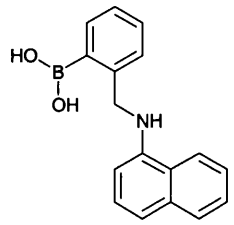

2-formylbenzeneboronic acid (0.20 g, 1.33 mmol) was dissolved in methanol (20 ml) and 1-aminonaphthalene (0.19 g, 1.33 mmol) was then added as a methanol (2 ml) solution. A drying tube was fitted and the reaction stirred at room temperature for 1 hour. Sodium borohydride (0.10 g, 2.66 mmol, 2 equiv.) was added slowly as a solid. After stirring for a further hour, the reaction mixture was poured on to ice-water (20 ml). A few drops of sodium hydroxide solution (1 M) were added to aid precipitation of the product. The precipitate was collected by suction filtration and dried in a dessicator to afford **16** (0.25 g, 68%) as an off-white solid: (HRMS: Found 547.1937, [M-2H_2O +

2 NOBA]$^+$. $C_{31}H_{26}BN_3O_6$ requires 547.1915); mp 74-77 °C (dec.); δ_H(300 MHz; CD_3OD; Me_4Si) 4.52 (2 H, s, ArC*H*$_2$-NHAr), 6.50 (1 H, d, *J* 6.0, Ar-*H*), 7.10-7.49 (8 H, m, Ar-*H*), 7.67-7.78 (1 H, m, Ar-*H*), 8.04-8.14 (1 H, m, Ar-*H*); δ_C(75 MHz; 50% $CDCl_3$ -50% CD_3OD; Me_4Si) 50.4, 107.4, 119.5, 122.7, 125.9, 126.2, 127.0, 127.6, 127.8, 128.2, 129.6, 130.1, 136.1, 145.3; *m/z* (FAB) 547 ([M-2H_2O + 2 NOBA]$^+$, 100%).

(2-boronobenzyl)-[4-(4-nitrophenylazo)-naphthalen-1-yl]-amine (17)

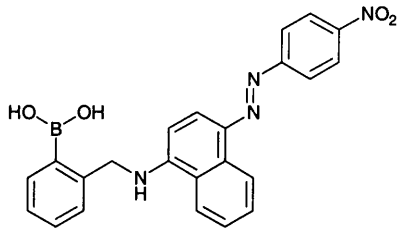

The procedure to form **10** was repeated using 2-(boronobenzyl)-naphthalen-1-yl-amine (0.10 g, 0.36 mmol) instead of (2-borono-benzyl)-*m*-tolyl-amine (all other reagents were used in the same mole ratios), to afford a dark solid, **17,** (0.13 g, 85%): (Found: C, 64.1; H, 4.5; N, 13.1. $C_{23}H_{19}N_4O_4$ requires C, 64.8; H 4.5; N 13.1%); (HRMS: Found 696.2143, ([M- 2H_2O + 2 NOBA]$^+$. $C_{37}H_{29}BN_6O_8$ requires 696.2140); mp >120 °C (dec.); λ_{max}(pH 8.65, 0.05 mol dm^{-3} NaCl, 52.1% MeOH: 47.9% H_2O w/w)/nm 539 (ε/dm^3 mol^{-1} cm^{-1} 45070); ν_{max}(KBr)/cm^{-1} 1574 (N=N), 1538 and 1318 (NO_2); δ_H(300 MHz; 50% $CDCl_3$ - 50% CD_3OD; Me_4Si) 4.27 (2 H, s, ArC*H*$_2$-NHAr), 6.64 (1 H, d, *J* 9.0, Ar-*H*), 7.24-7.73 (6 H, m, Ar-*H*), 7.95-8.13 (4 H, m, Ar-*H*), 8.36 (2 H, d, *J* 9.0, Ar-*H*), 9.02 (1 H, d, *J* 9.0, Ar-*H*); δ_C(75 MHz; 50% $CDCl_3$ - 50% CD_3OD; Me_4Si) 51.5, 108.2, 119.0, 123.7, 126.1, 126.9, 128.1, 128.9, 130.3, 131.0, 131.1, 132.5, 135.4, 136.9, 137.3, 142.8, 145.1, 150.5, 152.4, 160.5; *m/z* (FAB) 697 ([MH- 2H_2O + 2 NOBA]$^+$, 100%).

(2-boronobenzyl)-(3-methoxyphenyl)-amine (18)

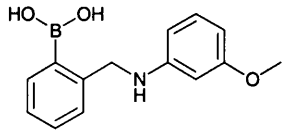

2-formylbenzeneboronic acid (0.50 g, 3.33 mmol) and *m*-anisidine (0.41 g, 3.33 mmol) were mixed in absolute ethanol (45 ml) and benzene (5 ml). A Dean and Stark trap was fitted to permit the azeotropic removal of water, and the reaction mixture heated at reflux overnight (18 hours). After cooling, the solvent was removed *in vacuo* to afford a yellow oil. Sodium borohydride (0.25 g, 6.66 mmol, 2 equiv.) was added slowly to the oil in dry methanol (40 ml). The reaction was left to stir at room temperature for 2 hours and then poured into ice-water (20 ml). The aqueous solution was extracted with dichloromethane (3 x 50 ml). The organic extracts were combined, dried over $MgSO_4$, filtered and stripped of solvent. Precipitation from chloroform by hexane afforded **18** (0.78 g, 91%) as a light yellow solid: (HRMS: Found 527.1882, $[M\text{-}2H_2O + 2\ NOBA]^+$. $C_{28}H_{26}BN_3O_7$ requires 527.1864); mp 50-56 °C (dec.); δ_H(300 MHz; CD_3OD; Me_4Si) 3.84 (3 H, s, Ar-OC*H*$_3$), 4.73 (2 H, s, ArC*H*$_2$-NHAr), 6.92-7.12 (3 H, m, Ar-*H*), 7.39-7.50 (4 H, m, Ar-*H*), 7.87 (1 H, m, Ar-*H*); δ_C(75 MHz; CD_3OD; Me_4Si) 57.1, 58.8, 110.9, 116.7, 117.2, 130.9, 132.5, 132.9, 133.9, 137.4, 137.5, 138.3, 163.0; *m/z* (FAB) 527 ($[M\text{-}2H_2O + 2\ NOBA]^+$, 100%).

(2-borono-5-methoxybenzyl)-*m*-tolylamine (19)

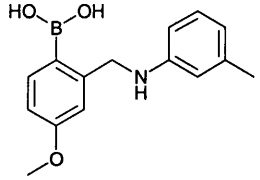

The procedure to form **18** was repeated using 4-methoxy-2-formylphenylboronic acid (0.50 g, 2.78 mmol) and *m*-toluidine (0.30 g, 2.78 mmol) as the reactants, to yield **19** (0.30 g, 40%) as an orange solid: (HRMS: Found 541.2036, $[M\text{-}2H_2O + 2\ NOBA]^+$.

$C_{29}H_{28}BN_3O_7$ requires 541.2020); mp 64-68 °C (dec.); δ_H(300 MHz; CD_3OD; Me_4Si) 2.13 (3 H, s, Ar-C*H*$_3$), 3.69 (3 H, s, Ar-OC*H*$_3$), 4.21 (2 H, s, ArC*H*$_2$-NHAr), 6.45-7.30 (7 H, m, Ar-*H*); δ_C(75 MHz; CD_3OD; Me_4Si) 22.1, 49.7, 56.0, 113.7, 113.9, 114.5, 114.9, 119.8, 122.8, 130.0, 130.3, 130.9, 134.0, 140.3; *m/z* (FAB) 540 ([M-H -2H_2O + 2 NOBA]$^+$, 100%).

4-chloro-2-methylbenzeneboronic acid (20)

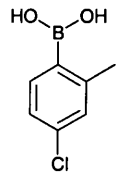

Magnesium powder (2.01 g, 82.7 mmol, 1.1 equiv.) was added to dry THF (40 ml) under a nitrogen atmosphere. 2-bromo-5-chlorotoluene (15.45 g, 75.2 mmol) was slowly syringed into solution. A catalytic amount of 1,2-dibromoethane was added to help initiate the reaction. The solution was heated to reflux for 1 hour until no more magnesium was reacting. The Grignard solution was then filtered under nitrogen into a pressure equalised dropping funnel. The Grignard was added slowly dropwise to trimethylborate (19.53 g, 188 mmol, 2.5 equiv.) in THF (40 ml) cooled to –78 °C. After addition was complete, the reaction was left to stir overnight and allowed to warm to room temperature. The reaction mixture was acidified with 15% aqueous hydrochloric acid (60 ml) and stirred for 30 minutes. The resulting magnesium bromide precipitate was filtered off. The filtrate was extracted with diethyl ether (3 x 50 ml). The organic extracts were combined, dried over $MgSO_4$, filtered and stripped of solvent. The resulting off-white solid was recrystallised from methanol-water to afford **20** (3.81 g, 30%) as a white solid: (HRMS: Found 170.0301. $C_7H_8BO_2Cl$ requires 170.0306); mp 193-195 °C; δ_H(300 MHz; CD_3OD; Me_4Si) 2.29 (3 H, s, Ar-C*H*$_3$), 7.03-7.42 (3 H, m,

Ar-*H*); δ_C(75 MHz; CD_3OD; Me_4Si) 22.2, 126.4, 130.5, 134.2, 136.1, 144.0; *m/z* (EI) 170 ($[M]^+$, 85%), 152 ($[M\text{-}H_2O]^+$, 100).

(2-borono-5-chlorobenzyl)-*m*-tolylamine (21)

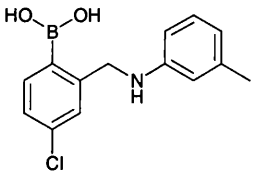

4-chloro-2-methylbenzeneboronic acid (1.50 g, 8.80 mmol) was mixed in carbon tetrachloride (25 ml). A reflux condensor and a pressure equalised dropping funnel, containing bromine (7.03 g, 44.0 mmol, 5 equiv.) in carbon tetrachloride (20 ml), were fitted to the reaction vessel. The boronic acid solution was heated to gentle reflux until all solid had dissolved. The bromine solution was then added dropwise over the period of 1 hour, whilst reflux was maintained. A lamp was shined upon the reaction throughout the bromine addition. Reflux was continued for a further hour after addition was complete. The solvent was removed *in vacuo* to afford an off-white solid, a mixture of the mono and dibrominated products. This was dissolved in chloroform (50 ml) and added to water (50 ml). After cooling on an ice bath, 15% sodium hydroxide solution was added to raise the pH of the aqueous phase to above 11. The solution was stirred vigourously for 1 hour. The chloroform layer was removed and the aqueous phase acidified with 1 M hydrochloric acid. The aqueous layer was extracted with diethyl ether (3 x 50 ml), the organic extracts combined, dried over $MgSO_4$ and filtered. The solvent was stripped to yield a white solid, the alcohol hydrolysis product of the monobrominated reactant. The chloroform layer was re-extracted with 15% sodium hydroxide. The aqueous layer was acidified and extracted with diethyl ether (3 x 50 ml). After combination of the organic extracts, drying ($MgSO_4$) and filtration, the solvent was removed *in vacuo* to afford an off-white solid, the aldehyde hydrolysis product of the dibrominated reactant. The procedure to form **2** was repeated using the aldehyde

product (0.62 g, 3.33 mmol) and *m*-toluidine (0.36 g, 3.33 mmol), to yield **21** (0.39 g, 43%) as a white solid: (HRMS: Found 545.1528, $[M\text{-}2H_2O + 2\ NOBA]^+$. $C_{28}H_{25}BN_3O_6Cl$ requires 545.1525); mp 62-66 °C (dec.); δ_H(300 MHz; CD_3OD; Me_4Si) 2.13 (3 H, s, Ar-C*H*$_3$), 4.21 (2 H, s, ArC*H*$_2$-NHAr), 6.45-6.61 (3 H, m, Ar-*H*), 6.88-6.99 (1 H, m, Ar-*H*), 7.07-7.28 (3 H, m, Ar-*H*); δ_C(75 MHz; CD_3OD; Me_4Si) 22.0, 51.5, 114.9, 118.5, 123.0, 126.7, 127.9, 130.2, 134.1, 135.6, 140.1, 148.5; *m/z* (FAB) 545 ($[M\text{-}2H_2O + 2\ NOBA]^+$, 100%).

_N,N'_-Bis-(2-boronobenzyl)-methylene-3,3-dianiline (22)

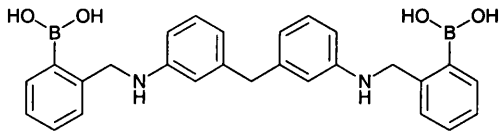

The procedure to form **18** was repeated using 2-formylphenylboronic acid (0.50 g, 3.33 mmol, 2 equiv.) and 3,3'-methylenedianiline (0.33 g, 1.67 mmol) as the reactants, to yield **22** (0.72 g, 93%) as a white solid: (HRMS: Found 1006.3745, $[M\text{-}4H_2O + 4\ NOBA]^+$. $C_{55}H_{48}B_2N_6O_{12}$ requires 1006.3745); mp 129-135 °C (dec.); δ_H(300 MHz; CD_3OD; Me_4Si) 3.71 (2 H, s, ArC*H*$_2$-Ar), 4.32 (4 H, s, ArC*H*$_2$-NHAr), 6.45-6.68 (6 H, m, Ar-*H*), 6.90-7.01 (2 H, m, Ar-*H*), 7.07-7.41 (8 H, m, Ar-*H*); δ_C(75 MHz; CD_3OD; Me_4Si) 43.8, 51.6, 115.0, 118.0, 120.9, 121.7, 127.6, 129.1, 130.4, 134.0, 144.0, 145.8; *m/z* (ESI) 429 ($[M\text{-}2H_2O]^+$, 100%).

_N,N'_-Bis-(2-boronobenzyl)-benzene-1,3-diamine (23)

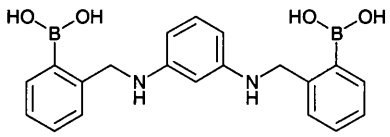

The procedure to form **16** was repeated with 2-formylbenzeneboronic acid (0.40 g, 2.67 mmol, 2 equiv.) and *m*-phenylenediamine (0.14 g, 1.33 mmol) to afford **23** (0.46 g, 92%) as an off-white solid: (HRMS: Found 916.3092, $[M\text{-}4H_2O + 4\ NOBA]^+$.

$C_{48}H_{42}B_2N_6O_{12}$ requires 916.3045); mp 175-177 °C (dec.); δ_H(300 MHz; CD_3OD; Me_4Si) 4.24 (4 H, s, ArCH_2-NHAr), 6.24 (1 H, s, Ar-*H*), 6.29 (2 H, d, *J* 9.0, Ar-*H*), 6.93 (1 H, t, *J* 9.0, Ar-*H*), 7.14-7.36 (8 H, m, Ar-*H*); δ_C(75 MHz; CD_3OD; Me_4Si) 50.2, 103.6, 108.4, 125.5, 126.3, 128.2, 128.8, 128.9, 131.2, 144.3, 148.1; *m/z* (FAB) 916 ([M-4H_2O + 4 NOBA]$^+$, 100%).

2-{(2-hydroxyethyl)-[3-methyl-4-(4-nitrophenylazo)-phenyl]-amino}-ethanol (24)

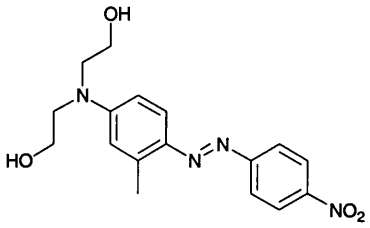

4-nitroaniline (0.18 g, 1.28 mmol) was mixed in water (2 ml), methanol (2 ml) and hydrochloric acid (2 ml, 5.0 M) and then cooled to 0-5 °C on an ice-bath. A chilled solution of sodium nitrite (0.11 g, 1.54 mmol, 0.2 M) was added dropwise. Excess nitrite was destroyed by the addition of sulphamic acid. *m*-tolyldiethanolamine (0.25 g, 1.28 mmol) was dissolved in methanol (4 ml) and dilute hydrochloric acid (2 ml, 1 M), then added dropwise to the reaction mixture, which quickly turned a red colour. Sodium acetate was added to raise the pH of the solution to 4 and this was then left to stir at 0-5 °C for 3 hours. Sodium hydroxide (2 M) was slowly added to raise the pH to 7. The resulting precipitate was collected by suction filtration and dried in a dessicator overnight to afford **24** (0.39 g, 89%) as a dark red solid: HRMS Found 344.1480, $C_{17}H_{20}N_4O_4$ requires 344.1485; mp >120 °C (dec.); λ_{max}(0.05 M NaCl, 33.3% MeOH: 66.7% H_2O w/w, pH 7.07)/nm 500 (ε/dm^3 mol^{-1} cm^{-1} 31620); ν_{max}(KBr disk)/cm^{-1} 1604 (N=N), 1507 and 1336 (NO_2); δ_H(300 MHz; 90% $CDCl_3$-10%CD_3OD; Me_4Si) 2.62 (3 H, s, Ph-CH_3), 3.51 (4 H, m, -NCH_2CH_2OH), 4.68 (4 H, m, -NCH$_2$CH_2OH), 6.45-6.55 (2 H, m, Ph-*H*), 7.58-7.65 (1 H, d, Ph-*H*), 7.72 (2 H, d, Ph-*H*), 8.12 (2 H, d, Ph-*H*); δ_C(125 MHz; 90% $CDCl_3$-10% CD_3OD; Me_4Si) 21.8, 58.3, 63.5, 114.1, 116.5, 121.0,

126.2, 128.3, 145.8, 146.8, 150.7, 155.4, 160.7; m/z (EI) 344 ($[M]^+$, 19%) 313 ($[M-CH_2OH]^+$, 100).

Alizarin Red S monohydrate (25)

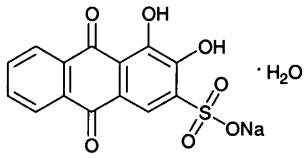

A certified sample of Alizarin Red S monohydrate (sodium salt of 3,4-dihydroxy-9,10-dioxo-2-anthracenesulfonic acid) was purchased from the Aldrich Chemical Co. Ltd. and was used as received in all of the various titrations described herein.

3.3 UV-Visible Absorbance Measurements

Absorption-pH titration of 3, 4, 5, 6, 7, 10, 14 and 17

The UV-visible absorption spectra of **3** (5.66×10^{-5} mol dm^{-3}), **4** (4.66×10^{-5} mol dm^{-3}), **5** (5.47×10^{-5} mol dm^{-3}), **6** (7.33×10^{-5} mol dm^{-3}), and **7** (5.34×10^{-5} mol dm^{-3}) in a 0.05 mol dm^{-3} NaCl 33% methanol: 67% water (w/w) solution, were all recorded as the pH was changed from pH 2 to 12 in approximate intervals of 0.5 pH units. The pH was controlled using minimum volumes of sodium hydroxide and hydrochloric acid solutions. The same experiment was repeated with **10** (1.86×10^{-5} mol dm^{-3}) in a 0.05 mol dm^{-3} NaCl 67% methanol: 33% water (w/w) solution, **14** (1.57×10^{-5} mol dm^{-3}) in a 0.05 mol dm^{-3} NaCl 52.1% methanol: 47.9% water (w/w) solution, and **17** (1.76×10^{-5} mol dm^{-3}) in a 0.05 mol dm^{-3} NaCl 50% methanol: 50% water (w/w) solution.

Absorption-pH titrations of 3, 4, 5, 6, 7, 10, 14 and 17 in the presence of D-Fructose

The previous experiment was repeated with the addition of 0.05 mol dm^{-3} D-fructose to the solution in all cases.

Absorption-Saccharide titrations of 3, 4, 5, 6, 7, 10 and 17 at pH 11.32

The UV-visible absorption spectra of **3** (2.83×10^{-5} mol dm^{-3}), **4** (3.26×10^{-5} mol dm^{-3}), **5** (2.74×10^{-5} mol dm^{-3}), **6** (5.86×10^{-5} mol dm^{-3}), **7** (4.27×10^{-5} mol dm^{-3}), **10** (2.09×10^{-5} mol dm^{-3}), and **17** (1.76×10^{-5} mol dm^{-3}) in a pH 11.32 buffer (0.01000 mol dm^{-3} KCl, 0.002771 mol dm^{-3} $NaHCO_3$, 0.002771 mol dm^{-3} Na_2CO_3 in 52.1 wt% methanol: 47.9 wt% water),[144] were recorded as increasing amounts of various saccharides were added to the solution.

Absorption-Saccharide titrations of 3, 10, 14 and 17 at pH 8.21

The UV-visible absorption spectra of **3** ($2.83x10^{-5}$ mol dm^{-3}), **10** ($2.00x10^{-5}$ mol dm^{-3}), **14** ($3.14x10^{-5}$ mol dm^{-3}) and **17** ($1.76x10^{-5}$ mol dm^{-3}) in a pH 8.21 buffer (0.01000 mol dm^{-3} KCl, 0.002752 mol dm^{-3} $KHPO_4$, 0.002757 mol dm^{-3} Na_2HPO_4 in 52.1 wt% methanol: 47.9 wt% water),[144] were recorded as increasing amounts of various saccharides were added to the solution.

Absorption-Potassium Halide titrations of 3, 10, 12, 14 and 17 in methanol

The UV-visible absorption spectra of **3** ($3.16x10^{-5}$ mol dm^{-3}), **10** ($2.93x10^{-5}$ mol dm^{-3}), **12** ($2.89x10^{-5}$ mol dm^{-3}), **14** ($1.57x10^{-5}$ mol dm^{-3}) and **17** ($1.76x10^{-5}$ mol dm^{-3}) in HPLC methanol, were recorded as increasing amounts of potassium halide salts were added to the solution. The titrations were performed under a nitrogen atmosphere. After each addition of salt, the solutions were allowed to stir for at least 2 minutes before absorbance measurements were made, to allow complete dissolution of the salt.

Absorption-pH titrations of Alizarin Red S monohydrate (25)

The UV-visible absorption spectra of **25** ($7.36x10^{-5}$ mol dm^{-3}) in a 0.05 mol dm^{-3} NaCl 50% methanol: 50% water (w/w) solution was recorded as the pH was changed from pH 2 to 12 in approximate intervals of 0.5 pH units. The pH was controlled using minimum volumes of sodium hydroxide and hydrochloric acid solutions. The titration was repeated in the presence of 0.005 mol dm^{-3} phenylboronic acid.

Absorption-Boronic acid titrations of 25 at pH 8.21

The UV-visible absorption spectra of **25** ($9.60x10^{-5}$ mol dm^{-3}) in a pH 8.21 buffer (0.01000 mol dm^{-3} KCl, 0.002752 mol dm^{-3} $KHPO_4$, 0.002757 mol dm^{-3} Na_2HPO_4 in

52.1 wt% methanol: 47.9 wt% water)[144] were recorded as increasing amounts of various boronic acids were added to the solution.

4 Conclusions

"It is good to have an end to journey toward; but it is the journey that matters, in the end."

Ursula K. Le Guin, 1929-

This research has shown that it is possible to synthesise a variety of boronic acid appended dyes using relatively simple, clean and mild reaction conditions. The interaction of saccharides with these dyes has shown spectral responses in all cases, although the extent of the change varies subtly with each dye structure. Dye **3**, containing an azo chromophore, and dye **14**, a tricyanovinyl derivative, have both experienced enhanced spectral changes upon the addition of saccharide. This leads to large visible colour changes being detected in both molecules, at pH 11.32 and pH 8.21 respectively. Indeed, the spectral shifts are the biggest reported to date in such systems.

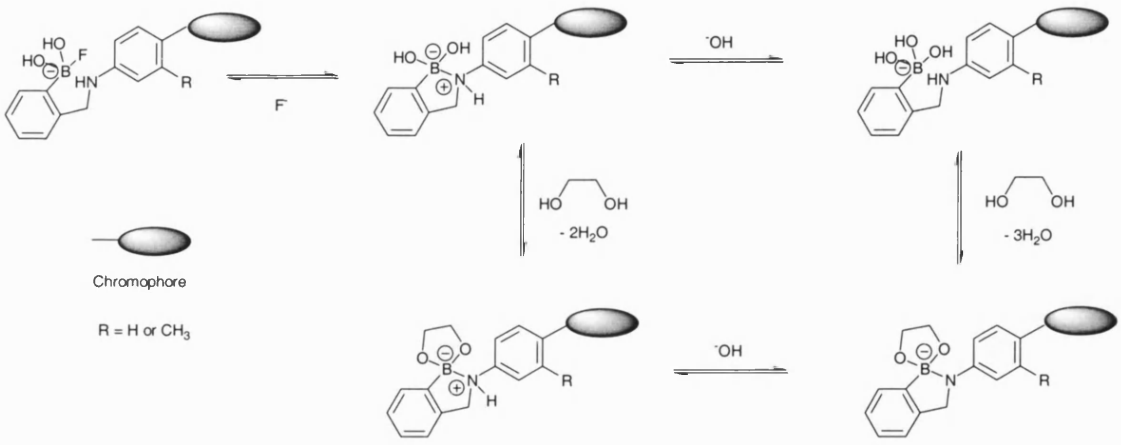

Scheme 22: Schematic to represent the interaction of saccharide and fluoride with boronic acid chromophores showing deprotonated saccharide-bound boron-nitrogen bonded species

The key structural element that leads to the improved spectral responses of these dyes is thought to be the presence of the proton on the anilinic nitrogen secondary centre. Scheme 22 shows the proposed equilibria for this explanation. The strengthening of the boron-nitrogen interaction upon saccharide binding to the boronic acid, in combination with the electron-withdrawing nature of the chromophores, seems to facilitate the deprotonation of the anilinic nitrogen hydrogen. This leads to the formation of a deprotonated saccharide-bound boron-nitrogen bonded species, which is electronically different from the unbound boronic acid species. Hence a colour change is observed

upon saccharide binding. The highly electron-withdrawing tricyanovinyl group of dye **14** lowers the pK_a of the dye compared to azo derivatives. This enables the formation of the deprotonated saccharide-bound boron-nitrogen species at near neutral pH. Boronic acid dyes that cannot form this deprotonated saccharide bound boron-nitrogen bonded species, either for structural or steric reasons, give smaller spectral changes. Scheme 23 shows the proposed equilibria for these dye structures.

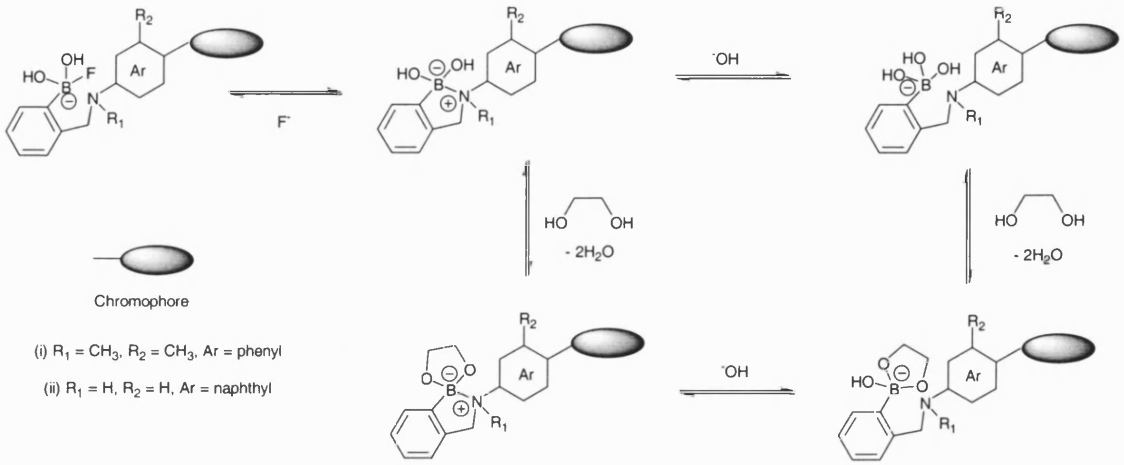

Scheme 23: Schematic to represent the interaction of saccharide and fluoride with boronic acid chromophores showing no deprotonated boron-nitrogen bonded species

Attempts to introduce a second boronic acid binding site into the azo dye system for the recognition of D-glucose have proved unsuccessful. However, future endeavour could lead to the development of a D-glucose selective colour sensor. The unproductive efforts so far have concentrated on adding the second boronic acid unit to the aromatic ring where the chromophore is coupled. Figure 72 shows how it might be viable to link a second boronic acid to the first boronic acid ring system. By changing the length of the linker unit it may be possible to change the selectivity towards different saccharides. Only one chromophore needs to be coupled to the molecule for a binding event to be signalled. The second boronic acid moiety can be used solely for binding purposes.

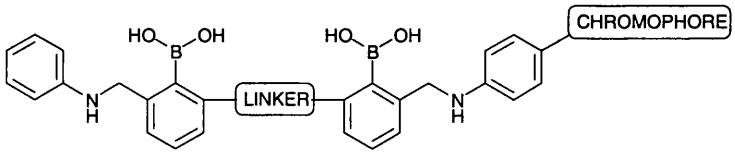

Figure 72: Schematic to represent a possible D-glucose selective colour sensor

The fluoride work with the boronic acid dyes represents the first example where chromophores containing a boronic acid receptor unit have been used to detect fluoride ion binding events colorimetrically. The use of these molecules has resulted in high fluoride selectivity, with no interference observed from other halide ions. The spectral changes observed are thought to be caused by the fluoride ion breaking the boron-nitrogen bond present in these molecules to form a tetrahedral boronate adduct, in a similar manner to the addition of hydroxide ion to the dyes in the pH titrations (see Scheme 22 and Scheme 23). With appropriate modifications of the chromophore and Lewis acid-binding site, fluoride selectivity could be fine tuned to any desired fluoride concentration range. Polymer support would also increase the sensitivity of the sensor, possibly to the range of concentration of fluoride in drinking water supplies. It is therefore conceivable that this work could lead to the development of colorimetric fluoride sensors for a variety of industrial and medicinal applications.

It has been shown that the commercially available Alizarin Red S undergoes a large visible colour change upon complexation with a variety of simple boronic acids. This could prove to be a very useful colorimetric detection method for the many researchers working with boronic acids. It should be stressed that the system will also work as a fluorescent sensor. Further work is needed to develop this colorimetric system towards an independent scale of boronic acid binding affinity to diols. Recent work has shown that Alizarin Red S can also be used as a competitive assay for the colorimetric study of the binding of boronic acids to D-fructose.[162] With further research, Alizarin Red S and

other similar dye molecules could feasibly be developed into selective systems for other saccharides, and not just for D-fructose.

5 References

"If I have seen further than others, it is by standing upon the shoulders of giants."

Isaac Newton, 1642-1727

1 T. D. James, K. R. A. S. Sandanayake, and S. Shinkai, *Angew. Chem., Int. Ed. Engl.*, 1996, **35**, 1911.

2 J. H. Hartley, T. D. James, and C. J. Ward, *J. Chem. Soc., Perkin Trans. 1*, 2000, 3155.

3 A. Suzuki, *J. Organomet. Chem.*, 1999, **576**, 147.

4 R. N. Fedoak, M. D. Gershon, and M. Field, *Gasteroenterology*, 1989, **96**, 37.

5 H. Yasuda, T. Kurokawa, Y. Fuji, A. Yamashita, and S. Ishibashi, *Biochim. Biophys. Acta.*, 1990, **1021**, 114.

6 P. Baxter, J. Goldhill, P. T. Hardcastle, and C. J. Taylor, *Gut.*, 1990, **31**, 817.

7 L. J. Elsaa and L. E. Rosenberg, *J. Clinic. Invest.*, 1969, **48**, 1845.

8 S. De Marchi, E. Cecchin, A. Basil, G. Proto, W. Donadon, A. Jengo, D. Schinella, A. Jus, D. Villalta, P. De Paoli, G. Santini, and F. Tesio, *J. Nephrol.*, 1984, **4**, 280.

9 T. Yamamoto, Y. Seino, H. Fukumoto, G. Koh, H. Yano, N. Inagaki, Y. Yamada, K. Inoue, T. Manabe, and H. Imura, *Biochem. Biophys. Res. Commun.*, 1990, **170**, 223.

10 For more information see the Diabetes UK website: www.diabetes.org.uk.

11 R. W. Cattrall, '*Chemical sensors*', Oxford University Press, 1997.

12 A. P. Davis and R. S. Wareham, *Angew. Chem., Int. Ed. Engl.*, 1999, **38**, 2978.

13 A. P. Davis and R. S. Wareham, *Angew. Chem., Int. Ed. Engl.*, 1998, **37**, 2270.

14 A. P. Davis, S. Menzer, J. J. Walsh, and D. J. Williams, *Chem. Commun.*, 1996, 453.

15 A. P. Davis and J. J. Walsh, *Chem. Commun.*, 1996, 449.

16 K. M. Bhattarai, A. P. Davis, J. J. Perry, C. J. Walter, S. Menzer, and D. J. Williams, *J. Org. Chem.*, 1997, **62**, 8463.

17 A. S. Droz and F. Diederich, *J. Chem. Soc., Perkin Trans. 1*, 2000, 4224.

18 G. Das and A. D. Hamilton, *Tetrahedron Lett.*, 1997, **38**, 3675.

19 A. Michaelis and P. Becker, *Ber. Dtsch. Chem. Ges.*, 1882, **15**, 180.

20 A. Michaelis and P. Becker, *Ber. Dtsch. Chem. Ges.*, 1880, **13**, 58.

21 W. Seaman and J. R. Johnson, *J. Am. Chem. Soc.*, 1931, **53**, 711.

22 M. L. Lappert, *Chem. Rev.*, 1956, **56**, 959.

23 K. Torssell, *Arkiv Kemi*, 1957, **10**, 473.

24 H. G. Kuivila, A. H. Keough, and E. J. Soboczenski, *J. Org. Chem.*, 1954, **19**, 780.

25 M. L. Wolfrom and J. Solms, *J. Org. Chem.*, 1956, **21**, 815.

26 J. M. Sugihara and C. M. Bowman, *J. Am. Chem. Soc.*, 1958, **80**, 2443.

27 J. P. Lorand and J. O. Edwards, *J. Org. Chem.*, 1959, **24**, 769.

28 S. David, '*The Molecular and Supramolecular Chemistry of Carbohydrates: A Chemical Introduction to the Glycosciences*', Oxford University Press, 1997.

29 K. Tsukagoshi and S. Shinkai, *J. Org. Chem.*, 1991, **56**, 4089.

30 K. Kondo, Y. Shiomi, M. Saisho, T. Harada, and S. Shinkai, *Tetrahedron*, 1992, **48**, 8239.

31 Y. Shiomi, M. Saisho, K. Tsukagoshi, and S. Shinkai, *J. Chem. Soc., Perkin Trans. 1*, 1993, 2111.

32 T. D. James, K. R. A. S. Sandanayake, R. Iguchi, and S. Shinkai, *J. Am. Chem. Soc.*, 1995, **117**, 8982.

33 J. C. Norrild and H. Eggert, *J. Am. Chem. Soc.*, 1995, **117**, 1479.

34 J. C. Norrild and H. Eggert, *J. Chem. Soc., Perkin Trans. 2*, 1996, 2583.

35 M. Bielecki, H. Eggert, and J. C. Norrild, *J. Chem. Soc., Perkin Trans. 2*, 1999, 449.

36 W. Yang, H. He, and D. G. Drueckhammer, *Angew. Chem., Int. Ed. Engl.*, 2001, **40**, 1714.

37 A. P. de Silva, H. Q. N. Gunaratne, T. Gunnlaugsson, A. J. M. Huxley, C. P. McCoy, J. T. Rademacher, and T. E. Rice, *Chem. Rev.*, 1997, **97**, 1515.

38 J. Yoon and A. W. Czarnik, *J. Am. Chem. Soc.*, 1992, **114**, 5874.

39 H. Suenaga, M. Mikami, K. Sandanayake, and S. Shinkai, *Tetrahedron Lett.*, 1995, **36**, 4825.

40 H. Suenaga, H. Yamamoto, and S. Shinkai, *Pure Appl. Chem.*, 1996, **68**, 2179.

41 T. D. James, K. R. A. S. Sandanayake, and S. Shinkai, *Angew. Chem., Int. Ed. Engl.*, 1994, **33**, 2207.

42 K. Sandanayake, T. D. James, and S. Shinkai, *Chem. Lett.*, 1995, 503.

43 C. R. Cooper and T. D. James, *Chem. Commun.*, 1997, 1419.

44 C. R. Cooper and T. D. James, *J. Chem. Soc., Perkin Trans. 1*, 2000, 963.

45 K. Sandanayake, S. Imazu, T. D. James, M. Mikami, and S. Shinkai, *Chem. Lett.*, 1995, 139.

46 S. Arimori, L. I. Bosch, C. J. Ward, and T. D. James, *Tetrahedron Lett.*, 2001, **42**, 4553.

47 T. Imada, H. Kijima, M. Takeuchi, and S. Shinkai, *Tetrahedron Lett.*, 1995, **36**, 2093.

48 T. Imada, H. Kijima, M. Takeuchi, and S. Shinkai, *Tetrahedron*, 1996, **52**, 2817.

49 M. Takeuchi, T. Imada, and S. Shinkai, *J. Am. Chem. Soc.*, 1996, **118**, 10658.

50 M. Takeuchi, T. Imada, and S. Shinkai, *Bull. Chem. Soc. Japan*, 1998, **71**, 1117.

51 S. Arimori, M. Takeuchi, and S. Shinkai, *Chem. Lett.*, 1996, 77.

52 T. Mizuno, M. Takeuchi, and S. Shinkai, *Tetrahedron*, 1999, **55**, 9455.

53 T. Mizuno, M. Yamamoto, M. Takeuchi, and S. Shinkai, *Tetrahedron*, 2000, **56**, 6193.

54 M. J. Deetz and B. D. Smith, *Tetrahedron Lett.*, 1998, **39**, 6841.

55 Y. Kanekiyo, Y. Ono, K. Inoue, M. Sano, and S. Shinkai, *J. Chem. Soc., Perkin Trans. 2*, 1999, 557.

56 Y. Kanekiyo, K. Inoue, Y. Ono, M. Sano, S. Shinkai, and D. N. Reinhoudt, *J. Chem. Soc., Perkin Trans. 2*, 1999, 2719.

57 T. Ishi-i, K. Nakashima, and S. Shinkai, *Chem. Commun.*, 1998, 1047.

58 T. Ishi-i, K. Nakashima, S. Shinkai, and A. Ikeda, *J. Org. Chem.*, 1999, **64**, 984.

59 S. J. Gardiner, B. D. Smith, P. J. Duggan, M. J. Karpa, and G. J. Griffin, *Tetrahedron*, 1999, **55**, 2857.

60 M. F. Paugam, J. A. Riggs, and B. D. Smith, *Chem. Commun.*, 1996, 2539.

61 M. F. Paugam, J. T. Bien, B. D. Smith, L. A. J. Chrisstoffels, F. deJong, and D. N. Reinhoudt, *J. Am. Chem. Soc.*, 1996, **118**, 9820.

62 S. P. Draffin, P. J. Duggan, and S. A. M. Duggan, *Org. Lett.*, 2001, **3**, 917.

63 R. J. Ferrier, *Adv. Carbohydr. Chem. Biochem.*, 1978, **35**, 31.

64 V. Bhaskar, P. J. Duggan, D. G. Humphrey, G. Y. Krippner, V. McCarl, and D. A. Offermann, *J. Chem. Soc., Perkin Trans. 1*, 2001, 1098.

65 H. R. Snyder and C. Weaver, *J. Am. Chem. Soc.*, 1948, **70**, 232.

66 H. S. Snyder and S. L. Meisel, *J. Am. Chem. Soc.*, 1948, **70**, 774.

67 H. Gilman, L. Santucci, D. R. Swayampi, and R. O. Ranck, *J. Am. Chem. Soc.*, 1957, **79**, 2898.

68 A. P. Russell, in '*Method and means for detecting polyhydroxyl compounds*', WO 91/04488, 1991.

69 N. Nagasaki, H. Shinmori, and S. Shinkai, *Tetrahedron Lett.*, 1994, **35**, 2201.

70 H. Shinmori, M. Takeuchi, and S. Shinkai, *J. Chem. Soc., Perkin Trans. 2*, 1996, 1.

71 M. Takeuchi, M. Taguchi, H. Shinmori, and S. Shinkai, *Bull. Chem. Soc. Japan*, 1996, **69**, 2613.

72 K. R. A. S. Sandanayake and S. Shinkai, *J. Chem. Soc., Chem. Commun.*, 1994, 1083.

73 H. Shinmori, M. Takeuchi, and S. Shinkai, *J. Chem. Soc., Perkin Trans. 2*, 1998, 847.

74 K. Koumoto and S. Shinkai, *Chem. Lett.*, 2000, 856.

75 K. Koumoto, M. Takeuchi, and S. Shinkai, *Supramol. Chem.*, 1998, **9**, 203.

76 C. J. Davis, P. T. Lewis, M. E. McCarroll, M. W. Read, R. Cueto, and R. M. Strongin, *Org. Lett.*, 1999, **1**, 331.

77 P. T. Lewis, C. J. Davis, L. A. Cabell, M. He, M. W. Read, M. E. McCarroll, and R. M. Strongin, *Org. Lett.*, 2000, **2**, 589.

78 F. Frantzen, K. Grimsrud, D. Heggli, and E. Sundrehagen, *Clin. Chim. Acta*, 1997, **263**, 207.

79 N. E. Pawlowski, D. D. Russell, and K. M. Robotti, in '*Boronic Acid Dyes*', US 5108502, 1992.

80 L. A. Cabell, M. K. Monahan, and E. V. Anslyn, *Tetrahedron Lett.*, 1999, **40**, 7753.

81 J. J. Lavigne and E. V. Anslyn, *Angew. Chem., Int. Ed. Engl.*, 1999, **38**, 3666.

82 J. H. Hartley and T. D. James, *Tetrahedron Lett.*, 1999, **40**, 2597.

83 M. S. Frant and J. W. Ross, *Science*, 1966, **154**, 1553.

84 A. Bianchi, K. Bowman-James, and E. Garcia-Espana, '*Supramolecular Chemistry of Anions*', Wiley-VCH, 1997.

85 P. D. Beer and D. K. Smith, *Prog. Inorg. Chem.*, 1997, **46**, 1.

86 P. D. Beer and P. A. Gale, *Angew. Chem., Int. Ed. Engl.*, 2001, **40**, 487.

87 R. Belcher, M. A. Leonard, and T. S. West, *Talanta*, 1959, **2**, 92.

88 R. Belcher, M. A. Leonard, and T. S. West, *J. Chem. Soc.*, 1959, 3577.

89 R. Belcher and T. S. West, *Talanta*, 1961, **8**, 853.

90 R. Belcher and T. S. West, *Talanta*, 1961, **8**, 863.

91 M. A. Leonard and T. S. West, *J. Chem. Soc.*, 1960, 4477.

92 S. S. Yamamura, M. A. Wade, and J. H. Sikes, *Anal. Chem.*, 1962, **34**, 1308.

93 J. L. Sessler, M. J. Cyr, V. Lynch, E. McGhee, and J. A. Ibers, *J. Am. Chem. Soc.*, 1990, **112**, 2810.

94 M. Shionoya, H. Furuta, V. Lynch, A. Harriman, and J. L. Sessler, *J. Am. Chem. Soc.*, 1992, **114**, 5714.

95 J. L. Sessler, M. Cyr, H. Furuta, V. Kral, T. Mody, T. Morishima, M. Shionoya, and S. Weghorn, *Pure Appl. Chem.*, 1993, **65**, 393.

96 P. A. Gale, L. J. Twyman, C. I. Handlin, and J. L. Sessler, *Chem. Commun.*, 1999, 1851.

97 S. Camiolo and P. A. Gale, *Chem. Commun.*, 2000, 1129.

98 H. Miyaji, W. Sato, and J. L. Sessler, *Angew. Chem., Int. Ed. Engl.*, 2000, **39**, 1777.

99 P. A. Gale, J. L. Sessler, V. Kral, and V. Lynch, *J. Am. Chem. Soc.*, 1996, **118**, 5140.

100 M. M. G. Antonisse, B. H. M. Snellink-Ruel, I. Yigit, J. F. J. Engbersen, and D. N. Reinhoudt, *J. Org. Chem.*, 1997, **62**, 9034.

101 C. B. Black, B. Andrioletti, A. C. Try, C. Ruiperez, and J. L. Sessler, *J. Am. Chem. Soc.*, 1999, **121**, 10438.

102 S. Mason, J. M. Llinares, M. Morton, T. Clifford, and K. Bowman-James, *J. Am. Chem. Soc.*, 2000, **122**, 1814.

103 K. Niikura, A. P. Bisson, and E. V. Anslyn, *J. Chem. Soc., Perkin Trans. 2*, 1999, 1111.

104 A. Metzger, V. M. Lynch, and E. V. Anslyn, *Angew. Chem., Int. Ed. Engl.*, 1997, **36**, 862.

105 A. Metzger and E. V. Anslyn, *Angew. Chem., Int. Ed. Engl.*, 1998, **37**, 649.

106 L. A. Cabell, M. D. Best, J. J. Lavigne, S. E. Schneider, D. M. Perreault, M. K. Monahan, and E. V. Anslyn, *J. Chem. Soc., Perkin Trans. 2*, 2001, 315.

107 H. E. Katz, *J. Am. Chem. Soc.*, 1985, **107**, 1420.

108 H. E. Katz, *J. Org. Chem.*, 1985, **50**, 5027.

109 H. E. Katz, *J. Am. Chem. Soc.*, 1986, **108**, 7640.

110 M. T. Reetz, C. M. Niemeyer, and K. Harms, *Angew. Chem., Int. Ed. Engl.*, 1991, **30**, 1472.

111 M. T. Reetz, C. M. Niemeyer, and K. Harms, *Angew. Chem., Int. Ed. Engl.*, 1991, **30**, 1474.

112 C. Dusemund, K. Sandanayake, and S. Shinkai, *J. Chem. Soc., Chem. Commun.*, 1995, 333.

113 H. Yamamoto, A. Ori, K. Ueda, C. Dusemund, and S. Shinkai, *Chem. Commun.*, 1996, 407.

114 A. Ori and S. Shinkai, *J. Chem. Soc., Chem. Commun.*, 1995, 1771.

115 C. R. Cooper, N. Spencer, and T. D. James, *Chem. Commun.*, 1998, 1365.

116 A. Yuchi, J. Sakurai, A. Tatebe, H. Hattori, and H. Wada, *Anal. Chim. Acta*, 1999, **387**, 189.

117 A. Yuchi, A. Tatebe, S. Kani, and T. D. James, *Bull. Chem. Soc. Japan*, 2001, **74**, 509.

118 M. Nicolas, B. Fabre, and J. Simonet, *Chem. Commun.*, 1999, 1881.

119 H. Shiratori, T. Ohno, K. Nozaki, I. Yamazaki, Y. Nishimura, and A. Osuka, *Chem. Commun.*, 1998, 1539.

120 H. Shiratori, T. Ohno, K. Nozaki, and A. Osuka, *Chem. Commun.*, 1999, 2181.

121 M. Nicolas, B. Fabre, G. Marchand, and J. Simonet, *Eur. J. Org. Chem.*, 2000, 1703.

122 M. Nicolas, B. Fabre, and J. Simonet, *Electrochim. Acta*, 2001, **46**, 1179.

123 E. N. Abrahart, '*Dyes and their Intermediates*', Edward Arnold, 1977.

124 P. Gordon and P. Gregory, '*Organic Chemistry in Colour*', Springer-Verlag, 1987.

125 W. Wang, G. Springsteen, S. Gao, and B. Wang, *Chem. Commun.*, 2000, 1283.

126 A. M. G. Campana, F. A. Barrero, and M. R. Ceba, *Analyst*, 1992, **117**, 1189.

127 N. Chimpalee, D. Chimpalee, B. Boonyanitchayakul, and D. T. Burns, *Anal. Chim. Acta*, 1993, **282**, 643.

128 K. A. Bello and J. Griffiths, *J. Chem. Soc., Chem. Commun.*, 1986, 1639.

129 B. C. McKusick, R. E. Heckert, T. L. Cairns, D. D. Coffman, and H. F. Mower, *J. Am. Chem. Soc.*, 1958, **80**, 2806.

130 J. R. Roland and B. C. McKusick, *J. Am. Chem. Soc.*, 1961, **83**, 1652.

131 M. L. Schilling, H. E. Katz, and D. I. Cox, *J. Org. Chem.*, 1988, **53**, 5538.

132 A. K. Y. Jen, Y. J. Liu, Y. Cai, V. P. Rao, and L. R. Dalton, *J. Chem. Soc., Chem. Commun.*, 1994, 2711.

133 V. P. Rao, K. Y. Wong, A. K. Y. Jen, and K. J. Drost, *Chem. Mater.*, 1994, **6**, 2210.

134 X. Wang, J. I. Chen, S. Marturunkakul, L. Li, J. Kumar, and S. K. Tripathy, *Chem. Mater.*, 1997, **9**, 45.

135 H. E. Katz, K. D. Singer, J. E. Sohn, C. W. Dirk, L. A. King, and H. M. Gordon, *J. Am. Chem. Soc.*, 1987, **109**, 6561.

136 D. N. Dhar, *Chem. Rev.*, 1967, **67**, 611.

137 T. D. James, P. Linnane, and S. Shinkai, *Chem. Commun.*, 1996, 281.

138 C. R. Cooper and T. D. James, *Chem. Lett.*, 1998, 883.

139 H. Zollinger, '*Color Chemistry*', VCH, 1991.

140 C. S. De Ligny and M. Rehbach, *Recl. Trav. Chim. Pays-Bas*, 1960, **79**, 727.

141 J. H. Hartley, '*Saccharide Accelerated Hydrolysis of Boronic Acid Imines*', PhD Thesis, University of Birmingham, 2001.

142 T. D. James, K. R. A. S. Sandanayake, and S. Shinkai, *Supramol. Chem.*, 1995, **6**, 141.

143 B. Valeur, J. Pouget, J. Bourson, M. Kaschke, and N. P. Ernsting, *J. Phys. Chem.*, 1992, **96**, 6545.

144 D. D. Perrin and B. Dempsey, '*Buffers for pH and Metal Ion Control*', Chapman & Hall, 1974.

145 C. J. Ward, P. Patel, P. R. Ashton, and T. D. James, *Chem. Commun.*, 2000, 229.

146 N. B. Chapman and J. Shorter, '*Advances in Linear Free Energy Relationships*', Plenum Press, 1972.

147 L. P. Hammett, '*Physical Organic Chemistry*', McGraw-Hill, 1970.

148 S. Jacobson and R. Pizer, *J. Am. Chem. Soc.*, 1993, **115**, 11216.

149 J. Griffiths, '*Colour and Constitution of Organic Molecules*', Academic Press, 1976.

150 C. J. Ward, P. Patel, and T. D. James, *Chem. Lett.*, 2001, 406.

151 P. R. Westmark, S. J. Gardiner, and B. Smith, *J. Am. Chem. Soc.*, 1996, **118**, 11093.

152 G. W. Kabalka, *Expert Opinion on Therapeutic Patents*, 1998, **8**, 545.

153 F. J. Green, '*The Sigma-Aldrich Handbook of Stains, Dyes and Indicators*', Aldrich Chemical Company, 1991.

154 F. P. Schmidtchen and M. Berger, *Chem. Rev.*, 1997, **97**, 1609.

155 D. G. Hall, J. Tailor, and M. Gravel, *Angew. Chem., Int. Ed. Engl.*, 1999, **38**, 3064.

156 K. A. Thompson and D. G. Hall, *Chem. Commun.*, 2000, 2379.

157 C. Pourbaix, F. Carreaux, B. Carboni, and H. Deleuze, *Chem. Commun.*, 2000, 1275.

158 S. Arimori, J. H. Hartley, M. L. Bell, C. S. Oh, and T. D. James, *Tetrahedron Lett.*, 2000, **41**, 10291.

159 S. Arimori, C. J. Ward, and T. D. James, *Chem. Commun.*, 2001, in press.

160 L. Szebellady and S. Tomay, *Z. Anal. Chem.*, 1936, **107**, 26.

161 S. L. Wiskur, J. J. Lavigne, H. Ait-Haddou, V. Lynch, Y. Hung Chiu, J. W. Canary, and E. V. Anslyn, *Org. Lett.*, 2001, **3**, 1311.

162 G. Springsteen and B. Wang, *Chem. Commun.*, 2001, 1608.

6 Appendix

"If we knew what it was we were doing, it would not be called research, would it?"

Albert Einstein, 1879-1955

6.1 Absorption-pH Titrations

Appendix 1: Absorption-pH spectral changes of dye **4** (4.66 x 10^{-5} mol dm^{-3})

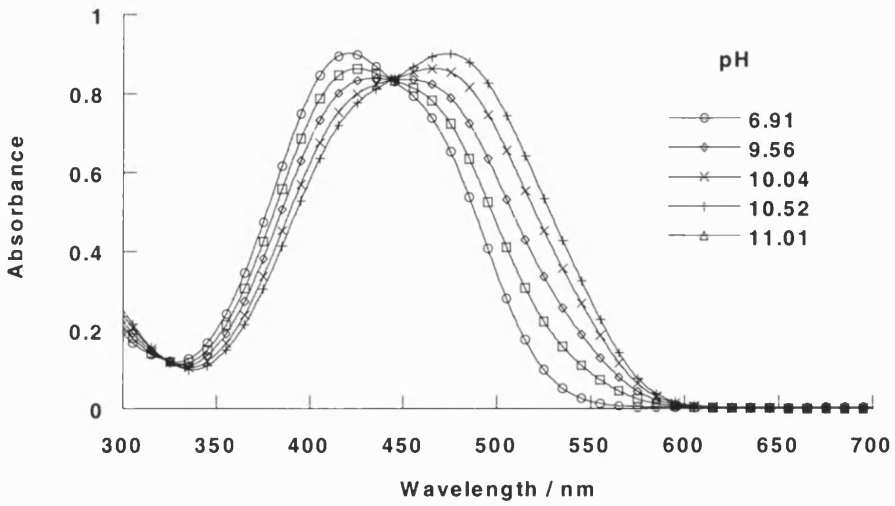

Appendix 2: Absorption-pH spectral changes of dye **4** (4.66 x 10^{-5} mol dm^{-3}) with 0.05 mol dm^{-3} D-fructose

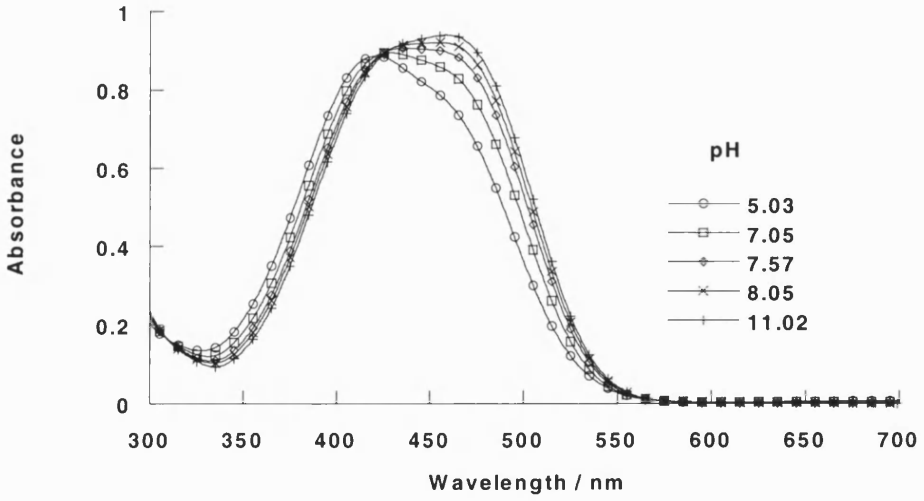

Appendix 3: Absorption-pH profile of dye **4** with and without D-fructose at 450 nm

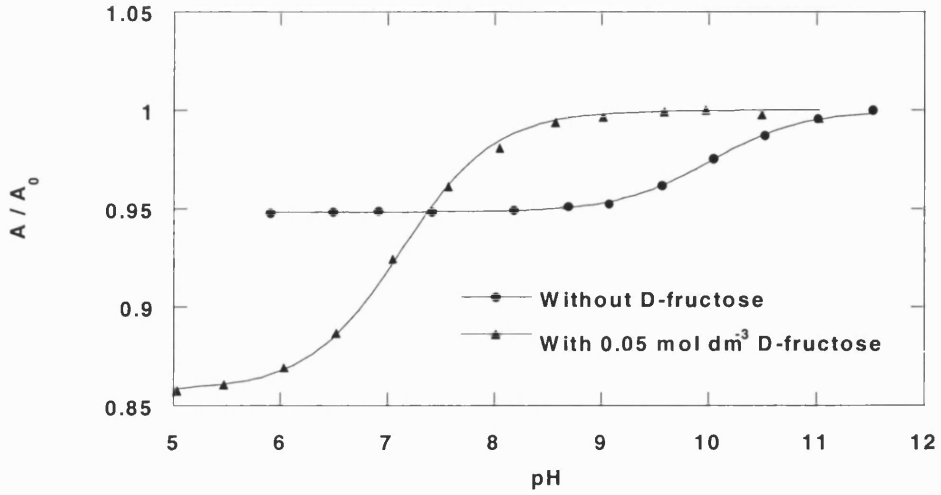

Appendix 4: Absorption-pH spectral changes of dye **5** (5.47×10^{-5} mol dm^{-3})

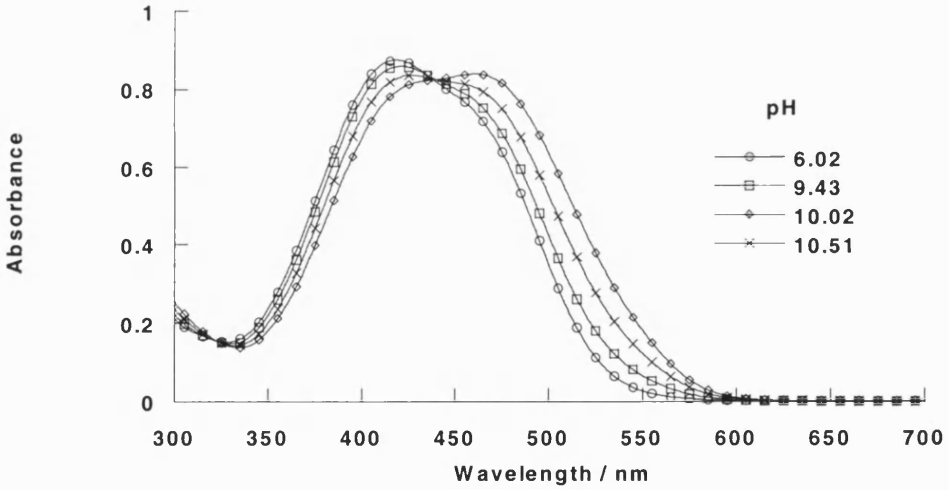

Appendix 5: Absorption-pH spectral changes of dye **5** (5.47×10^{-5} mol dm^{-3}) with 0.05 mol dm^{-3} D-fructose

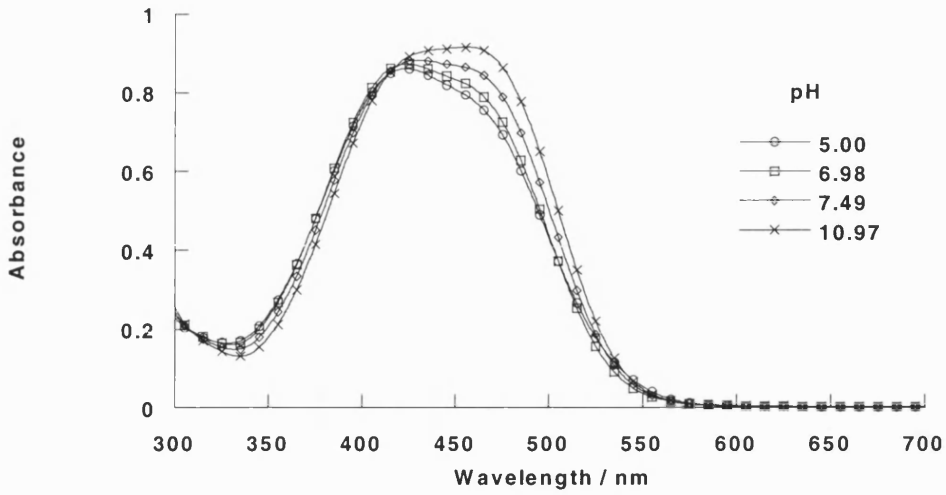

Appendix 6: Absorption-pH profile of dye **5** with and without D-fructose at 450 nm

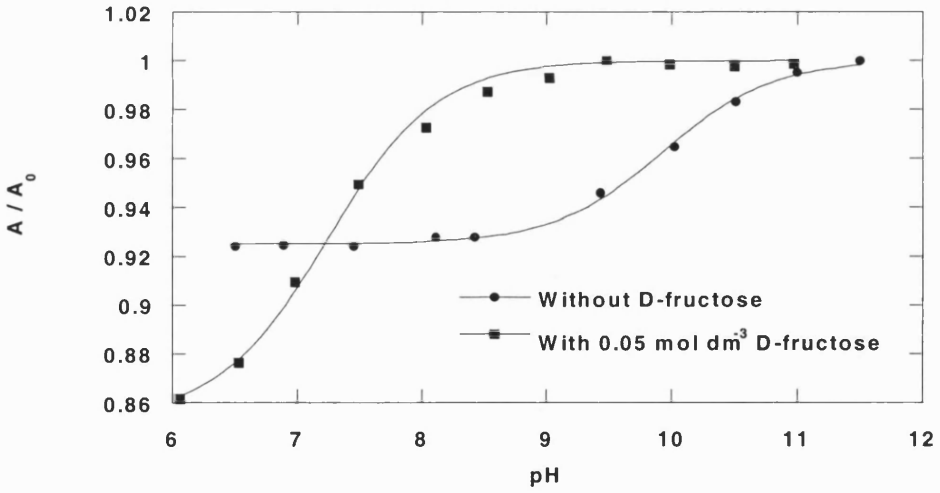

Appendix 7: Absorption-pH spectral changes of dye **6** (7.33 x 10^{-5} mol dm^{-3})

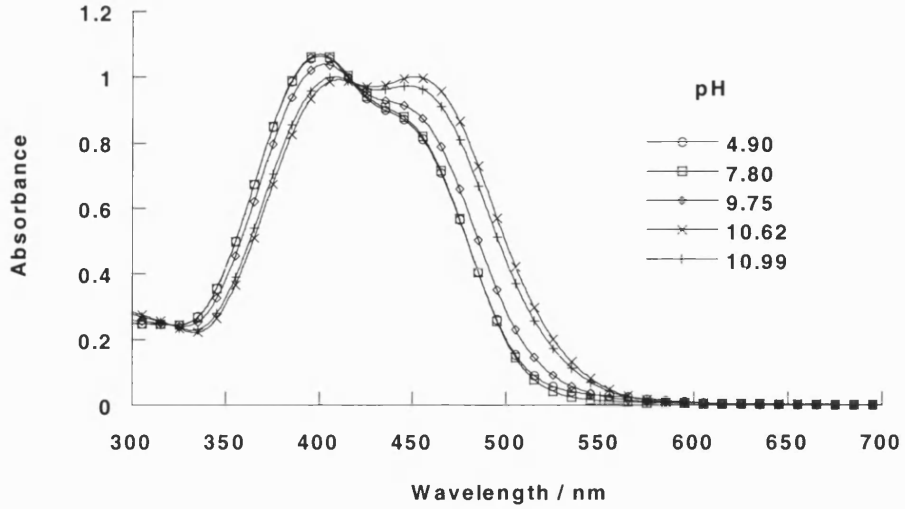

Appendix 8: Absorption-pH spectral changes of dye **6** (7.33 x 10^{-5} mol dm^{-3}) with 0.05 mol dm^{-3} D-fructose

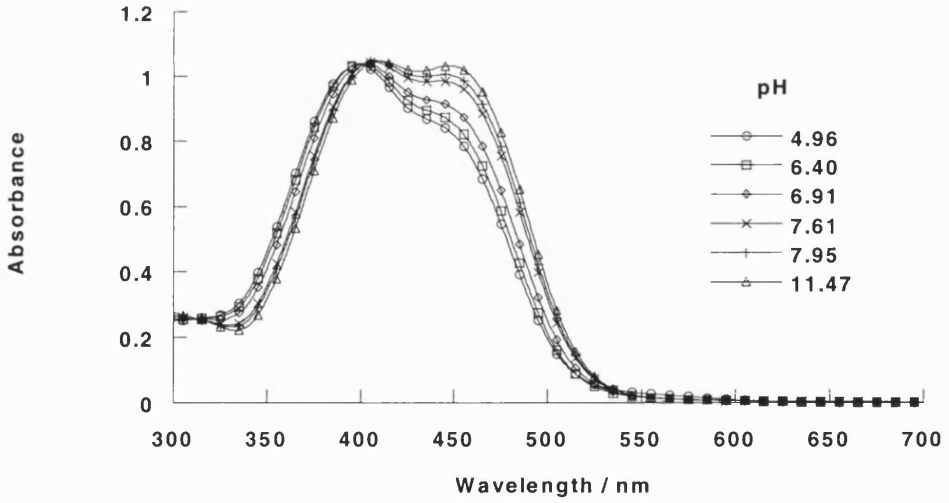

Appendix 9: Absorption-pH profile of dye **6** with and without D-fructose at 450 nm

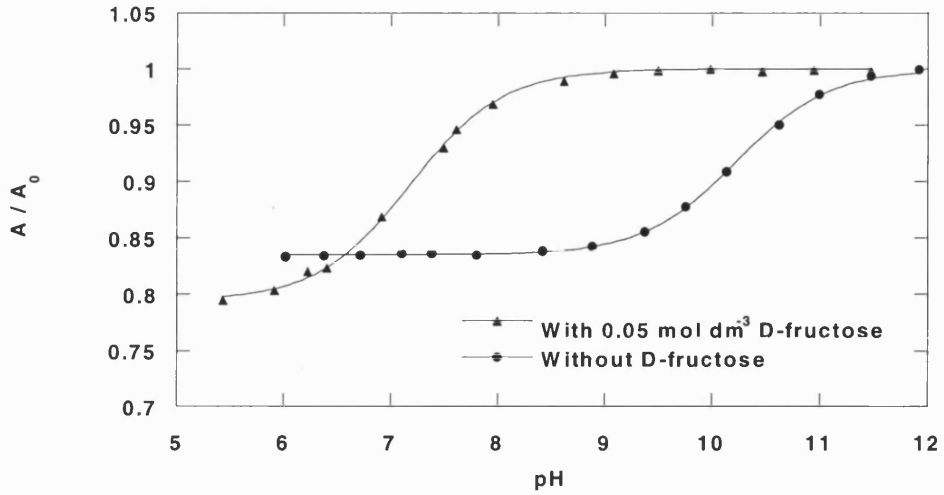

Appendix 10: Absorption-pH spectral changes of dye **10** (1.86×10^{-5} mol dm^{-3})

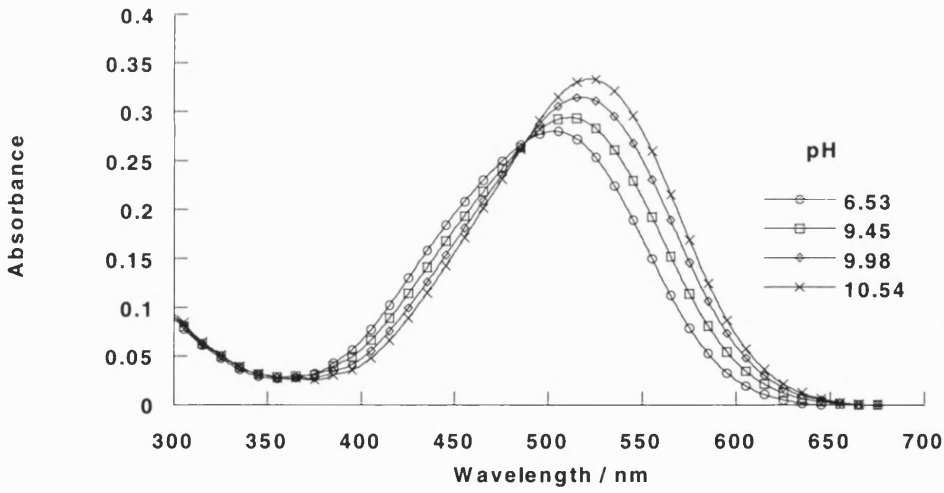

Appendix 11: Absorption-pH spectral changes of dye **10** (1.86 x 10^{-5} mol dm^{-3}) with 0.05 mol dm^{-3} D-fructose

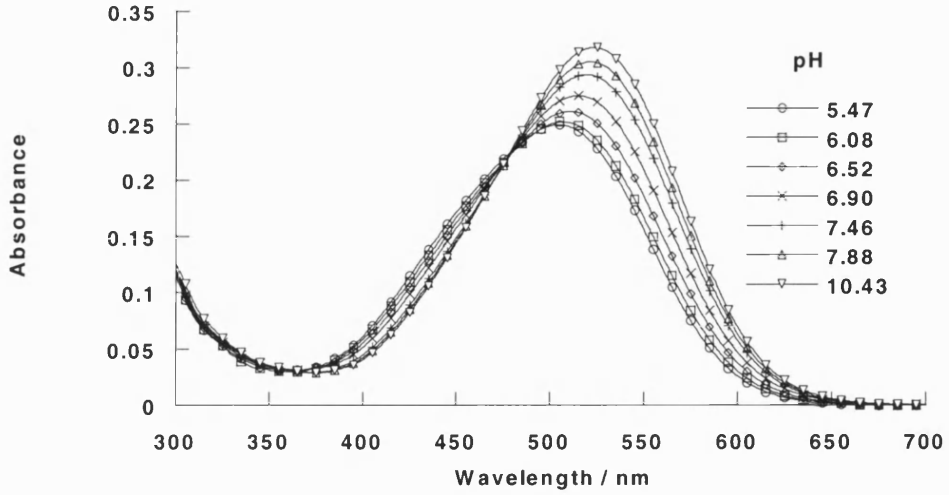

Appendix 12: Absorption-pH profile of dye **10** with and without D-fructose at 590 nm

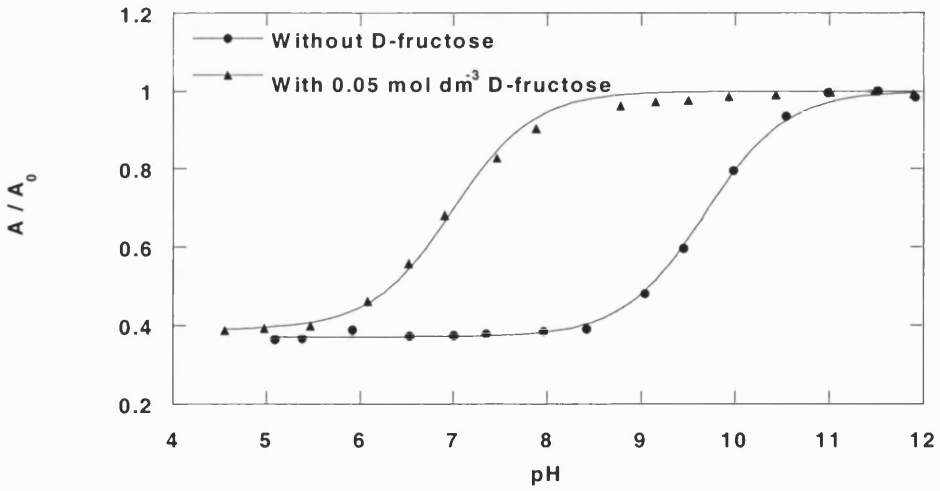

Appendix 13: Absorption-pH spectral changes of dye **17** (1.76 x 10^{-5} mol dm^{-3})

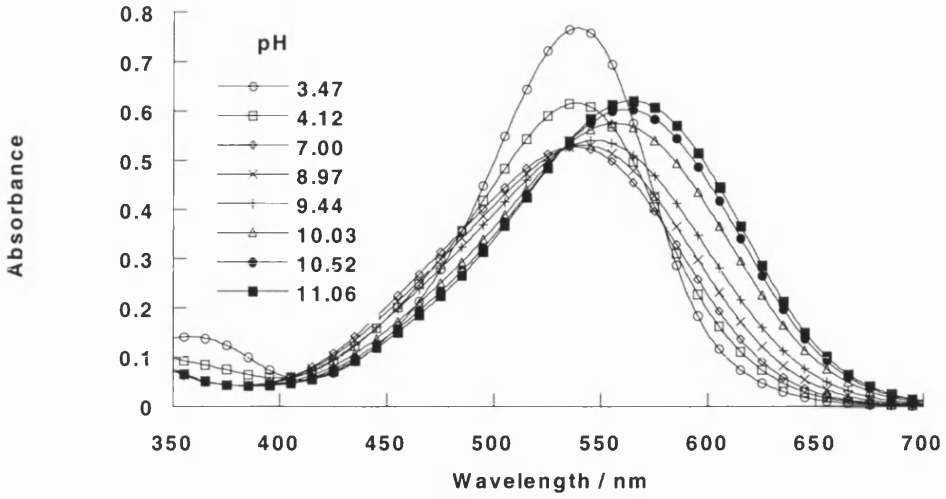

Appendix 14: Absorption-pH spectral changes of dye **17** (1.76 x 10^{-5} mol dm^{-3}) with 0.05 mol dm^{-3} D-fructose

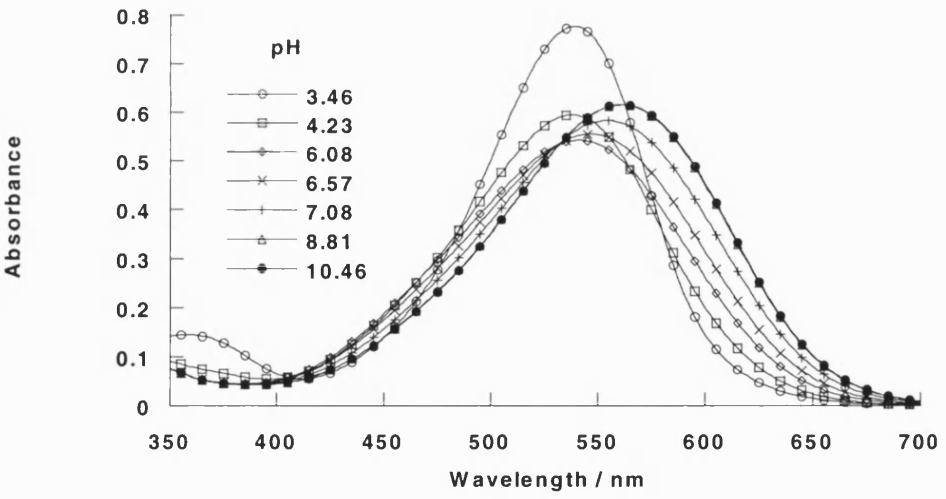

Appendix 15: Absorption-pH profile of dye **17** with and without D-fructose at 590 nm

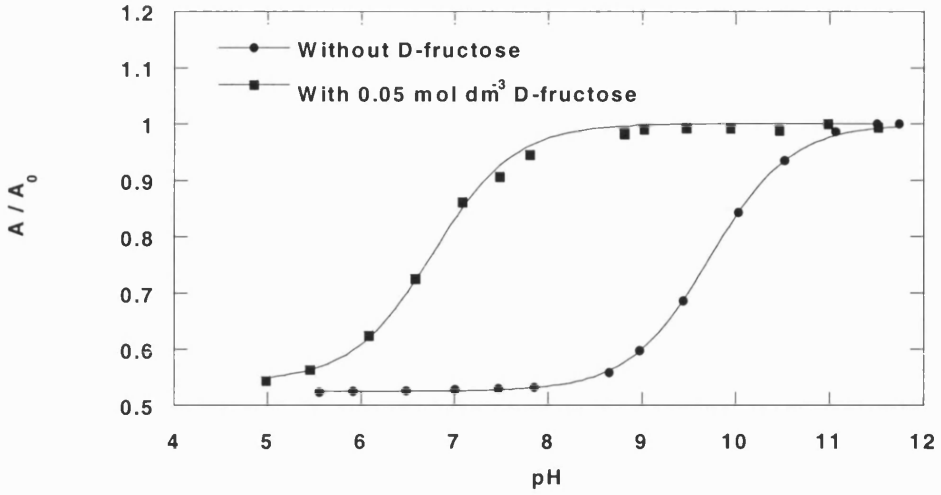

6.2 Absorption-Saccharide Titrations

Appendix 16: Absorption spectral changes of dye **3** (2.83×10^{-5} mol dm^{-3}) with increasing concentration of D-fructose at pH 11.32

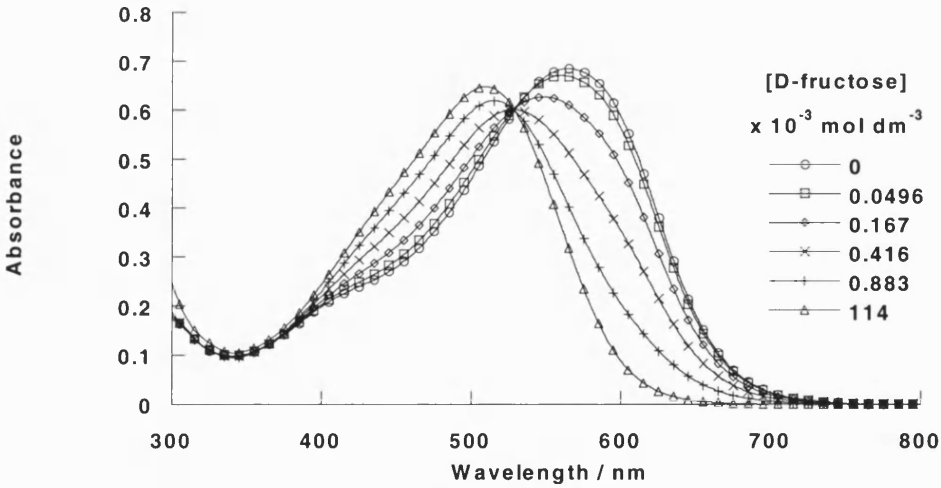

Appendix 17: Curve fit to determine the stability constant at 509 nm of dye **3** with D-fructose at pH 11.32

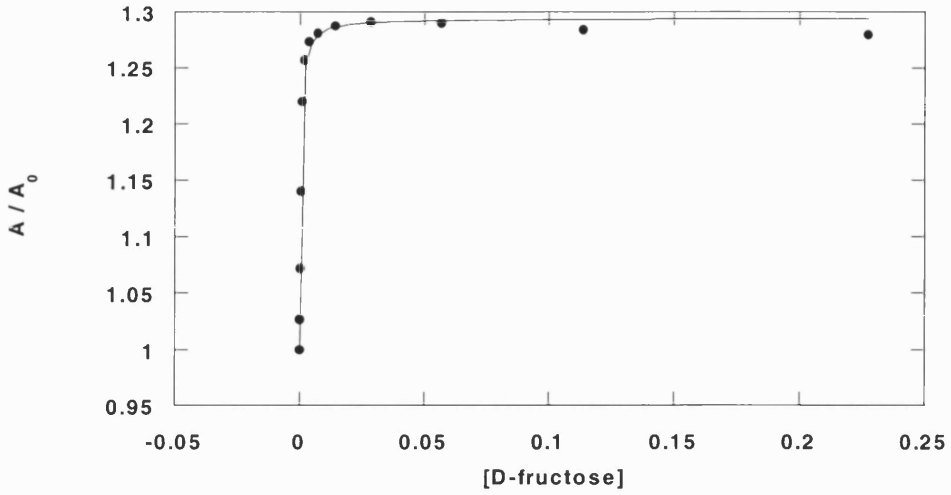

Appendix 18: Absorption spectral changes of dye **3** (2.83×10^{-5} mol dm^{-3}) with increasing concentration of ethylene glycol at pH 11.32

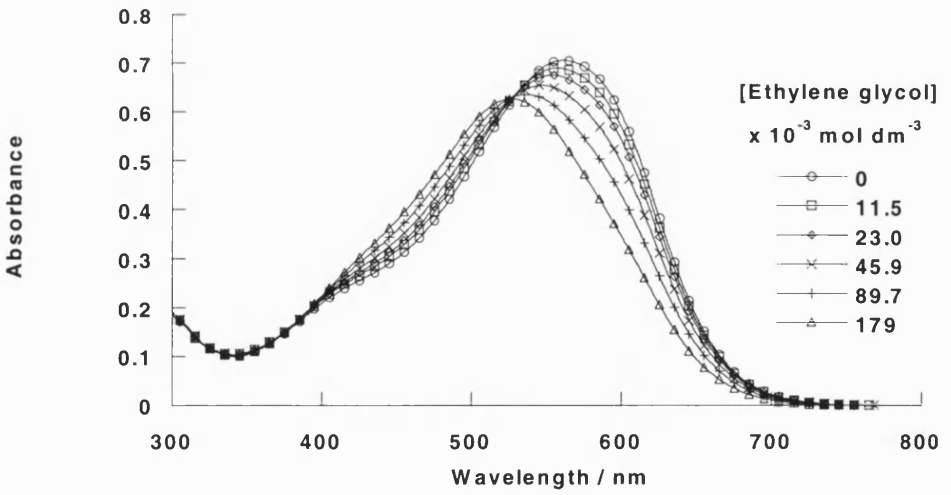

Appendix 19: Curve fit to determine the stability constant at 564 nm of dye **3** with ethylene glycol at pH 11.32

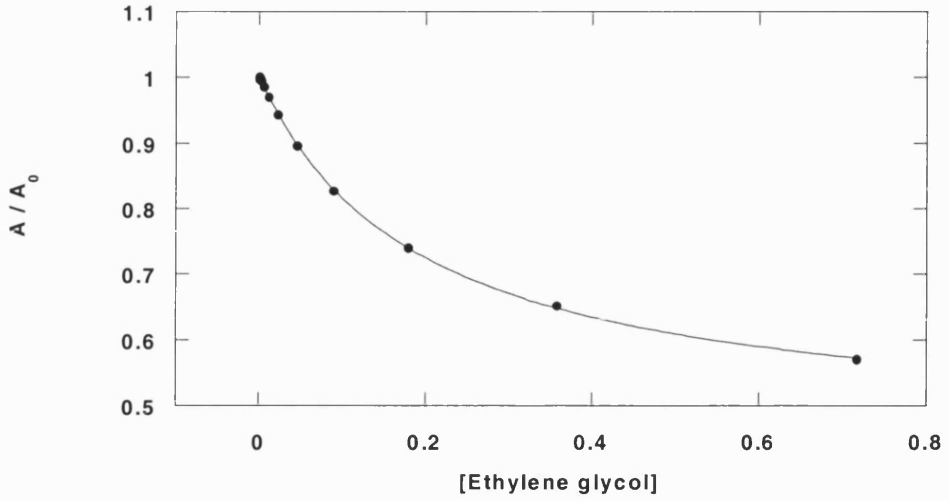

Appendix 20: Curve fit to determine the stability constant at 509 nm of dye **3** with D-fructose at pH 8.21

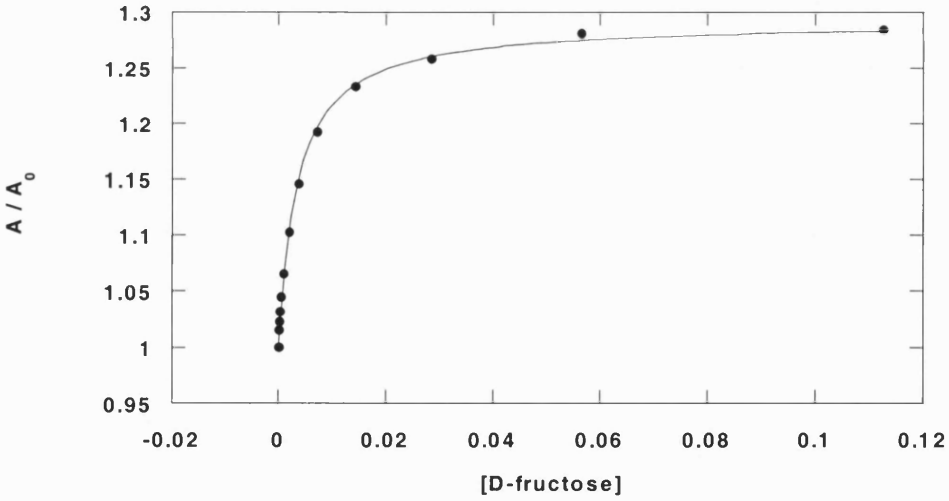

Appendix 21: Absorption spectral changes of dye **3** (2.83 x 10^{-5} mol dm^{-3}) with increasing concentration of D-glucose at pH 8.21

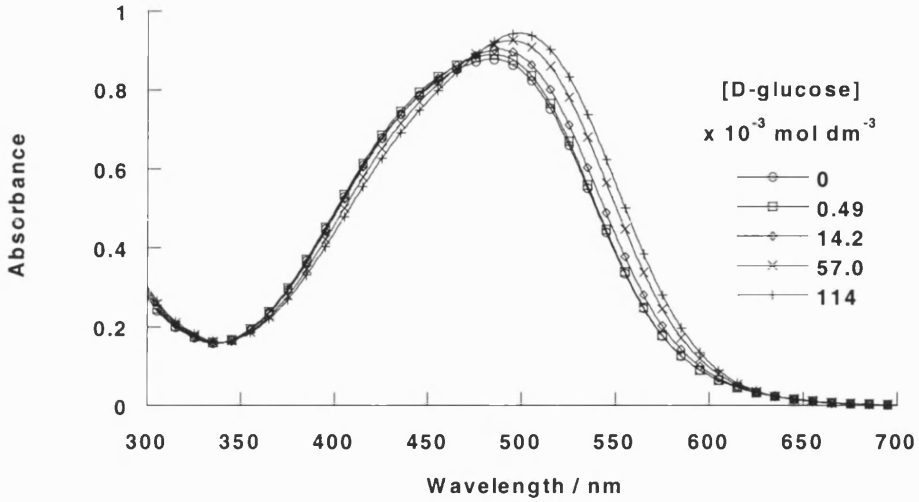

Appendix 22: Curve fit to determine the stability constant at 509 nm of dye **3** with D-glucose at pH 8.21

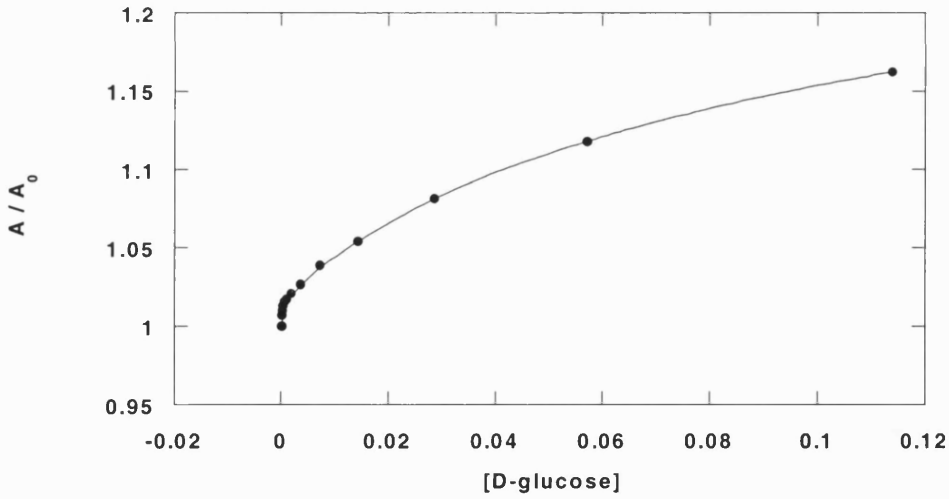

Appendix 23: Absorption spectral changes of dye **4** (3.26 x 10^{-5} mol dm^{-3}) with increasing concentration of D-fructose at pH 11.32

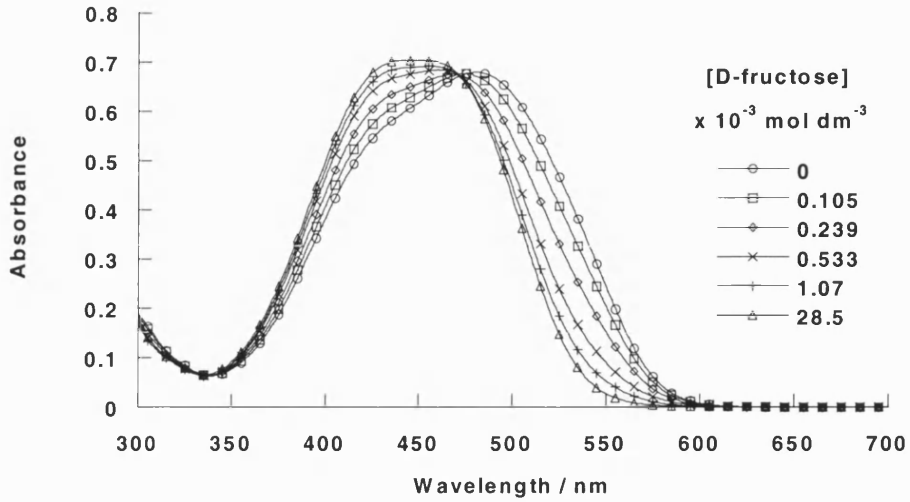

Appendix 24: Curve fit to determine the stability constant at 451 nm of dye **4** with D-fructose at pH 11.32

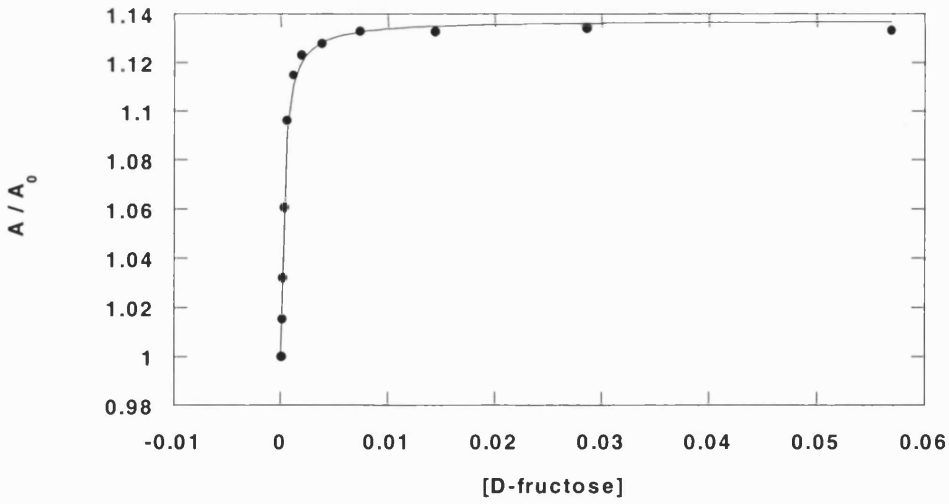

Appendix 25: Absorption spectral changes of dye **4** (3.26 x 10^{-5} mol dm^{-3}) with increasing concentration of D-glucose at pH 11.32

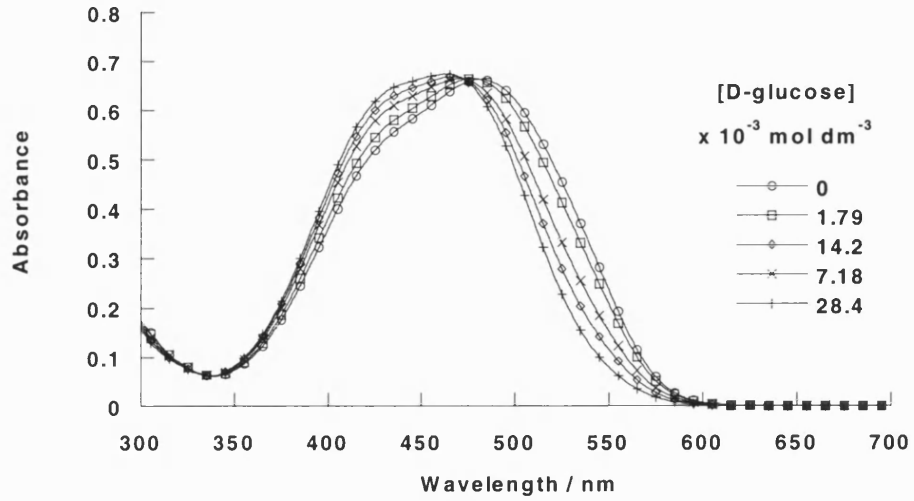

Appendix 26: Curve fit to determine the stability constant at 458 nm of dye **4** with D-glucose at pH 11.32

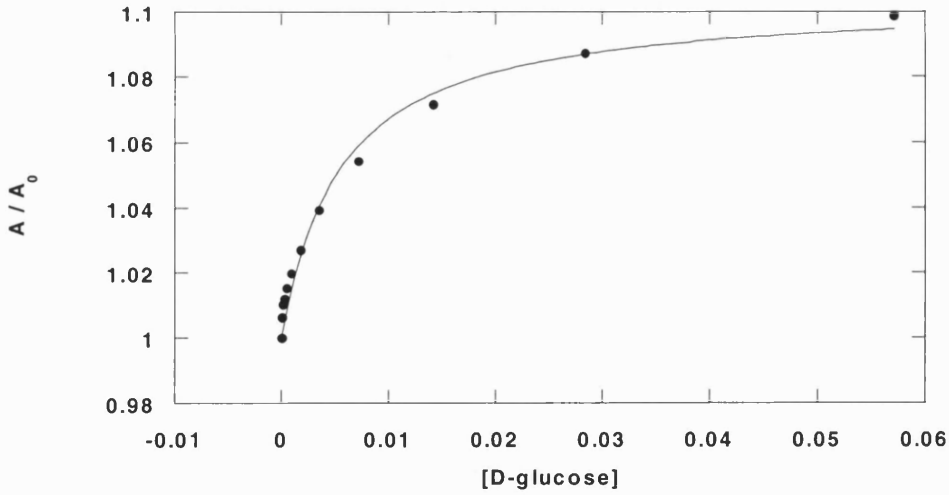

Appendix 27: Absorption spectral changes of dye **5** (2.74 x 10^{-5} mol dm^{-3}) with increasing concentration of D-fructose at pH 11.32

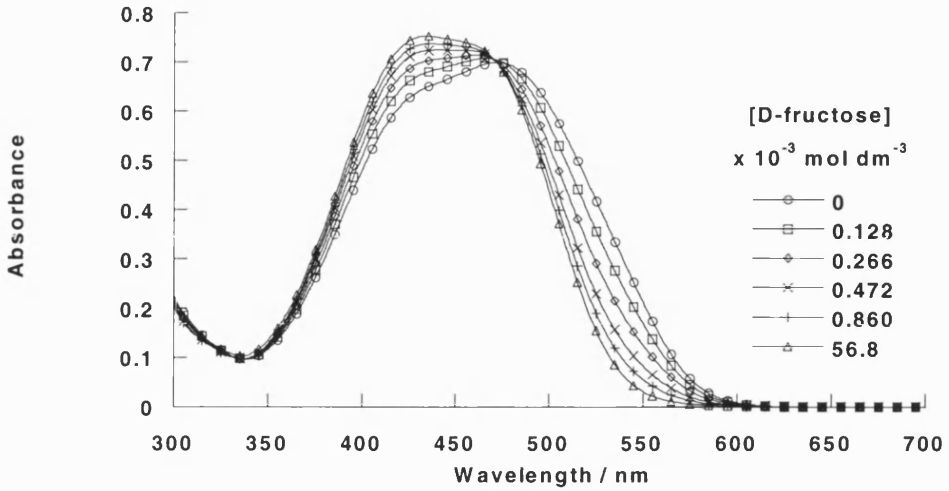

Appendix 28: Curve fit to determine the stability constant at 429 nm of dye **5** with D-fructose at pH 11.32

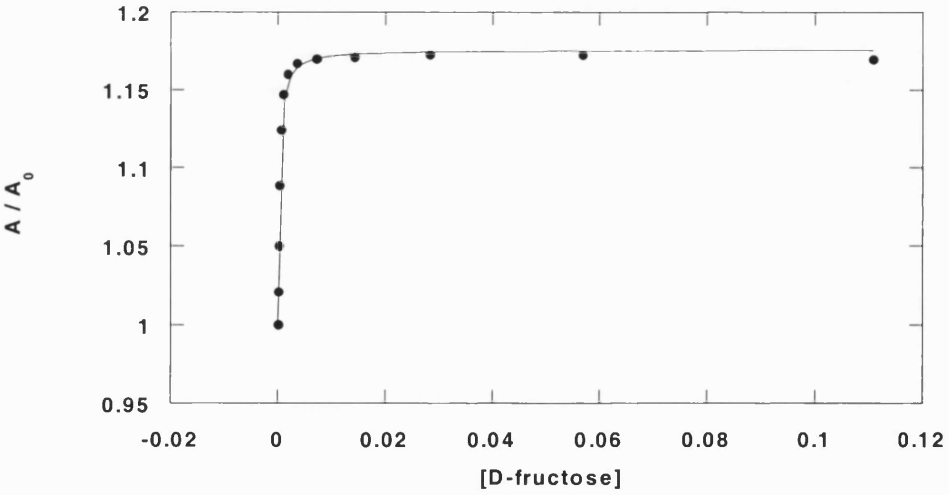

Appendix 29: Absorption spectral changes of dye **5** (2.74 x 10^{-5} mol dm^{-3}) with increasing concentration of D-glucose at pH 11.32

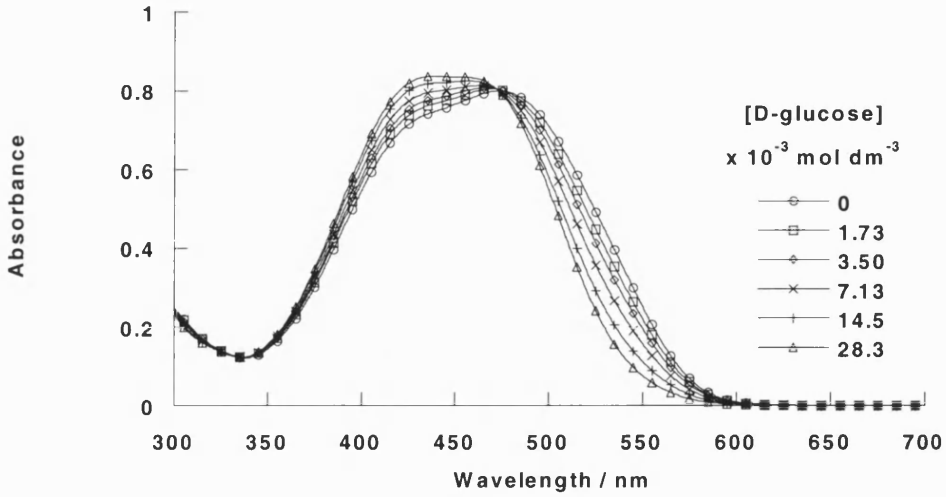

Appendix 30: Curve fit to determine the stability constant at 432 nm of dye **5** with D-glucose at pH 11.32

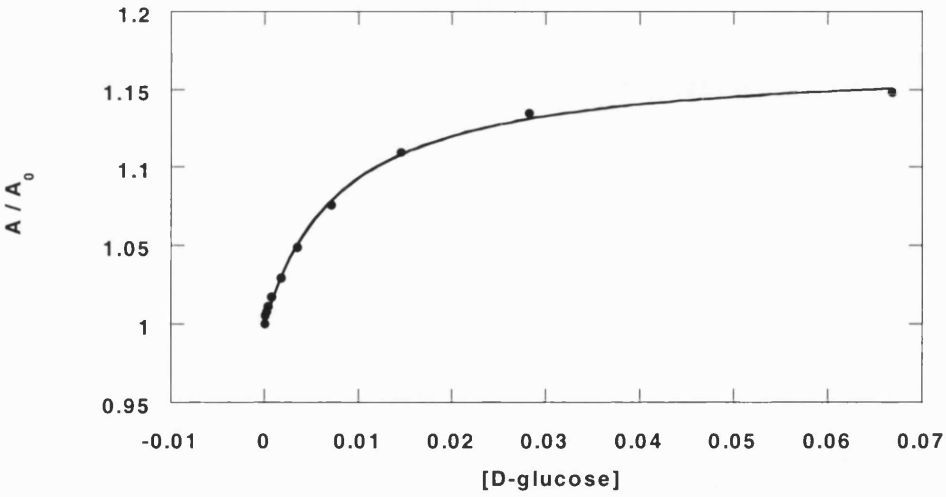

Appendix 31: Absorption spectral changes of dye **6** (5.86 x 10^{-5} mol dm^{-3}) with increasing concentration of D-fructose at pH 11.32

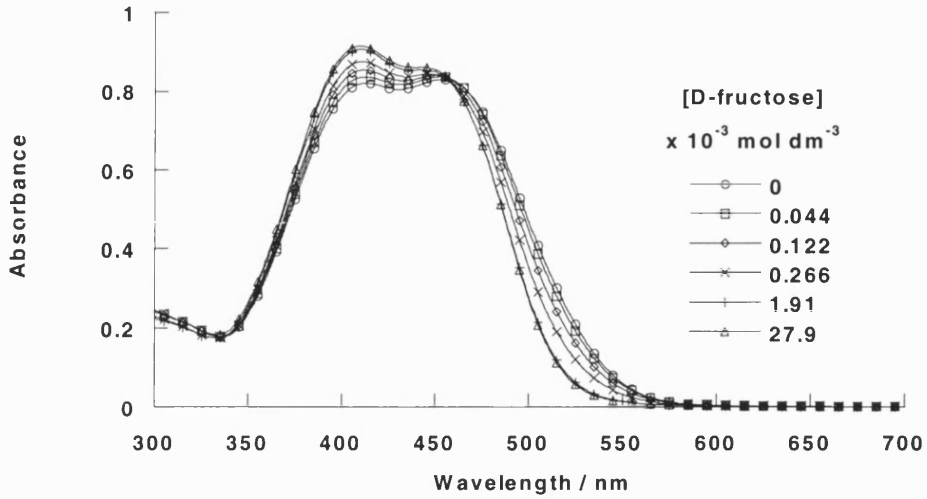

Appendix 32: Curve fit to determine the stability constant at 409 nm of dye **6** with D-fructose at pH 11.32

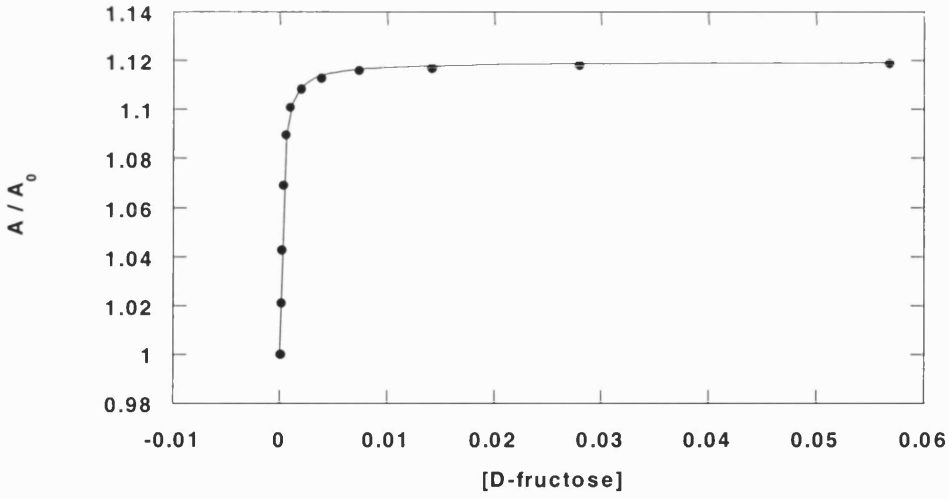

Appendix 33: Absorption spectral changes of dye **6** (5.86 x 10^{-5} mol dm^{-3}) with increasing concentration of D-glucose at pH 11.32

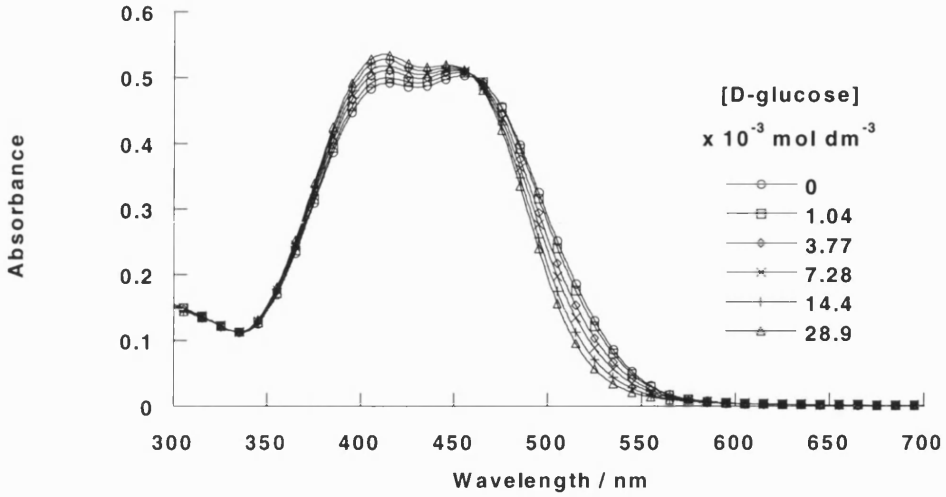

Appendix 34: Curve fit to determine the stability constant at 411 nm of dye **6** with D-fructose at pH 11.32

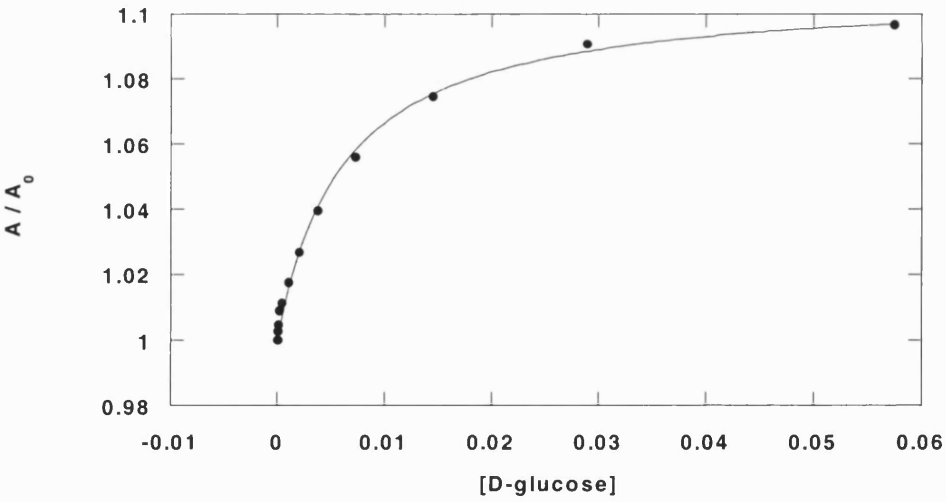

Appendix 35: Absorption spectral changes of dye **7** (4.27 x 10^{-5} mol dm^{-3}) with increasing concentration of D-fructose at pH 11.32

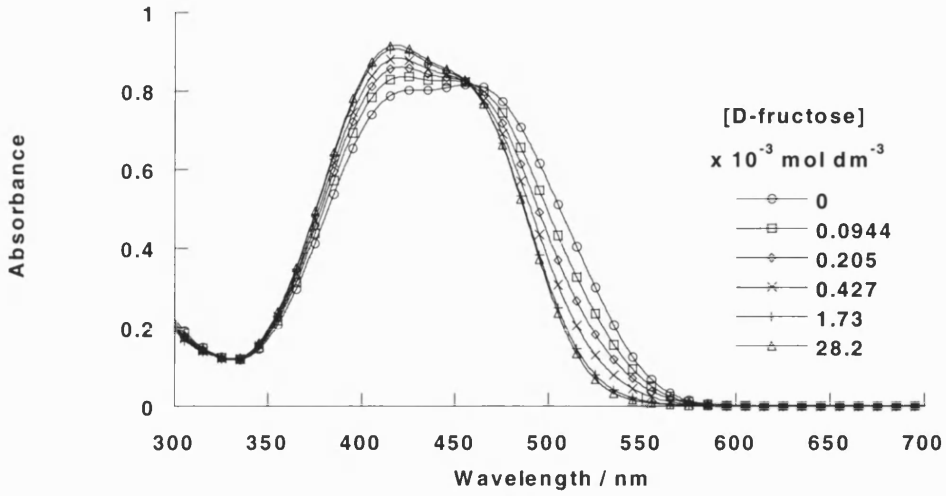

Appendix 36: Curve fit to determine the stability constant at 418 nm of dye **7** with D-fructose at pH 11.32

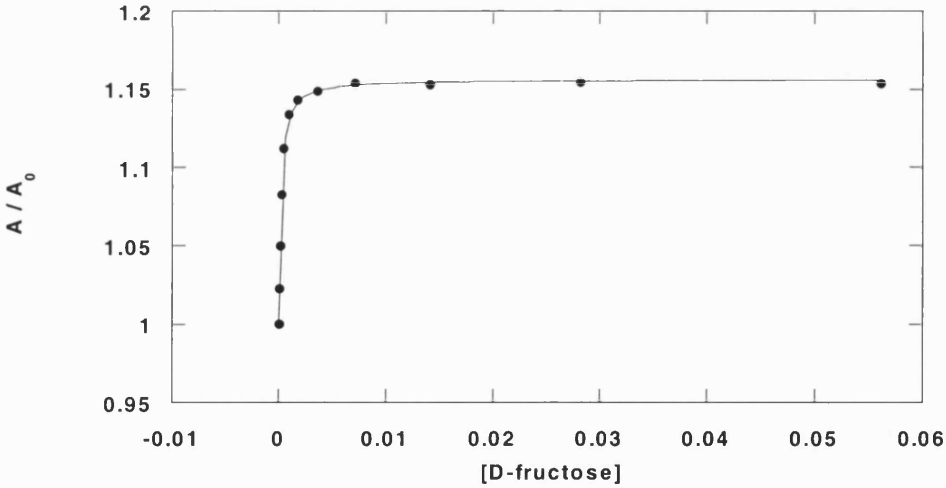

Appendix 37: Absorption spectral changes of dye **7** (4.27 x 10^{-5} mol dm^{-3}) with increasing concentration of D-glucose at pH 11.32

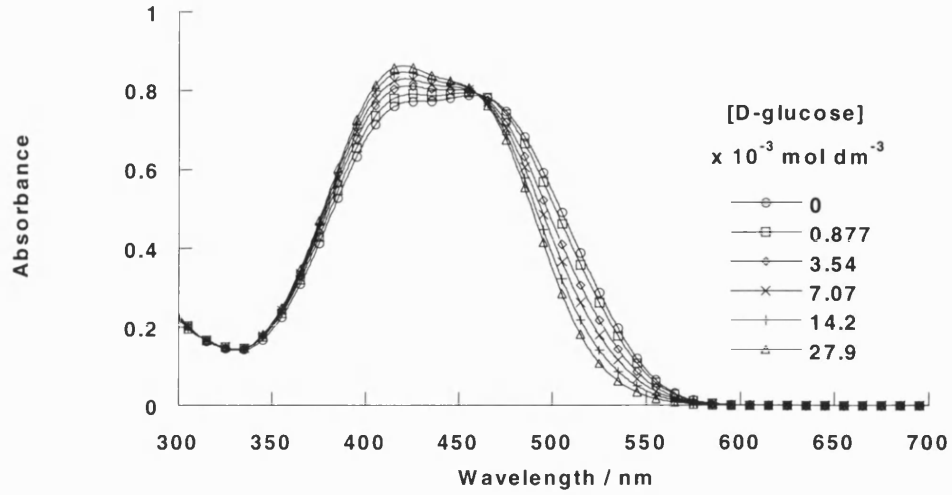

Appendix 38: Curve fit to determine the stability constant at 418 nm of dye **7** with D-glucose at pH 11.32

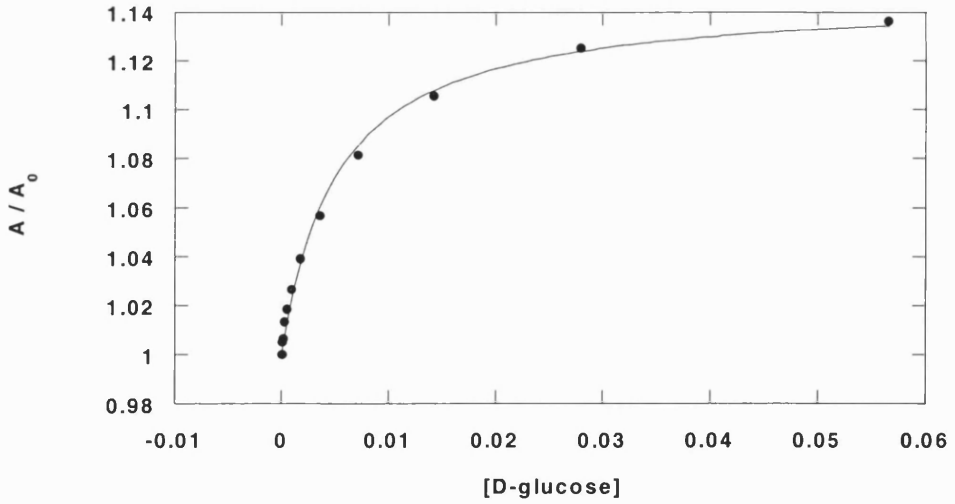

Appendix 39: Absorption spectral changes of dye **10** (2.09 x 10^{-5} mol dm^{-3}) with increasing concentration of D-glucose at pH 11.32

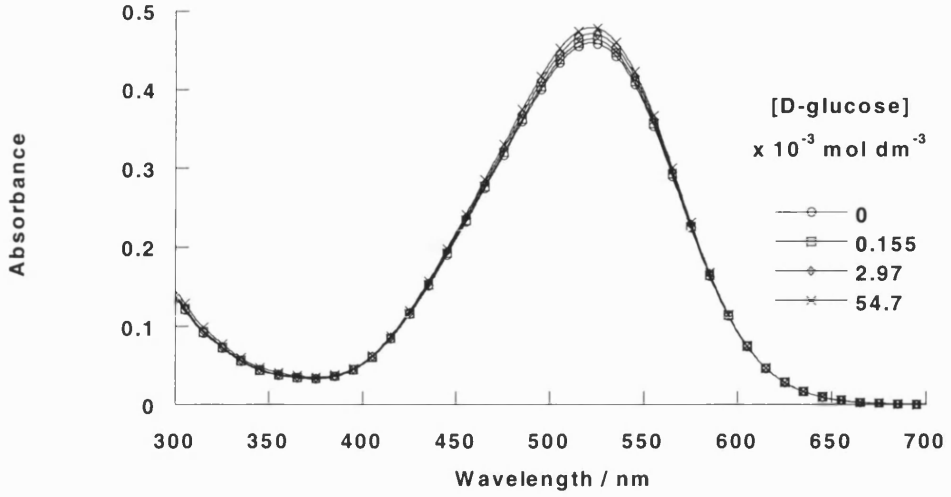

Appendix 40: Curve fit to determine the stability constant at 520 nm of dye **10** with D-fructose at pH 8.21

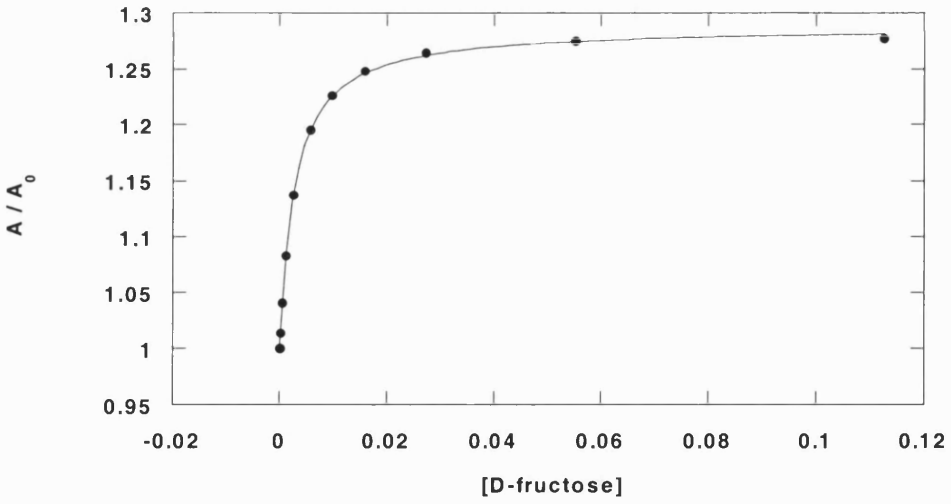

Appendix 41: Absorption spectral changes of dye **10** (2.00 x 10^{-5} mol dm^{-3}) with increasing concentration of D-glucose at pH 8.21

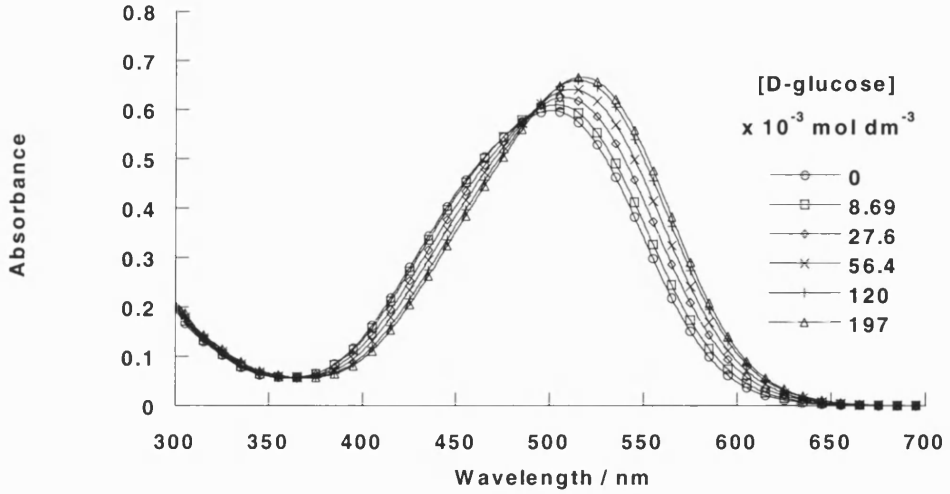

Appendix 42: Curve fit to determine the stability constant at 520 nm of dye **10** with D-glucose at pH 8.21

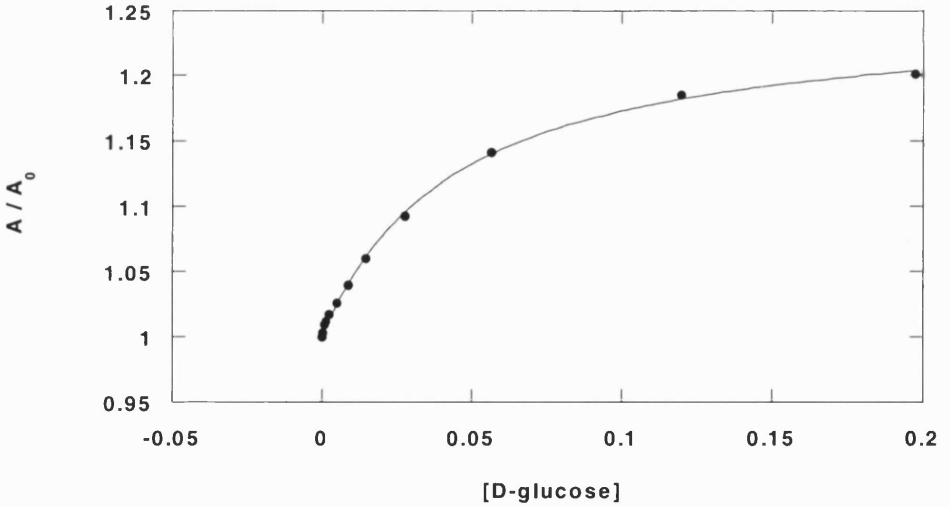

Appendix 43: Curve fit to determine the stability constant at 573 nm of dye **14** with D-fructose at pH 8.21

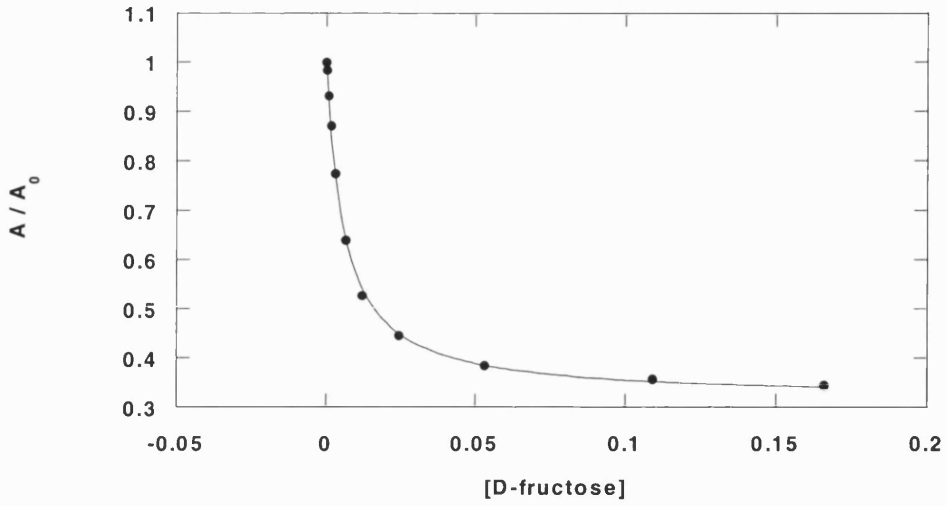

Appendix 44: Absorption spectral changes of dye **14** (3.14×10^{-5} mol dm^{-3}) with increasing concentration of D-glucose at pH 8.21

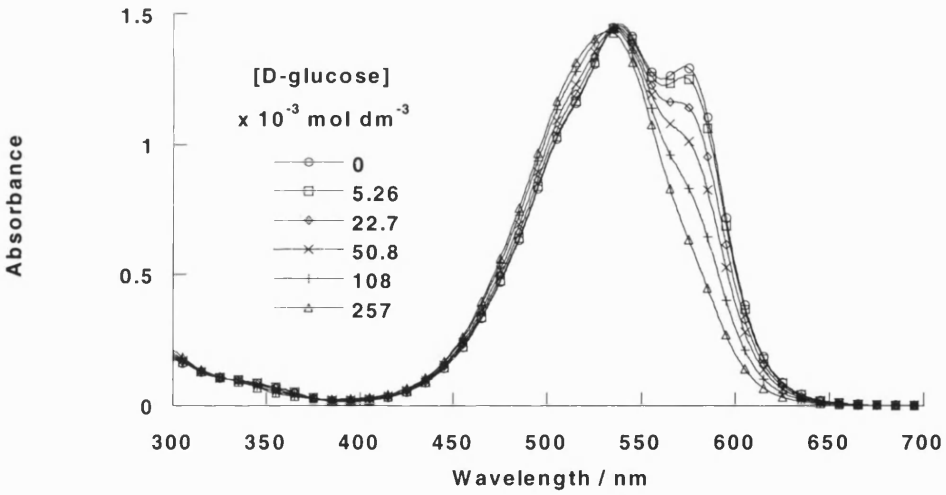

Appendix 45: Curve fit to determine the stability constant at 573 nm of dye **14** with D-glucose at pH 8.21

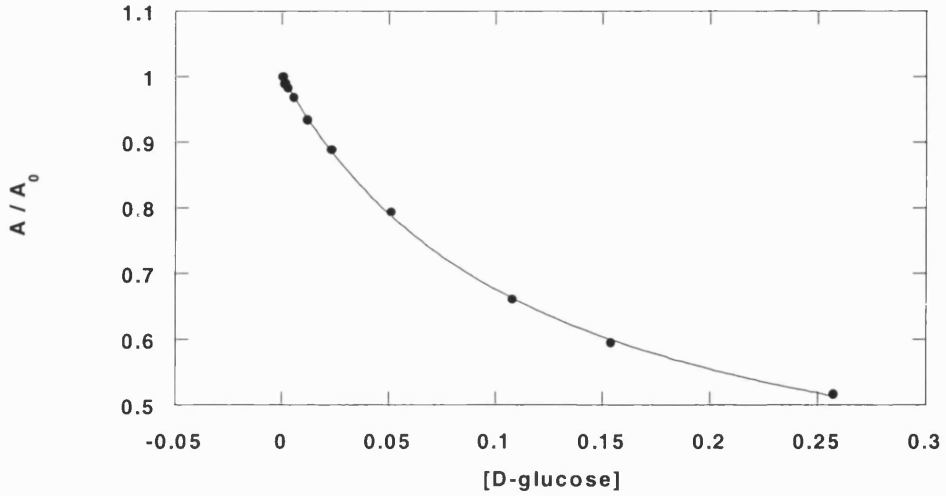

Appendix 46: Curve fit to determine the stability constant at 585 nm of dye **17** with D-fructose at pH 8.21

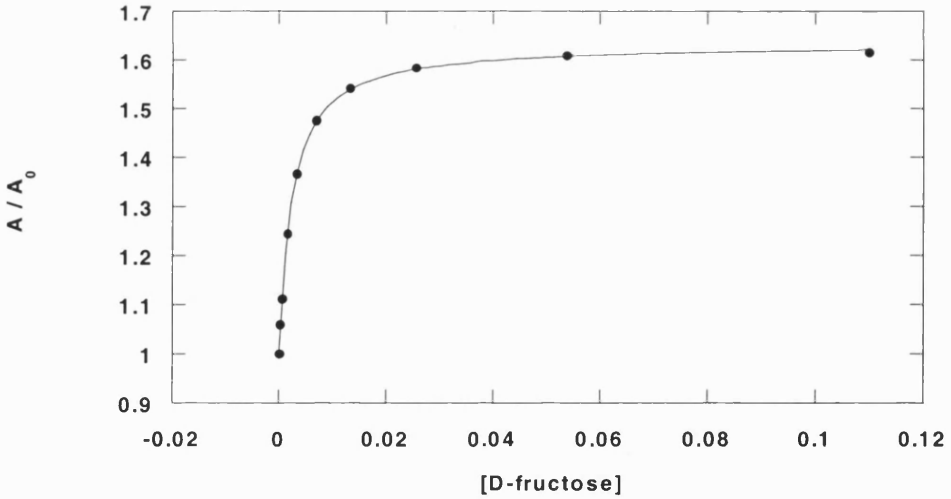

Appendix 47: Absorption spectral changes of dye **17** (1.76 x 10^{-5} mol dm^{-3}) with increasing concentration of D-glucose at pH 8.21

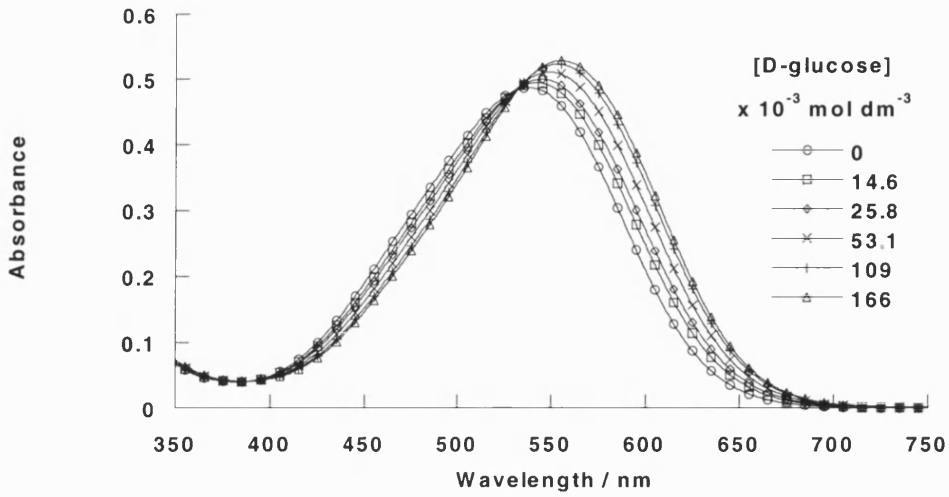

Appendix 48: Curve fit to determine the stability constant at 585 nm of dye **17** with D-glucose at pH 8.21

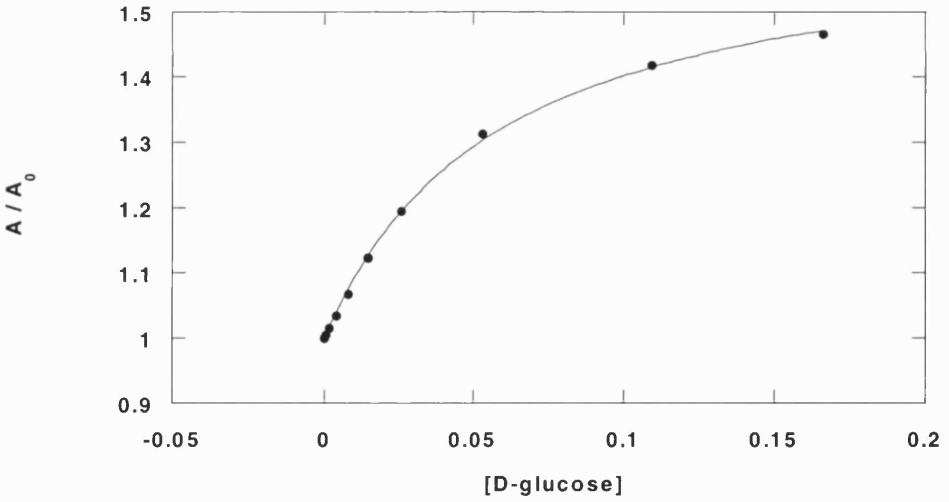

6.3 Absorption-Potassium Halide Titrations

Appendix 49: Absorption spectral changes of dye **3** (3.48 x 10^{-5} mol dm^{-3}) with increasing concentration of potassium bromide in methanol

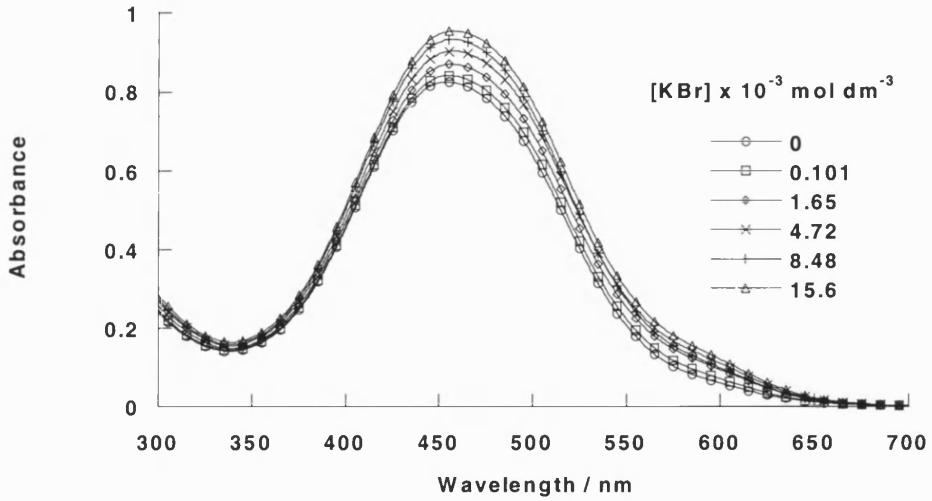

Appendix 50: Absorption spectral changes of dye **3** (3.48 x 10^{-5} mol dm^{-3}) with increasing concentration of potassium iodide in methanol

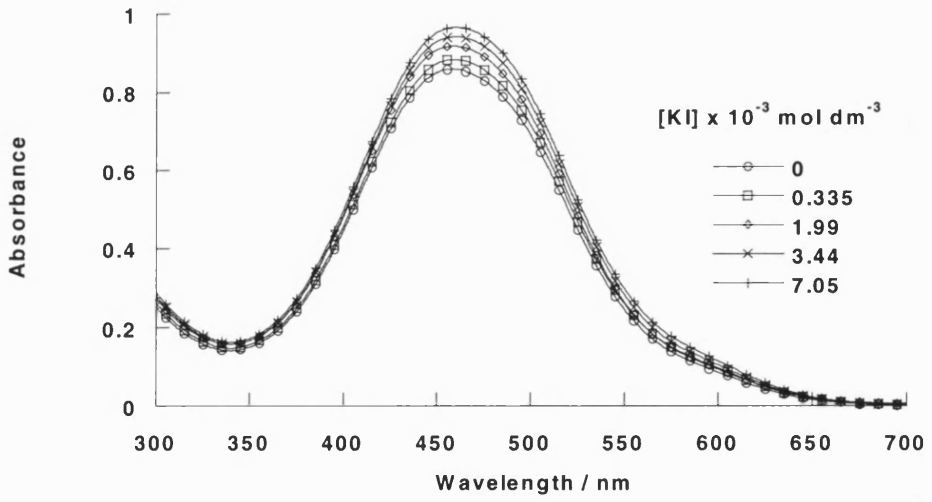

Appendix 51: Curve fit to determine the stability constant at 505 nm of dye **10** with potassium fluoride in methanol

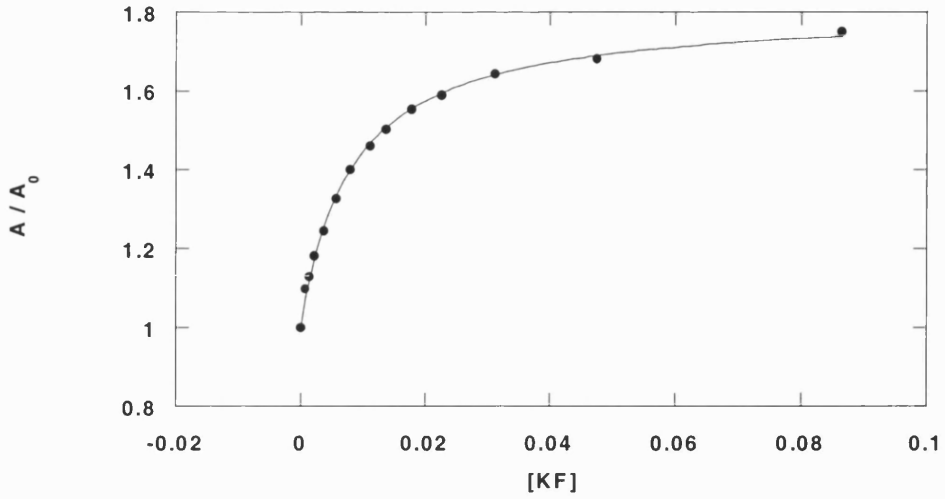

Appendix 52: Curve fit to determine the stability constant at 555 nm of dye **14** with potassium fluoride in methanol

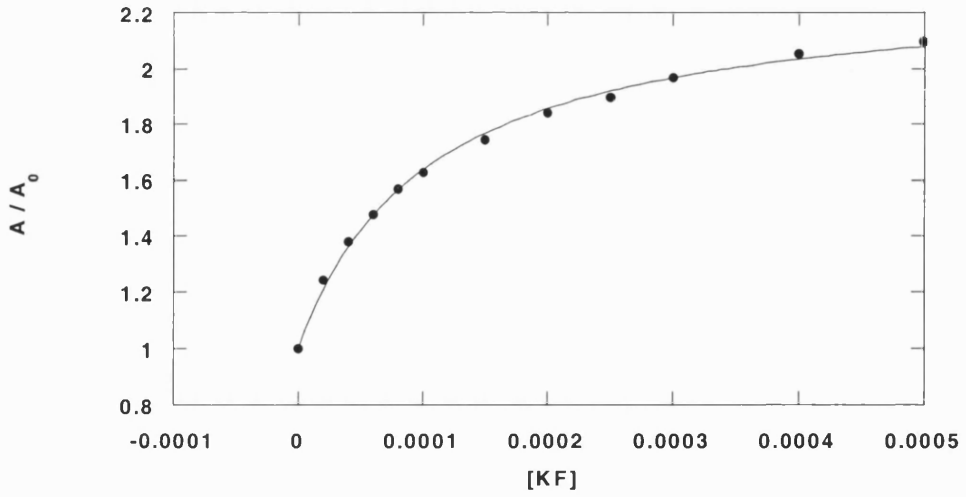

Appendix 53: Absorption spectral changes of dye **14** (1.57 x 10^{-5} mol dm^{-3}) with increasing concentration of potassium chloride in methanol

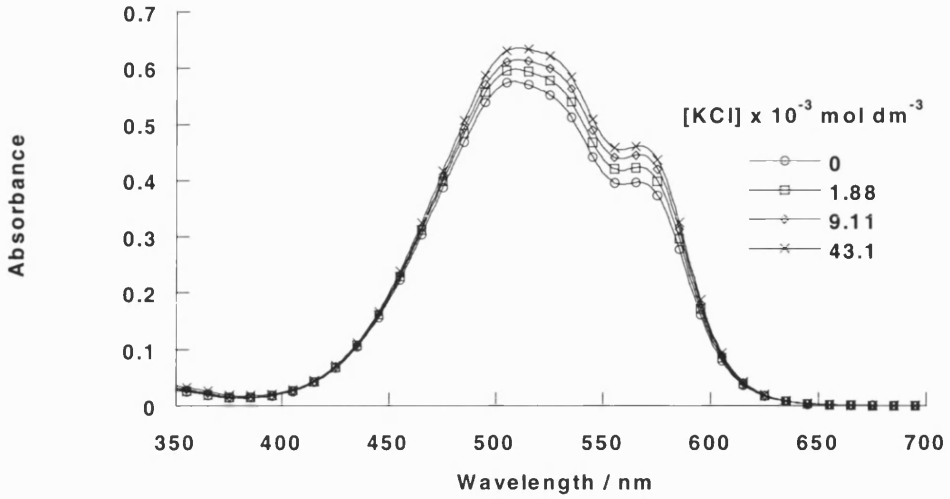

Appendix 54: Absorption spectral changes of dye **14** (1.57 x 10^{-5} mol dm^{-3}) with increasing concentration of potassium bromide in methanol

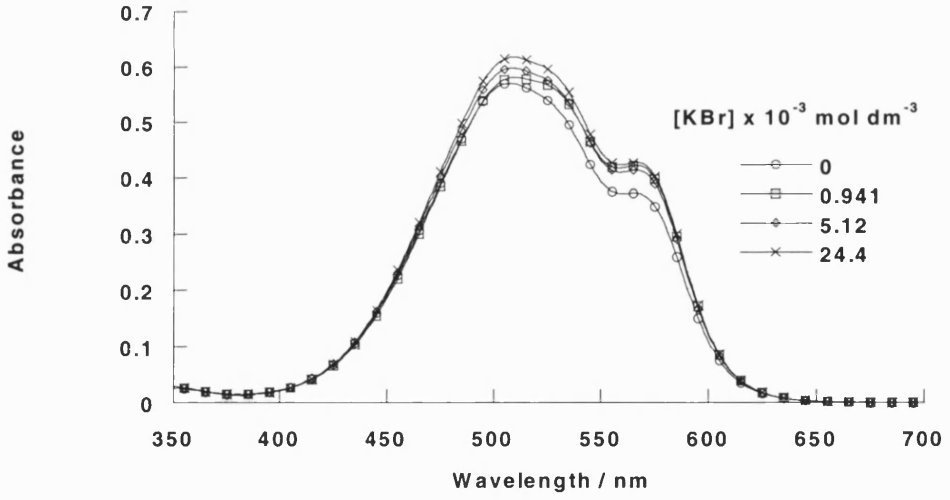

Appendix 55: Curve fit to determine the stability constant at 548 nm of dye **17** with potassium fluoride in methanol

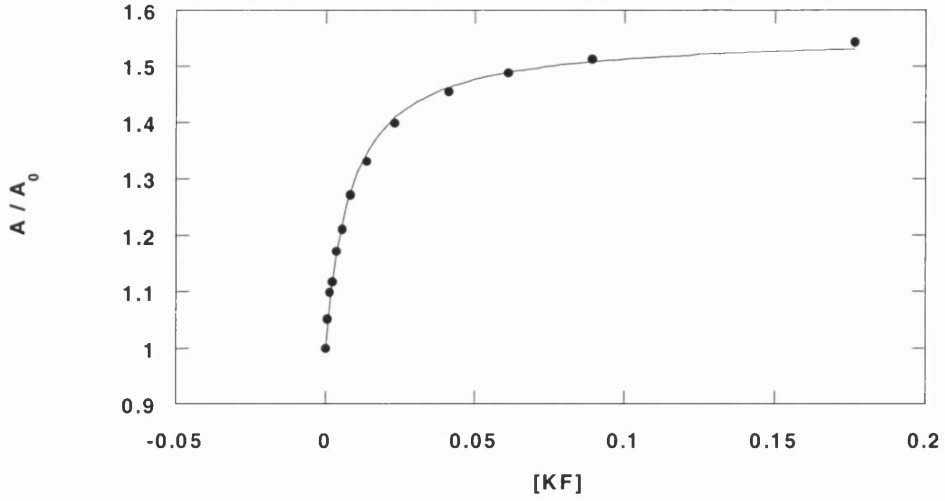

Appendix 56: Absorption spectral changes of dye **17** (1.76×10^{-5} mol dm^{-3}) with increasing concentration of potassium chloride in methanol

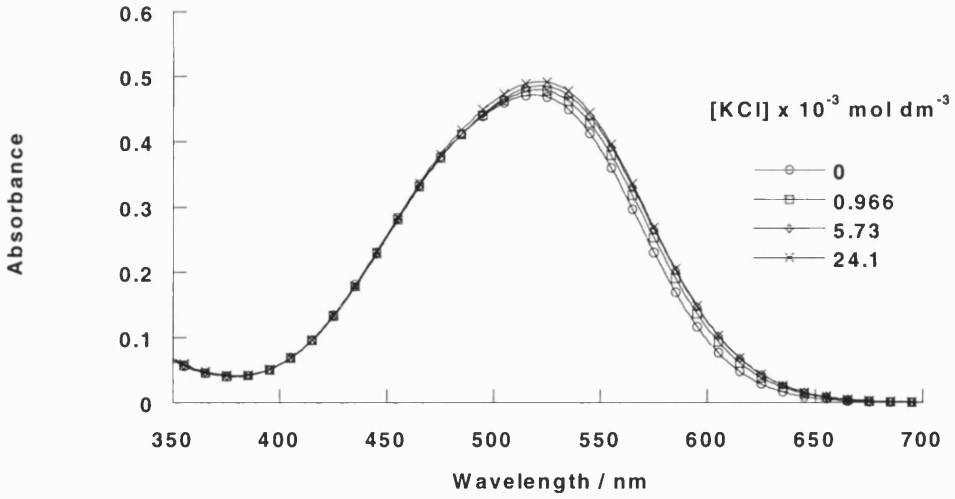

Appendix 57: Absorption spectral changes of dye **17** (1.76 x 10^{-5} mol dm^{-3}) with increasing concentration of potassium bromide in methanol

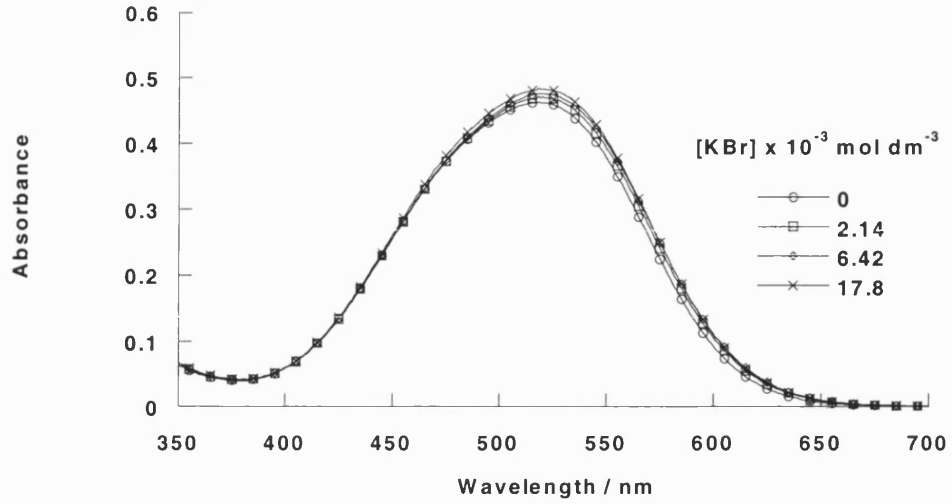

6.4 Absorption-Boronic Acid Titrations with Alizarin Red S

Appendix 58: Absorption spectral changes of dye **25** (9.60 x 10^{-5} mol dm^{-3}) with increasing concentration of boronic acid **12** at pH 8.21

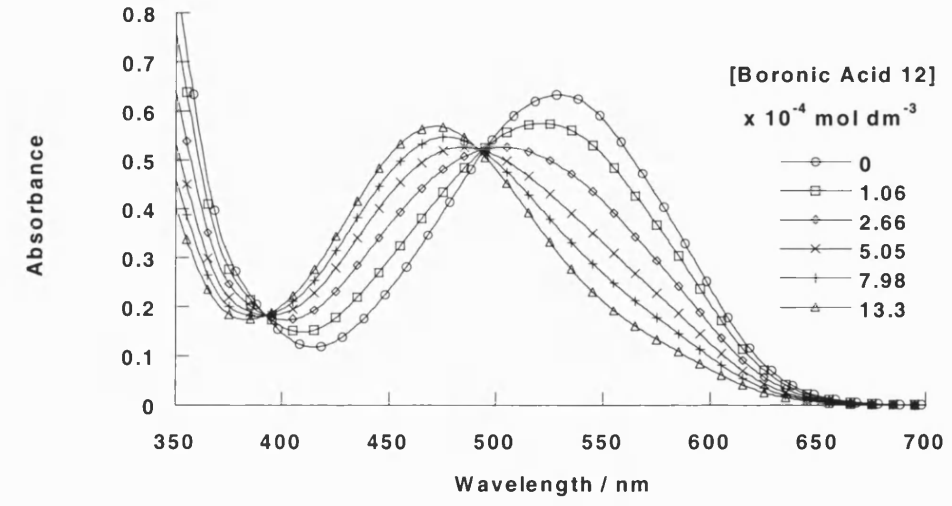

Appendix 59: Curve fit to determine the stability constant at 530 nm of dye **25** with boronic acid **12** at pH 8.21

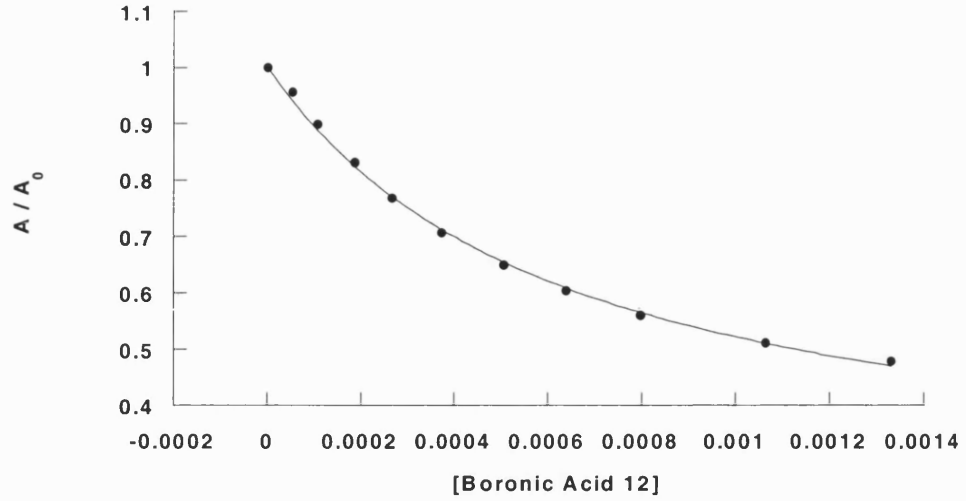

Appendix 60: Absorption spectral changes of dye **25** (9.60 x 10^{-5} mol dm^{-3}) with increasing concentration of benzyl-(2-boronobenzyl)-methylamine (**BBMA**) at pH 8.21

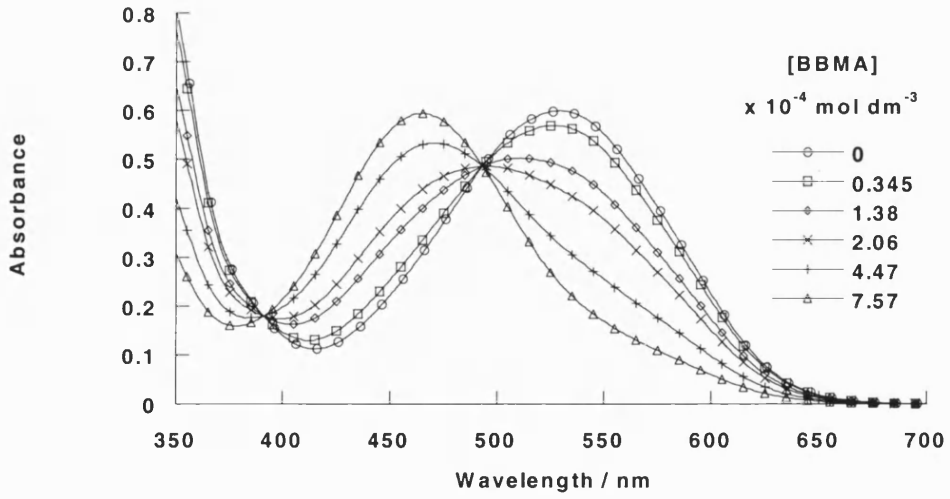

Appendix 61: Curve fit to determine the stability constant at 530 nm of dye **25** with benzyl-(2-boronobenzyl)-methylamine (**BBMA**) at pH 8.21

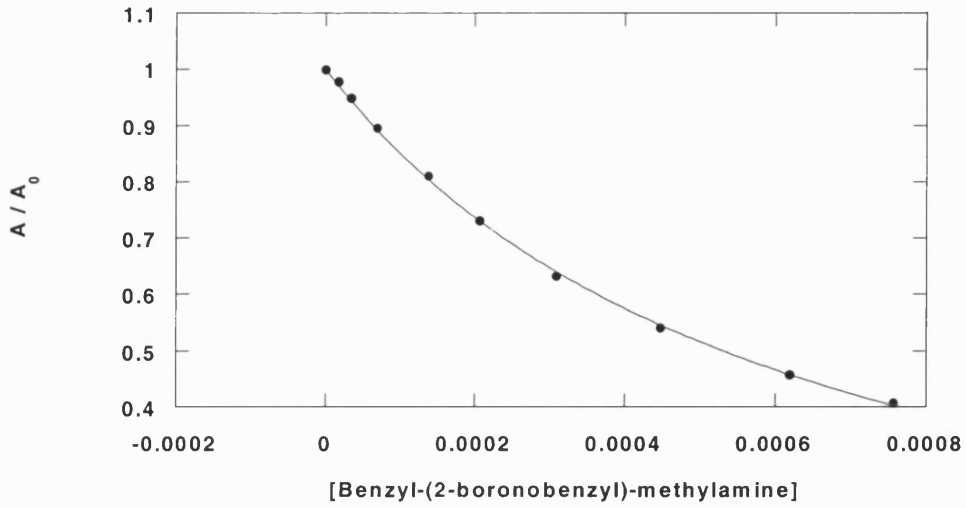

Appendix 62: Absorption spectral changes of dye **25** (9.60×10^{-5} mol dm^{-3}) with increasing concentration of 3-nitrophenylboronic acid (**3-NPBA**) at pH 8.21

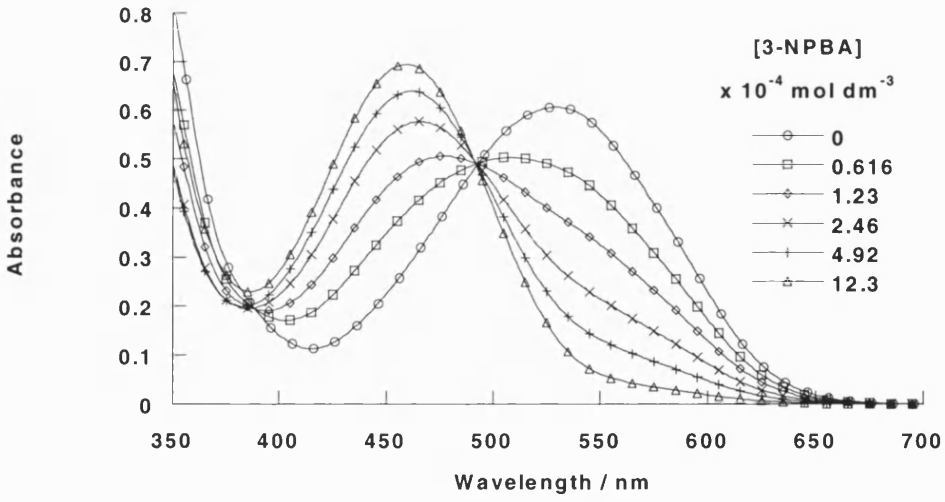

Appendix 63: Curve fit to determine the stability constant at 530 nm of dye **25** with 3-nitrophenylboronic acid (**3-NPBA**) at pH 8.21